



THE UNIVERSITY OF  
**WAIKATO**  
*Te Whare Wānanga o Waikato*

Research Commons

<http://researchcommons.waikato.ac.nz/>

## Research Commons at the University of Waikato

### Copyright Statement:

The digital copy of this thesis is protected by the Copyright Act 1994 (New Zealand).

The thesis may be consulted by you, provided you comply with the provisions of the Act and the following conditions of use:

- Any use you make of these documents or images must be for research or private study purposes only, and you may not make them available to any other person.
- Authors control the copyright of their thesis. You will recognise the author's right to be identified as the author of the thesis, and due acknowledgement will be made to the author where appropriate.
- You will obtain the author's permission before publishing any material from the thesis.

# The Volcanic Geology of the Western Tauranga Basin

A thesis

Submitted in partial fulfilment

of the requirements for

the Degree of

Master of Science in Earth Sciences

at the

University of Waikato

by

Annette N. Whitbread-Edwards

University of Waikato

1994

## Abstract

The western Tauranga basin is bounded to the north by the Tauranga Harbour and to the west by the Kaimai Range. It contains rhyolitic domes, ignimbrites, fluvial deposits and tephtras.

The oldest units are the Minden Rhyolites which are hypersthene, hornblende and biotite rhyolites. These form the dome complexes Minden Peak, Manawata and Kaikaikaroro. These domes are surrounded by the overlying Waiteariki Ignimbrite which is a dacitic ignimbrite made up of three flow units and contains co-eruptive lithics within its basal unit. The Te Puna Ignimbrite is a rhyolitic ignimbrite which is found in the coastal cliffs around western Tauranga Harbour. Fluvial material which is predominantly of volcanic origin lies unconformably below and on top of the Te Puna Ignimbrite. A number of tephtras overlie the rhyolites and ignimbrites in the area. These are: Pahoia Tephtras, Hamilton Ash, Rotoehu Ash, Mangaone, Oruanui, Okareka, Mamaku, Taupo and Kaharoa Tephtras.

Whole rock geochemistry shows that western Tauranga basin rocks are calc-alkaline, and have resulted from arc volcanism. The rocks have formed predominantly from crystal fractionation, with the rhyolites also resulting from crustal melting.

The Te Puna Ignimbrite contains pumice that ranges in SiO<sub>2</sub> content which indicates that the magma chamber was zoned. Upon eruption the magma chamber underwent simple inversion which is seen when comparing element composition and stratigraphic height. This eruption may have caused a caldera which is located east of Katikati.

The Tauranga basin lies between the Coromandel Volcanic Zone and the Taupo Volcanic Zone, and is a transitional zone in terms of age and geochemistry, shown by transitional incompatible trace element ratios.

## Acknowledgements

I would like to take this opportunity to thank the many people who helped in the production of this thesis.

Firstly I wish to thank my supervisor, Dr Roger Briggs, for his guidance and help when I needed it, and his sense of humour when I had new theories on my field area.

I also wish to thank the Bay of Plenty Regional Council for continuing the geological mapping project as their financial support of this thesis made life a lot easier.

Thanks to the staff in the Earth Science Department, the technical staff for their help when I needed to know something, Ian, Renat and Steve, and to the secretaries Sydney and Elaine.

Thanks to Ritchie Sims at the Geology Department, University of Auckland, for his help with the microprobing of my mineral samples. Also to Ken Palmer of Victoria University for prompt return of XRF analyses.

I wish to thank my field assistant and fellow masters student Glennis who made field work and shopping more fun. I also thank my fellow masters students who gave me helpful suggestions to my problems and entertainment when I needed it, namely Glen H., Annelisa, Mark, Ziggy, Glen M., Stuart, Brent, Maria and any one else I missed.

I wish to thank Mum and Dad for their financial and moral support over the last five years which made life more livable. Well Dad I have now finished and I might even get a job.

Finally I wish to thank my husband Alton, who **now** knows all there is to know about the Tauranga basin, and who gave me support and understanding when I needed it.

## Table of Contents

Title Page	i
Abstract	ii
Acknowledgements	iii
Table of Contents	iv
List of Figures	viii
List of Tables	x
<b>Chapter One : Introduction</b>	<b>1</b>
1.1 Introduction	1
1.2 Locality	1
1.3 Delineation of Field Area	1
1.4 Physiography of Area	4
1.5 Previous Literature	4
1.6 Objectives of Thesis	6
1.7 Regional Geology	7
1.8 Regional Stratigraphy and Petrography	7
<i>Coromandel Group</i>	8
<i>Whitianga Group</i>	8
<i>Whakamarama Group</i>	8
<i>Tauranaga Group</i>	10
<b>Chapter Two: Stratigraphy</b>	
2.1 Introduction	12
2.2 Minden Rhyolite	12
<i>Age</i>	12
<i>Source and distribution</i>	14
<i>Lithology</i>	14
2.3 Waiteariki Ignimbrite	16
<i>Age</i>	16
<i>Distribution</i>	16
<i>Lithology</i>	16
<i>Welding</i>	17

2.4 Matua Subgroup	18
<i>Lignite</i>	18
<i>Fluvial</i>	19
2.5 Te Puna Ignimbrite	19
<i>Age</i>	20
<i>Lithology</i>	20
2.6 Tephtras	24
<i>Pahoia Tephtras</i>	24
<i>Hamilton Ash</i>	24
<i>Rotehu Ash</i>	25
<b>Chapter Three: Petrology and Mineralogy</b>	<b>26</b>
3.1 Introduction	26
3.2 Rhyolites	26
3.2.1 Minden Peak	26
<i>Plagioclase</i>	37
<i>Quartz</i>	37
<i>Amphibole</i>	37
<i>Orthopyroxene</i>	37
<i>Biotite</i>	38
<i>Fe-Ti Oxides</i>	38
3.2.2 Kaikaikaroro	38
<i>Plagioclase</i>	38
<i>Quartz</i>	38
<i>Amphibole</i>	39
<i>Orthopyroxene</i>	39
<i>Biotite</i>	39
<i>Fe-Ti Oxides</i>	39
3.2.3 Manawata	39
<i>Plagioclase</i>	40
<i>Quartz</i>	40
<i>Amphibole</i>	40
<i>Orthopyroxene</i>	40
<i>Biotite</i>	40
<i>Fe-Ti Oxides</i>	41
3.3 Waiteariki Ignimbrite	41
<i>Plagioclase</i>	41
<i>Quartz</i>	42
<i>Amphibole</i>	42
<i>Orthopyroxene</i>	42

<i>Biotite</i>	42
<i>Fe-Ti Oxides</i>	42
<i>Pumice</i>	44
<i>Groundmass</i>	44
3.4 Te Puna Ignimbrite	44
<i>Quartz</i>	44
<i>Plagioclase</i>	45
<i>Amphibole</i>	45
<i>Orthopyroxene</i>	45
<i>Secondary Mineral</i>	45
<i>Groundmass</i>	45
<i>Pumice</i>	46
<i>Fe-Ti Oxides</i>	46
<b>Chapter Four : Petrochemistry</b>	48
4.1 Introduction	48
4.2 Classification	48
4.3 Major Element Chemistry	55
4.3.1 Rhyolites	55
4.3.2 Waiteariki Ignimbrite	57
4.3.3 Te Puna Ignimbrite	57
4.4 Trace Element Chemistry	57
4.5 Spider Diagrams	61
4.6 Fe-Ti Geothermometry	66
<b>Chapter Five : Te Puna Ignimbrite</b>	68
5.1 Introduction	68
5.2 Distribution	68
5.3 Mineralogy	68
5.4 Stratigraphic Section	69
5.5 Geochemistry	69
5.5.1 Pumice geochemistry	72
5.5.2 Pumice geochemistry related to stratigraphic height	75
5.6 Inversion of the Magma Chamber	78
5.7 Previous studies into zoned magma chambers	80
5.8 Discussion	80

<b>Chapter Six Conclusions</b>	81
6.1 Tectonic Setting	83
6.2 Comparison of the Tauranga basin to other Volcanic Zones	86
6.3 Caldera Identification	87
6.4 Evidence for the Katikati Caldera	88
<b>References</b>	92
<b>Appendices</b>	101

## List of Figures

### Chapter One

Fig 1.1	Major physiography features of the study area	2
Fig 1.2	Location and generalised geology of the study area	3
Fig 1.3	Generalised geology of the Coromandel Volcanic Zone.	9

### Chapter Two

Fig 2.1	Manawata Rhyolite Dome	15
Fig 2.2	Kaikaroro Rhyolite Dome surrounded by the Waiteariki Ignimbrite.	15
Fig 2.3	Waiteariki Ignimbrite at Mc Laren Falls	17
Fig 2.4	Dacitic lithic within the Waiteariki Ignimbrite	17
Fig 2.5	Te Puna Ignimbrite overlying Lignite	19
Fig 2.6	Stratigraphic column of Te Puna ignimbrite overlying Lignite at Omokoroa Point	21
Fig 2.7	Stratigraphic column of Te Puna Ignimbrite	22
Fig 2.8	Te Puna Ignimbrite showing two flow units	23
Fig 2.9	Te Puna Ignimbrite lithics within the Te Puna Ignimbrite	23

### Chapter Three

Fig 3.1	Spherulitic Minden Peak Rhyolite containing phenocrysts	27
Fig 3.2	An-Ab-Or classification diagram for plagioclase	30
Fig 3.3	Amphibole compositions	32
Fig 3.4	Classification of pyroxenes	36
Fig 3.5	Al-Mg-Fe+Mn ternary diagram for biotite	35
Fig 3.6	Photomicrograph of Kaikaroro Rhyolite	36
Fig 3.7	Photomicrograph of Waiteariki Ignimbrite	43
Fig 3.8	Photomicrograph of Te Puna Ignimbrite	43
Fig 3.8A	Photomicrograph of Te Puna pumice	47
Fig 3.8B	Photomicrograph of Te Puna pumice crossed polarised	47

### Chapter Four

Fig 4.1	Classification of Western Tauranga basin rocks	51
Fig 4.2	Na <sub>2</sub> O+K <sub>2</sub> O vs SiO <sub>2</sub> diagram of rock types	52
Fig 4.3	Total alkali vs silica plot	53
Fig 4.4	AFM diagram of Western Tauranga basin rocks	54
Fig 4.5	Major element Harker diagrams	56
Fig 4.6	Trace element Harker diagrams	58
Fig 4.6	Trace element Harker diagrams continued	59

Fig 4.7A	Primitive mantle plot of representative samples.	62
Fig 4.7B	Chondrite mantle plot of representative samples.	63
Fig 4.7C	Primitive mantle plot comparisons to other areas	64
Fig 4.7D	Chondrite mantle plot comparisons to other areas	65

### Chapter Five

Fig 5.1	Stratigraphic section of Te Puna Ignimbrite on Clarke Rd	70
Fig 5.2	Major element Harker diagrams of Te Puna pumice	73
Fig 5.3	Trace element Harker diagrams of Te Puna pumice	74
Fig 5.4	Major elements vs stratigraphic height	76
Fig 5.5	Trace elements vs stratigraphic height	77
Fig 5.6	Inversion of a zoned magma chamber	79

### Chapter Six

Fig 6.1	Synoptic bathymetry and structure of souther Harve Trough - Bay of Plenty	84
Fig 6.2	Isostatic vertical gradient anomalies in the Tauranga area	89
Fig 6.3	Position of the proposed Katikati caldera	90

## List of Tables

### **Chapter One**

Table 1.1	Summarised stratigraphy and ages of the Tauranga basin	11
-----------	--	----

### **Chapter Two**

Table 2.1	Summarised stratigraphy of the Western Tauranga basin	13
-----------	---	----

### **Chapter Three**

Table 3.1	Modal data analyses of whole rock samples	28
Table 3.2	Representative microprobe analyses for plagioclase	29
Table 3.3	Representative microprobe analyses for amphiboles	31
Table 3.4	Representative microprobe analyses for biotite	31
Table 3.5	Representative microprobe analyses for orthopyroxenes	33

### **Chapter Four**

Table 4.1	Major and Trace element XRF analyses	49
Table 4.2	Major and Trace element XRF analyses	50
Table 4.3	Temperatures of Western Tauranga basin rocks	67

### **Chapter Five**

Table 5.1	Major and Trace element XRF analyses of Te Puna Pumice	71
Table 5.2	Comparison of incompatible trace element ratios	87

## *Chapter One*

# **Introduction**

# Chapter One

## Introduction

### 1.1 Introduction

The western Tauranga basin has never been studied to find out the local stratigraphy and geology. The current geological map which contains the area has become out-dated and the need for a new geological map has been realised. This lack of detailed local stratigraphy has led to geological mapping of the Tauranga basin in cooperation with the Bay of Plenty Regional Council (BOPRC) and previous MSc students.

### 1.2 Locality

The Tauranga basin is at the southern extent of the Hauraki Volcanic Region, which extends in a NNW direction from Poor Knights Island to beyond Tauranga. The Hauraki Volcanic Region consists of predominantly andesite-dacite volcanism in the mid-Miocene and rhyolite and ignimbrite volcanism more dominant in the late Miocene and Pliocene (Skinner 1986).

The Tauranga basin contains volcanic, fluvial and estuarine deposits. The basin is bounded by the Kaimai Range and Whakamarama Plateau in the west and the Papamoa Hills and the Mamaku Plateau to the south (fig 1.1).

### 1.3 Delineation of Field Area

The area studied consists of 115 km<sup>2</sup> of farmland, bush, horticulture, and residential areas. It is bounded to the north by the Tauranga Harbour, to the east by the Wairoa River and State Highway 29, and to the south by Ngamuwahine Road (fig 1.2).

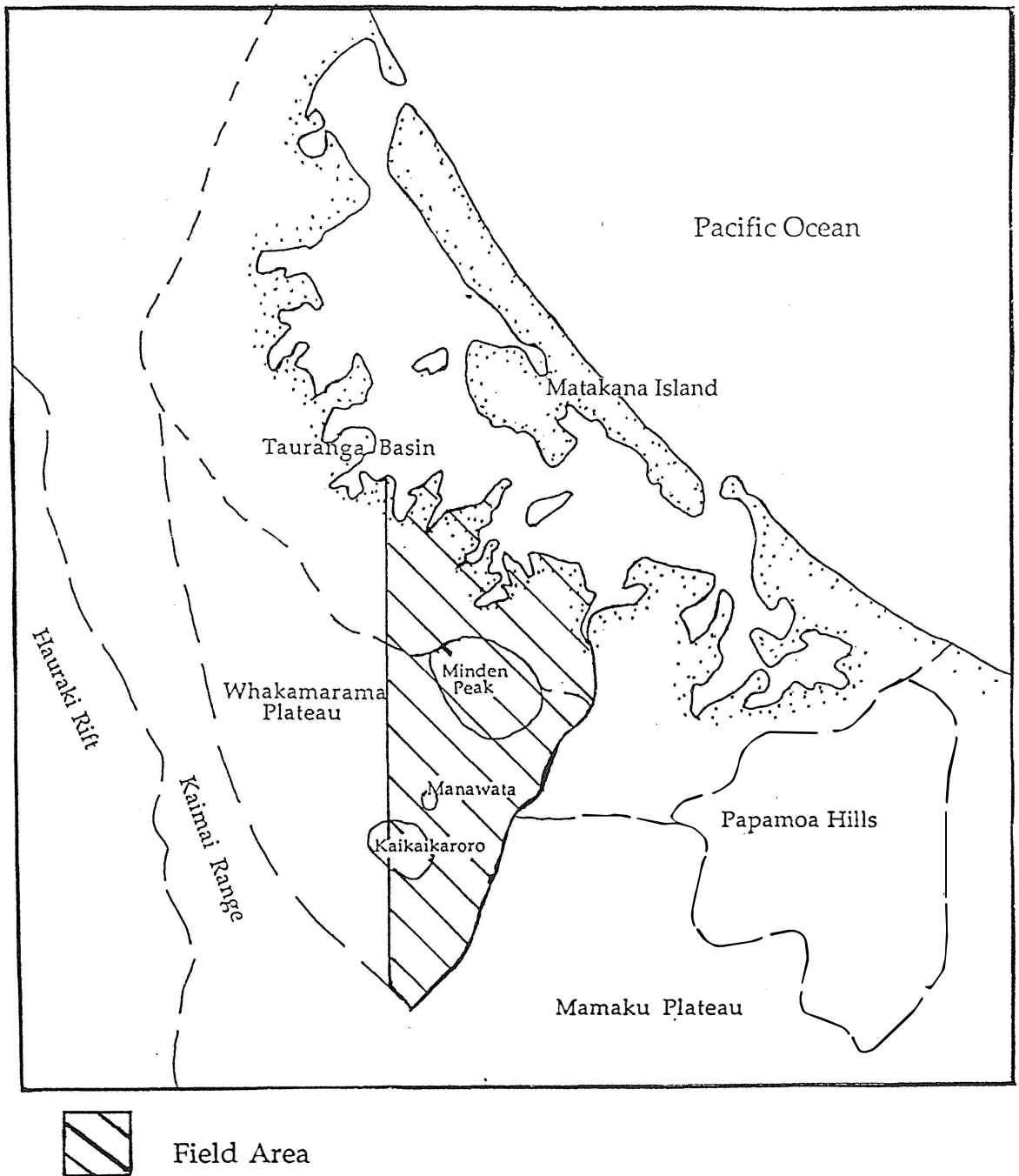
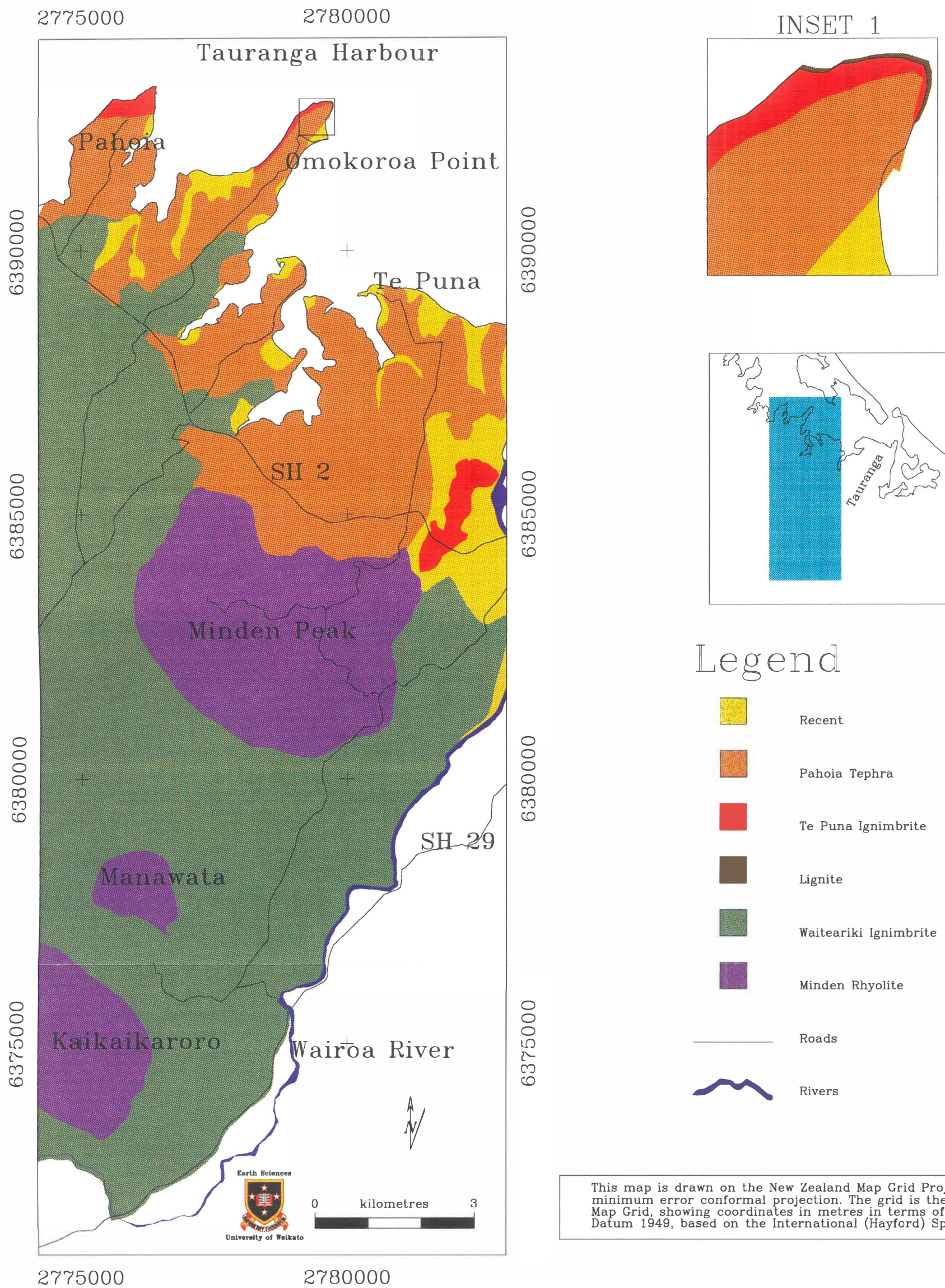


Fig 1.1 Major physiography features of the study area.



This map is drawn on the New Zealand Map Grid Projection, a minimum error conformal projection. The grid is the New Zealand Map Grid, showing coordinates in metres in terms of the Geodetic Datum 1949, based on the International (Hayford) Spheroid.

Fig 1.2 Location and Geology of Field Area.

## 1.4 Physiography of the Area

The dominant physiographic landform in the field area is the Whakamarama Plateau which dips 8-14°NE into the Tauranga basin (Harmsworth 1983). The plateau consists of the Waiteariki Ignimbrite which flowed around Minden Peak. The Waiteariki Ignimbrite becomes increasingly incised northeastward. It may once have extended further into the Tauranga Harbour, but over time it has been eroded back, forming the north-east trending peninsulas along the coastline.

The other major features are northeasterly aligned rhyolite domes, Kaikaikaroro, Manawata and Minden peak (fig 1.2). Kaikaikaroro (U14 746750) is a bush covered dome with a height of 444 m at the southern extent of the field area. The vegetation and rugged relief make access difficult and outcrops are confined to stream beds. To the northeast, Manawata (U14 762782) is a 317m dome which is covered by forest and farmland. Outcrops are highly weathered and confined to stream beds or as fallen boulders. Minden peak (U14 786832) at a height of 286m, is a flat topped rhyolite dome with lava flows. In places the rhyolite is weathered and has become highly unstable resulting in landslides, more recently in December 1983 and January 1986.

To the north of Minden peak, peninsulas which extend into the harbour, are covered by tephras up to 20m thick. The predominant unit is the Pahoia Tephra which contains thin pyroclastic flow deposits which are intercalated with white pumiceous fluvial sediments (Harmsworth 1983). The Pahoia Tephras are exposed around most of the coastline and are highly weathered. The weathering of the tephras to clay has resulted in a landslip at Omokoroa in 1979.

## 1.5 Previous Literature

The Hauraki Volcanic Region was first studied in the mid 19<sup>th</sup> Century due to an interest in mining in the region. The first geological and detailed investigations into the region was commissioned by the Geological Survey Branch of the Department of Mines. This resulted in the publication of bulletins which outlined the geology and economic value of the region (Fraser & Adams 1907, Fraser 1910, Henderson & Bartrum 1913, Morgan 1924).

Henderson and Bartrum (1913) studied the Aroha subdivision, which included the Tauranga basin. They produced a geological map of the area, and divided the rock types into series dependent on lithological and petrographic criteria. This also included a detailed study of the sediments in the area, mainly the Tauranga beds.

The Tauranga beds consist of conglomerates, sandstones and clays. Towards the base of the series there are seams of lignite which are at their thickest at Omokoroa, being measured at 4.27 m. They concluded that the coal-forming vegetation accumulated in place in elongated estuary-like depressions.

In 1963 geological investigations in the Kaimai Range resulted in the selection of an area for a tunnel linking Waharoa in the Hauraki Depression with Apata in the Tauranga basin. Healy (1967) produced a detailed study of the volcanic rocks of the area as part of a report investigating the proposed Kaimai Tunnel. Healy found that on the eastern side of the range, andesites were overlain by a series of younger ignimbrite sheets, pumice breccias, tuffs and interlayered sediments which slope down into the Tauranga basin (Ministry of Works and Development 1976).

Healy et al. (1964) mapped the geology of the Rotorua area which includes the Tauranga basin. They divided their rock types further based on lithology and composition. They separated the Waiteariki Ignimbrite from the dacites and likened it to the Papamoa Ignimbrite of similar age and composition.

Geophysical data of the Tauranga basin is presented in map form by Woodward and Ferry (1973) on the Isostatic Vertical Gradient Anomalies, Bouguer Anomalies and Isostatic Anomalies, and by Hunt and Whiteford (1979) on Magnetic Anomalies.

Stability investigations at Omokoroa and Minden Peak areas has been undertaken by Tonkin and Taylor (1991). Detailed investigation on the slope stability of Minden Peak found that the weathered rhyolite was prone to instability.

Known ages of the rocks within the Tauranga basin are limited. Stipp (1968) were determined potassium-argon ages of two andesites 2.95 Ma and 2.54 Ma for Beesons Island Volcanics in the Papamoa Hills. Kohn (1973) determined by Fission Track methods ages on the Waiteariki Ignimbrite at  $0.84 \pm 0.11$  Ma and the Aongatete Ignimbrite at  $0.86 \pm 0.14$  Ma. Rutherford (1978) determined an age of  $4.34 \pm 0.3$  by fission track methods at Mt

Maunganui. Kamp and Turner (pers com 1994) examined the magnetism of the Te Puna Ignimbrite and found that it was reversely magnetised and that is likely to be Matuyama reversed which indicates that it is older than 0.78 Ma.

Houghton and Cuthbertson (1989) produced a detailed geological map of the Kaimai Range which is adjacent to the area studied. This included a detailed description of rock units which are also present in the field area. A new subgroup was established, the Kaimai Subgroup which previously included the Beeson Island Volcanics, Waitawheta Dacites and Omaha Andesites. The petrographic subdivision into a dacitic and an andesitic formation was not sustainable as both lithologies occurred throughout the stratigraphic sequences.

They also established the Whakamarama Group, which are mid Pleistocene ignimbrites forming the Whakamarama plateau. This new group includes the Aongatete and Waiteariki Ignimbrites. The Te Puna Ignimbrite should now be included as it is a mid-Pleistocene ignimbrite which is at the northern end of the Whakamarama plateau.

Recently, detailed investigations of the geology of the region have been researched by MSc students. Morgan (1986) studied the geology of the Northern Mamaku Plateau. This was extended northwards by Hughes (1993) whose area included the Papamoa Ranges and eastern Tauranga Basin. Harmsworth (1983) studied the Quaternary stratigraphy of the Tauranga Basin. Bird (1981) studied the nature and causes of coastal landsliding on the Maungatapu peninsula within Tauranga.

## 1.6 Objectives of Thesis

- 1 To produce a geological map and ascertain the stratigraphic relations of the rocks in the Minden area, western Tauranga basin.
- 2 Study the field relationships and physical volcanology of local eruptives and investigate their possible source, emplacement processes, and relationship to each other.
- 3 Use laboratory methods to characterise the petrography, mineral chemistry, and whole-rock major and trace element geochemistry of the rocks in the Minden area.

- 4 To describe the nature and chemistry of the Te Puna Ignimbrite in detail.
- 5 To examine how the Tauranga basin relates to the Taupo Volcanic Zone and Coromandel Volcanic Zone.

## 1.7 Regional Geology

The Tauranga basin is located at the southern extent of the Hauraki Volcanic Region. It is also within the Central Volcanic Region (CVZ) based on maps of the New Zealand Geological Survey (NZ Geo. Surv. 1972,1973) which includes all Quaternary rhyolites within the region. The basin represents a transitional zone where rock types show characteristics of both the Hauraki Volcanic Region and the Taupo Volcanic Zone and where andesite ages indicate an apparent southeast migration with time (Stern 1986).

The NNW trending peninsula of the HVR is the result of the horst-graben nature of the basement rocks which have been overlain by Neogene arc volcanism. These NNW-striking faults are cross cut by NE-striking faults all along the Hauraki Volcanic Zone (Skinner 1986).

Northeasterly faults were mapped in the Tauranga basin between Tauranga and Te Puke by Healy et al. (1964) which are thought to link up to offshore faults. The NE-striking faults are almost all downthrown to the south progressively, lowering the Jurassic basement (Skinner 1986). This has resulted in no surface expression of the Jurassic basement in the Tauranga basin.

## 1.8 Regional Stratigraphy and Petrography

The Coromandel Volcanic Zone consists of the Coromandel and Kaimai Ranges. The CVZ varies in composition from basaltic to rhyolitic with a basement of late Jurassic Marine sedimentary rocks (Manaia Hill Group) (Fig 1.3) (Skinner 1986).

The stratigraphy within the Tauranga Basin is summarised in Table 1, and includes ages of dated units.

### *Coromandel Group*

The Coromandel Group ranges in composition from basic andesite to rhyodacite (Skinner 1986). Within the Tauranga basin, near the Papamoa range, the Beeson Island Volcanics outcrops as flows and centres. The Beeson Island Volcanics belong to the Kuaotunu Subgroup of the Coromandel Group. They are mid-Miocene to late Miocene with K-Ar ages of 16-7 Ma (Rutherford 1978, Cole 1979, Skinner 1986, 1993). These rocks are andesitic-dacitic in composition, characterised by hornblende - hypersthene  $\pm$  augite  $\pm$  biotite.

### *Whitianga Group*

The Whitianga Group includes the Minden Rhyolite Subgroup. This subgroup includes all hypersthene, hornblende and biotite rhyolites within the Coromandel-Bay of Plenty area, north of the Taupo Volcanic Zone (Houghton et al. 1989). Minden rhyolite outcrops as domes and flows within the Tauranga basin.

### *Whakamarama Group*

The Whakamarama Group is defined by Houghton and Cuthbertson (1989) as mid Pleistocene ignimbrites forming the Whakamarama plateau. It includes the Aongatete and Waiteariki Ignimbrite which are dacitic to andesitic. The Te Puna Ignimbrite should now be classed within the Whakamarama group as it is of mid-Pleistocene age of  $>0.78$  Ma (Kamp and Turner; pers com 1994) and it is at the northern extent of the Whakamarama plateau.

The Aongatete is a crystal poor ignimbrite with a high abundance of crystal-poor dacitic pumice. The crystals are andesine/labradorite-hypersthene-augite (Houghton and Cuthbertson 1989). It exceeds 490m thickness beneath the Tauranga basin.

The Waiteariki Ignimbrite overlies the Aongatete Ignimbrite. It is crystal-rich with plagioclase-hornblende-hypersthene-quartz-biotite-zircon. It has dacitic pumice which are cream, or black within the lenticular zone.

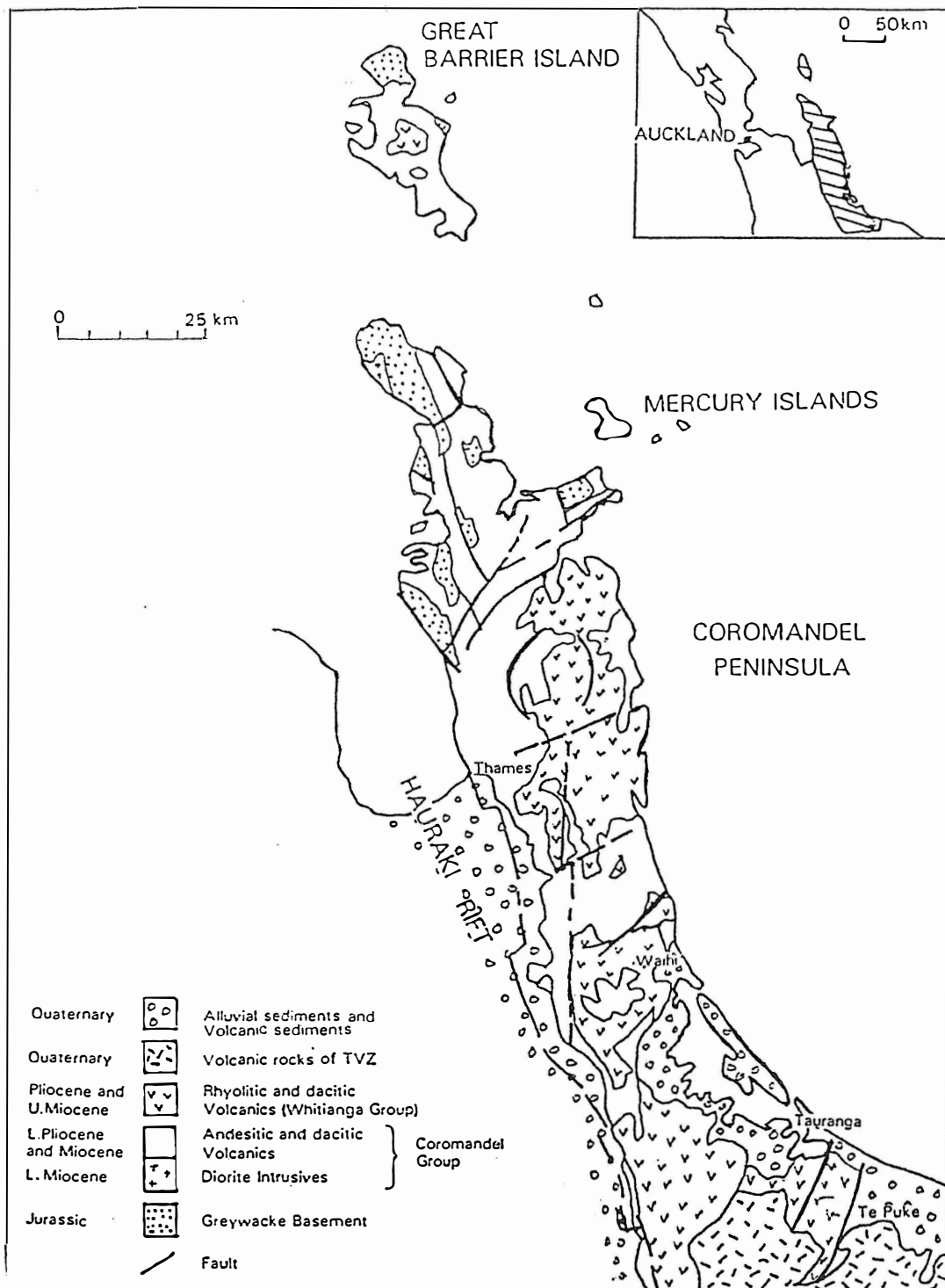


Fig 1.3 Generalised geology of the Coromandel Volcanic Zone (after Skinner 1986, Brathwaite 1989).

The Papamoa Ignimbrite is an informal member of the Whakamarama Group as it is of similar age to the Waiteariki Ignimbrite and also of dacitic composition (Houghton et al. 1989). It outcrops in the north-eastern sector of the Tauranga basin and consists of a lower layer which has a brown to yellow-tan matrix with protruding pumice of varying colours and mineralogy and an upper dense cream to grey rock with small white angular pumice (Hughes 1993).

### *Tauranga Group*

The Tauranga Group includes late Cenozoic deposits found in the Bay of Plenty, Hauraki lowland, Hamilton lowland, Lower Waikato and Manukau Harbour. It is made up of mainly pumiceous, terrestrial, estuarine and marine sediments (Kear and Schofield, 1978)

These units belong to the Matua Subgroup within the Tauranga Basin. It includes all Pleistocene sediments that overlie the Waiteariki Ignimbrite, which includes fluvial, estuarine strata, ignimbrites and airfall tephra (Harmsworth 1983).

The ignimbrites within the Tauranga basin are the Wairoa, Te Ranga, Waimakariri, Ohauiti, Kopurereroa and Merrick Ignimbrites (Harmsworth 1983, Hughes 1993). These ignimbrites are generally not found outside of the Tauranga basin.

Table 1.1 Summarised stratigraphy and ages of the Tauranga Basin after Healy et al. (1964), Stipp (1968), Kohn (1973), Rutherford (1978), Murphy and Seward (1981), Fransen (1982), Harmsworth (1983), Houghton and Cuthbertson (1989) Kohn et al. (1992), Hughes (1993), Kamp and Turner (pers com 1994).

Group Subgroup	Formation	Age	Comments
Rotorua	TVZ Tephtras		Widespread, thick deposits
	Mamaku Ig.	0.14± 0.08Ma	Thick, mantle deposit
	Merrick Ig.		
Tauranga Group Matua	Waimakariri Ig.	0.18 Ma	Large pumice, crystal rich
	Hamilton Ash	0.35 ±0.04 Ma	
	Pahoia Tephtras		Highly weathered tephtras and paleosols
	Kopurereroa Ig.		nonwelded
	Te Ranga Ig.		Sandy, nonwelded
	Ohauti Ig.		nonwelded
	Wairoa Ig. Fluvial		nonwelded gravels and sands
Whakamarama	Te Puna Ig.	>0.78 Ma	non to partially welded
	Waiteariki Ig.	0.84 ± 0.11 Ma	Dacitic, crystal rich
	Papamoia Ig.		Southern area of basin only
	Aongatete Ig.	0.86 ± 0.14 Ma 0.94 ± 0.13 Ma	Breccia Dacitic Tuff
Coromandel	Andesites	2.54 + 2.95 Ma	Flows and Strato Volcanoes
Coromandel Dacites	Dacites		Domes and Flows
Whitianga Minden Rhyolite	All Rhyolites in Coromandel Volcanic Zone	4.34 ± 0.38 Ma	Spherulitic domes and flows

*Chapter Two*

# Stratigraphy

# Chapter Two

## Stratigraphy

### 2.1 Introduction

The Western Tauranga basin is confined to the west of the Kaimai Range which is made up of rhyolitic, dacitic, and andesitic rocks. Within the basin the oldest exposed rocks are rhyolites which form dome complexes. These have been surrounded by the Aongatete and the Waiteariki Ignimbrites, of which only the Waiteariki is aerially exposed within the field area. These two ignimbrites are believed to have originated from the Kaimai Range.

After a period of time and erosion another ignimbrite was deposited, the Te Puna Ignimbrite. This was then followed by the deposition of the Pahoia Tephra, and late Pleistocene tephra which were derived from the Taupo Volcanic Zone.

Summarised stratigraphy of the western Tauranga basin is shown in Table 2.1.

### 2.2 Minden Rhyolite

Minden Rhyolite includes all hypersthene, hornblende and biotite rhyolites within the Coromandel-Bay of Plenty area, north of the Taupo Volcanic Zone (Houghton et al 1989). Rhyolitic volcanism is mainly attributed to single explosive centres and is usually associated to caldera formation, so grouping all rhyolites that occur in the Bay of Plenty and Coromandel together is not considered appropriate. Therefore rhyolites will be referred to by their apparent source as proposed by Hughes (1993). Rhyolites within the field area will be referred to as Minden Peak, Manawata and Kaikaikaroro.

#### *Age*

Manawata, Kaikaikaroro and Minden Peak are older than the overlying Whakamarama Group.

Table 2.1 Stratigraphy of the western Tauranga basin. Ages from Stipp (1968), Pullar et al. (1972), Kohn (1973) Rutherford (1978), Froggatt and Lowe (1990), Kohn et al. (1992), Kamp and Turner (pers com 1994).

<u>Group</u>	<u>Unit</u>	<u>Age</u>	<u>Lithology</u>
	Recent		Fluvial sediments and volcanic gravels and sands
	Taupo Tephra	1819 ± 17 yrs BP	Rhyolitic
	Mamaku Tephra	7250 ± 20	Rhyolitic
	Rotorua Tephra	12000	Rhyolitic
	Okareka Tephra	18000	
	Oruanui Tephra	19850 ± 310 yrs BP	Rhyolitic
	Mangaone Tephra	27730 ± 350	
	Rotoehu Ash	41700 ± 3500 yrs BP	Rhyolitic
	Hamilton Ash	35000 ± 0.04 yrs	
	Pahoia Tephras	300000 yrs	Rhyolitic
Tauranga Group -Matua subgroup	Fluvial sediments		Sediments containing volcanic gravels, sands and ash.
	Lignite	<0.78 Ma	Contains visible plant structures.
Whakamarama Group	Te Puna Ignimbrite	> 0.78 Ma	Crystal-rich rhyolitic ignimbrite with white and grey pumice.
	Waiteariki Ignimbrite	0.84 ± 0.11 Ma	Crystal-rich dacitic ignimbrite with cream and black pumice.
	Aongatete Ignimbrite	0.86 ± 0.14 Ma 0.94 ± 0.13 Ma	Crystal-poor dacitic ignimbrite with crystal poor dacitic pumice.
Whitianga Group -Minden Rhyolite	Manawata Kaikaikaroro Minden Peak		Grey spherulitic rhyolites with visible plagioclase, hornblende and quartz.

### *Source and distribution*

Within the Tauranga basin these rhyolites outcrop as dome and flow complexes. The domes have a linear relationship in a north-northeasterly direction, which suggests that their locations are fault related, possibly within the basement rocks.

The domes are steep sided complexes with few exposures which are limited to road cuttings and the Te Puna Quarry (U14 788842) in Minden Peak. The degree of weathering ranges from unweathered in places to highly weathered. No unweathered outcrops were found on Manawata.

### *Lithology*

Minden Peak Rhyolite is predominantly grey but also varies from cream to pink. Visible hornblende, biotite, quartz and plagioclase can be seen in hand specimen, and grain size is less than 2 mm. The rhyolite is spherulitic, and upon weathering the rock structure disintegrates. Flow banding can be seen on Minden Road, indicating flowage down the side of the dome.

Manawata Dome is a steep sided dome complex with a flat top (Fig 2.1). It is surrounded by the Waiteariki Ignimbrite, which suggests that it is older than the ignimbrite which flowed around it. Also where streams have incised the Waiteariki Ignimbrite around the dome, Manawata Rhyolite is exposed. The Manawata Rhyolite is also light grey and contains phenocrysts of quartz, plagioclase, hornblende and biotite within a spherulitic groundmass.

Kaikaikaroro Dome is thought to be older than the Waiteariki Ignimbrite ( $0.84 \pm 0.11$  Ma)(Kohn 1973) which overlies it. Kaikaikaroro (U14 746750) is a steep sided volcano and is surrounded by the Waiteariki Ignimbrite. Access is difficult due to the rugged terrain and bush cover (Fig 2.2). It is light grey and contains phenocrysts of quartz, plagioclase (up to 7 mm), hypersthene and hornblende (up to 5mm), surrounded by a spherulitic groundmass containing Fe-Ti oxide and zircon.



Fig 2.1 The Manawata Rhyolite dome (covered in pine trees) viewed from the east, surrounded by undulating hills underlain by the Waiteariki Ignimbrite.



Fig 2.2 View to the north, showing bush covered Kaikaikaroro Rhyolite(Kai) dome surrounded by Waiteariki Ignimbrite(Wai).

## 2.3 Waiteariki Ignimbrite

The Waiteariki Ignimbrite was first named by Healy et al. (1964). It belongs to the Whakamarama Group, which includes all mid-Pleistocene ignimbrites forming the Whakamarama plateau (Houghton and Cuthberton 1989).

### *Age*

The Waiteariki Ignimbrite is reversely magnetised (Cox 1969) and has a fission track age of  $0.84 \pm 0.11$  Ma (Kohn 1973).

### *Distribution*

The Waiteariki Ignimbrite is an extensive unit. It forms the dipping Whakamarama Plateau and underlies the Tauranga basin to depths of 50-100m. It was deposited prior to the uplift of the Kaimai Range as it is displaced by the Hauraki and Okauia faults into the Hauraki plains where it has been located in drill holes at a depth of 55m (Davidge 1982).

### *Lithology*

The Waiteariki Ignimbrite is 220m thick at its type section (T14 641797), where it can be divided into three flow units:

- 1 a soft non-welded to welded top between 50 and 70 m thick with extensive vapour phase alteration of pumice to cristobalite and alkali feldspar;
- 2 up to 150m of welded material containing alternatively moderately densely welded and very densely welded glassy lenticular zones;
- 3 a 3 to 5m thick nonwelded base consisting of pumiceous tuff breccia and ash (Houghton et al. 1989).

The Waiteariki Ignimbrite is a light grey-brown ignimbrite with 20% pumice which varies from lenticular cream pumice to black fiamme. It is densely welded with columnar jointing seen in outcrops (Fig 2.3). The Waiteariki Ignimbrite is unusually crystal rich with 30% crystals of plagioclase, quartz, hornblende, hypersthene and biotite.



Fig 2.3 The middle flow unit of the Waiteariki Ignimbrite at McLaren Falls showing columnar jointing.



Fig 2.4 Dacite lithic within the lower flow unit of the Waiteariki Ignimbrite at Ngamuwahine Road (U14 733737).

Lithics within the unit are dacitic. These lithics at Ngamuwahine Road (U14 736732) are large, up to 30 cm, indicating proximity to source (Fig 2.4).

In the basal part of the unit, co-eruptive lithics or lithics from the previous flow unit, can be found within the flow. This may suggest that an earlier flow unit may have been deposited before the main unit. This could have resulted in the incorporation of the lithic into the following flow

### *Welding*

The Waiteariki Ignimbrite becomes increasingly welded to the south. This results in a change in appearance from a soft pinky brown nonwelded ignimbrite in the north, to a dark brown welded ignimbrite in the south.

In the southern region of the field area, the Waiteariki Ignimbrite shows higher degrees of welding and post-eruptive devitrification. Samples at McLaren Falls contain spherulites which are thought to occur as the result of devitrification (Lofgren 1970). Where welding is greatest, the ignimbrite has a eutaxitic texture defined by fiamme.

## **2.4 Matua Subgroup**

### *Lignite*

Lignite is within the Matua Subgroup which includes all Pleistocene sediments which overlie the Waiteariki Ignimbrite within the Tauranga Basin (Harmsworth 1983). The lignite is exposed within the field area at Omokoroa Point and Te Puna estuary. It is also found at Matakana Island and Motuhoa Island. It underlies the Te Puna Ignimbrite at Omokoroa Point (Fig 2.5) and therefore is thought to be older than the Te Puna Ignimbrite (>0.78 Ma) (Kamp and Turner, pers com 1994). The lignite is black with plant structures, such as branches and logs still visible. At Omokoroa Point large ring like structures up to 3m in diameter may represent residual tree stumps.

The significance of the lignite is that it is a potential paleoenvironmental indicator. Hull (1977) suggests that the swamp from which the lignite formed grew at temperatures 3°C lower than at present with annual precipitation 800 to 900 mm higher than the present 1348mm per year.

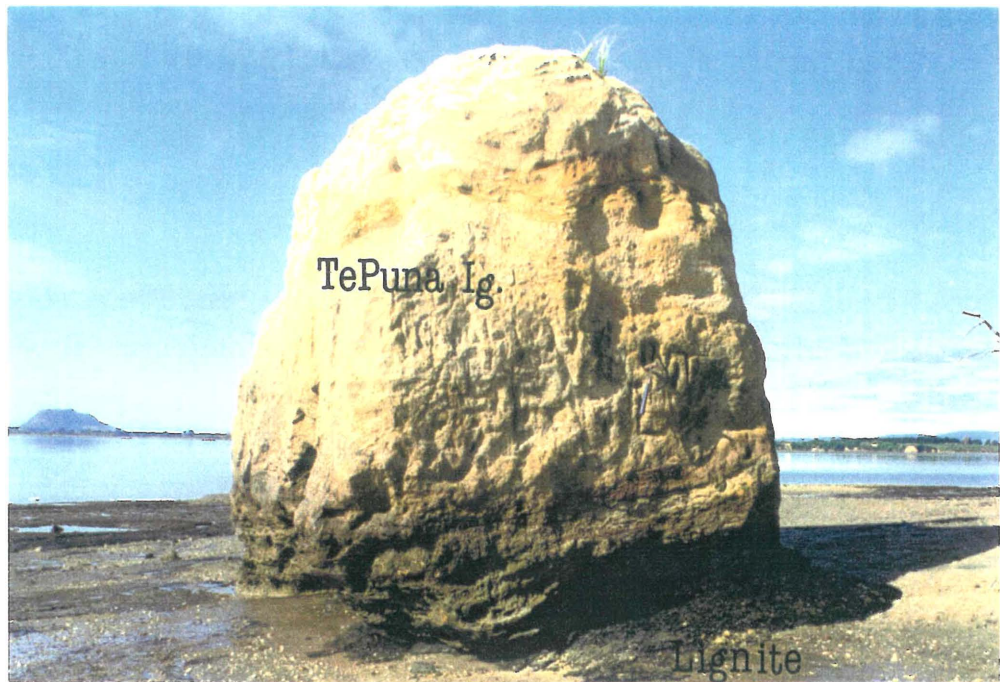


Fig 2.5 Te Puna Ignimbrite at Omokoroa Point overlying Lignite.

### *Fluvial Sediments*

Fluvial Sediments within the western Tauranga basin are predominantly pumiceous clays, sands and gravels. These fluvial beds are moderately to well sorted and commonly show cross-bedding.

The source of this material is from a volcanic terrain which has been eroded into the Tauranga basin. The clasts are mainly derived from previous pyroclastic flows, the Te Ranga Ignimbrite, Waimakariri Ignimbrite and Te Puna Ignimbrite, and airfall material mainly the Pahoia tephra (Harmsworth 1983).

## 2.5 Te Puna Ignimbrite

The Te Puna Ignimbrite was first described by Harmsworth (1983). It is exposed on Clarke Road (U14 825855) and in coastal sections at Omokoroa, at Pahoia Point where it forms the coastal cliffs, and also on Matakana Island.

### *Age*

The Te Puna Ignimbrite has not been radiometrically dated. Primary magnetisation within the ignimbrite is reversed which means that it is likely to be Matuyama reversed, and is therefore older than 0.78 Ma (Kamp and Turner pers com).

### *Lithology*

The Te Puna Ignimbrite is a nonwelded to partially welded buff brown ignimbrite. It contains 15-20% white to grey pumice which contains glomeroporphyritic plagioclase and quartz. The matrix of the ignimbrite is crystal-rich (25%) with visible plagioclase, quartz and hornblende.

Lithic abundance is poor (1-2%) and lithic types consist of grey, red, and green rhyolites. Also present is charcoal and the occasional lithic of obsidian.

The Te Puna Ignimbrite varies in thickness from >16 m at Clarke Road to 2 m at Omokoroa Point to 10 m at Pahoia Point. This variation in thickness is due to the undulating nature of the pre-existing topography and subsequent erosion.

At Omokoroa (U14 797928), the unit overlies lignite and fluvial pumice beds, which suggests that the ignimbrite flowed into a swamp or estuarine environment (Fig 2.6). The fluvial pumice beds may have resulted from plinian eruptions which occurred before the main ignimbrite forming eruption. The presence of chalazoidites and elutriation channels within the ignimbrite indicate that the eruption was high in water content. On Matakana Island lake sediments overlie the Te Puna Ignimbrite. These lake sediments may represent an intracaldera lake which formed after the eruption of the ignimbrite which caused the caldera collapse.

The Te Puna Ignimbrite contains a lithic-rich layer of rhyolite lithics up to 40mm in length and Te Puna Ignimbrite lithics (Fig 2.7, 2.8). The ignimbrite lithics are subrounded and up to 105 mm in length (Fig 2.9). The presence of Te Puna Ignimbrite lithics at the boundary between the two flow units, indicates two phases in the eruption, where the second pyroclastic flow incorporated ripped up ignimbrite lithics from the previous flow. Transportation of these reworked clasts resulted in their subrounded nature. The increase in rhyolite lithics at the flow unit boundary may represent a widening of the vent by

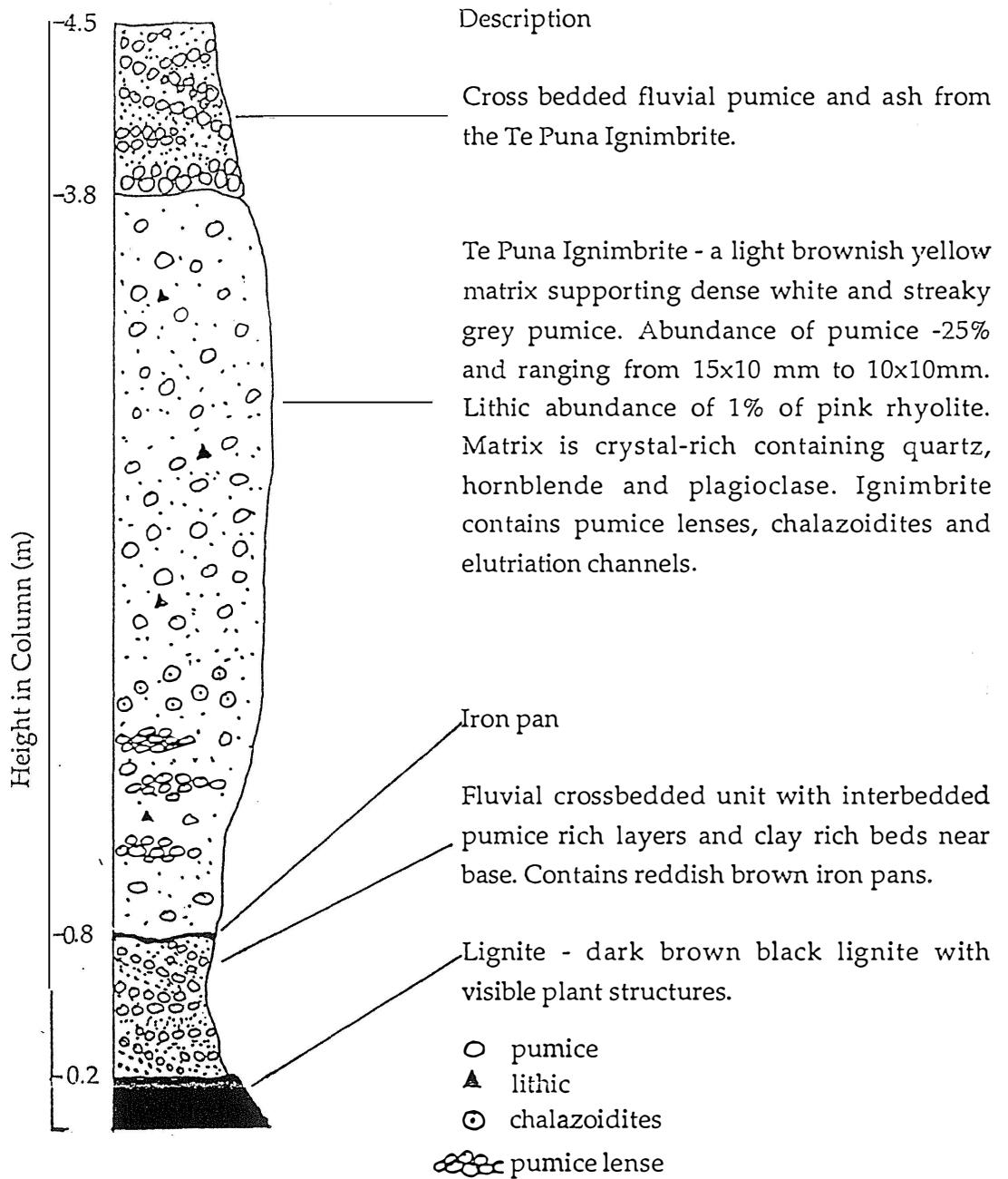


Fig 2. 6 Stratigraphic column of Te Puna Ignimbrite overlying lignite and fluvial material of the Tauranga Group, Omokoroa Point (U14 798928).

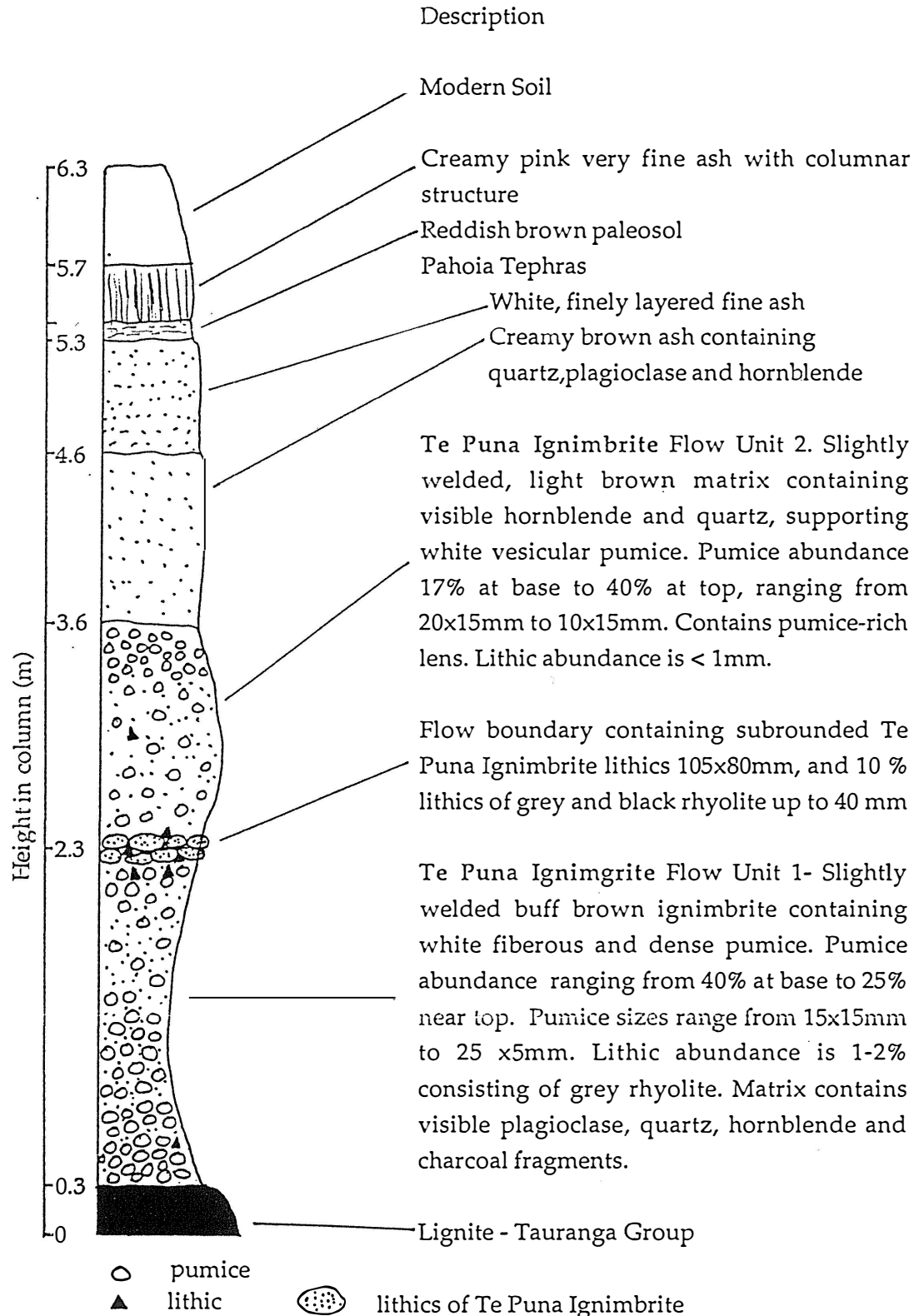


Fig 2.7 Stratigraphic column of Te Puna Ignimbrite and overlying ash beds at Omokoroa Point, U14 798927.

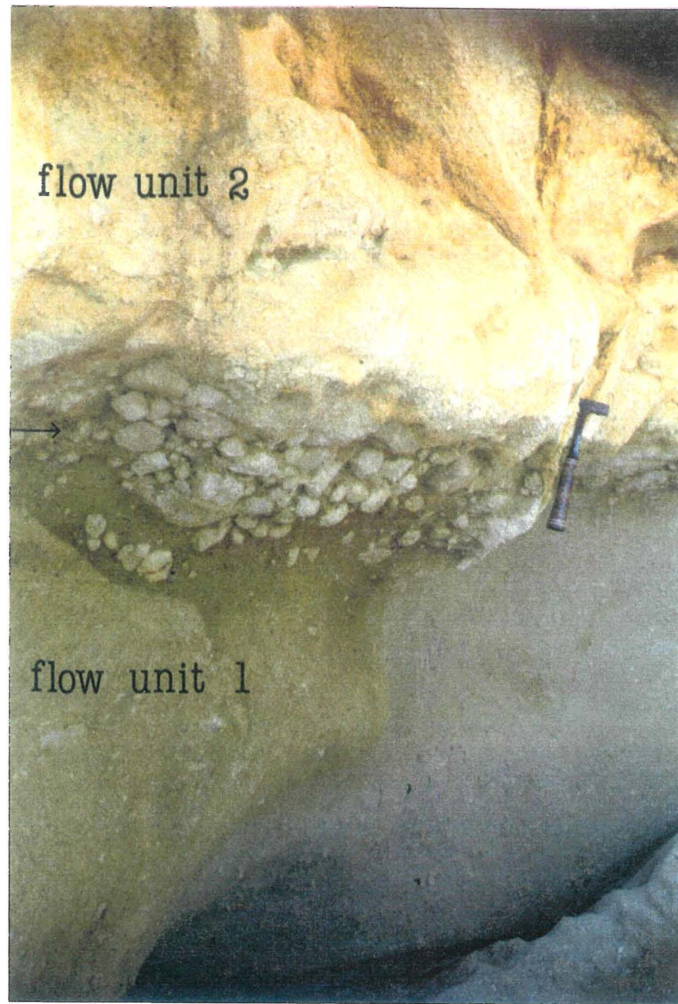


Fig 2.8 Te Puna ignimbrite lithics within the Te Puna Ignimbrite.



Fig 2.9 Subrounded Te Puna Ignimbrite lithics and Rhyolite lithics within the Te Puna Ignimbrite.

erosion. This increase in lithic abundance in the stratigraphic column can also indicate the time at which caldera collapse occurred.

## 2.6 Tephtras

Within the field area a number of tephra layers can be recognised. The thickest and most distinctive is the Pahoia Tephtras which underlies the Rotoehu and Hamilton Ash. Pullar et al (1973) also identified other less distinctive Holocene tephtras at Pahoia. They are; Mangaone Tephtra, Oruanui Tephtra, Okareka Tephtra, Rotorua Tephtra, Mamaku Tephtra, Taupo Tephtra, and Kaharoa Tephtra.

### *Pahoia Tephtras*

The Pahoia Tephtras are strongly weathered white and olive coloured tephtras which range in average thickness from 10-20 m. The Pahoia Tephtras unconformably overlie the Te Puna Ignimbrite at Clarkes Road, Omokoroa and Pahoia Point. Pullar et al. (1973) suggested an age range of 125 000 to 300 000 yr BP .

The Pahoia Tephtras are rhyolitic, normally graded, show shower bedding, and also contain thin (< 2m ) ignimbrites and interbedded paleosols. At Omokoroa Point 14 beds are informally named with upper contacts defined by colour and slight textural changes or by pale brown clay rich paleosols (2 to 15 cm thick) (Harmsworth 1983).

### *Hamilton Ash*

The Hamilton Ash Formation in the Tauranga Basin forms a thick (> 0.9m) yellow brown to dark reddish brown deeply weathered sequence in which paleosols are developed. At Omokoroa this sequence is 2.5 m thick while at Te Puna it is < 1.2 m (Harmsworth 1983). It can also be seen on the Whakamarama Plateau, in road cuttings, lying above the Waiteariki Ignimbrite. It has an age of 75000-150000 yrs BP (Pullar et al. 1973).

*Rotoehu Ash*

The Rotoehu Ash was first named by Healy et al. (1964). The tephra was erupted from the Okataina centre and is associated with the Rotoiti Breccia. It has an age of  $64 \pm 4$  ka (Wilson et al. 1992) and is at the base of the Quaternary tephra column. The bed shows prominent shower bedding and it is crystal rich with a calc-alkaline phenocryst assemblage.

*Chapter Three*

**Petrography  
and  
Mineralogy**

# Chapter Three

## Petrology and Mineralogy

### 3.1 Introduction

Petrography of the western Tauranga Basin was studied from 68 representative rock samples taken from the field area. Modal data was obtained from representative thin sections by point counting methods (Table 3.1). Polished sections were prepared for eleven selected samples of which the mineral chemistry was investigated by microprobing at the Department of Geology, University of Auckland. Representative chemical analyses of minerals are in Table 3.2, 3.3, 3.4, 3.5.

### 3.2 Rhyolites

There are three rhyolite domes, Minden Peak, Kaikaikaroro and Manawata, within the field area. Petrographically they are very similar, with phenocrysts of quartz, plagioclase, orthopyroxene, amphiboles, and biotite.

#### 3.2.1 Minden Peak

Minden Peak rhyolite is a grey to pink hypocrySTALLINE rock with medium (1-2mm) grain size. It has phenocrysts of plagioclase, quartz, hornblende and biotite set in a spherulitic groundmass (Fig 3.1), where spherulites have diameters of 1-2mm. Flow banding, where present, is defined by a variation of the matrix from pink to grey.

With weathering the rock varies in colour from cream to pink to grey. Weathering of the rhyolite between the spherulites can cause the spherulites to become detached and result in the disintegration of the structure of the rock.

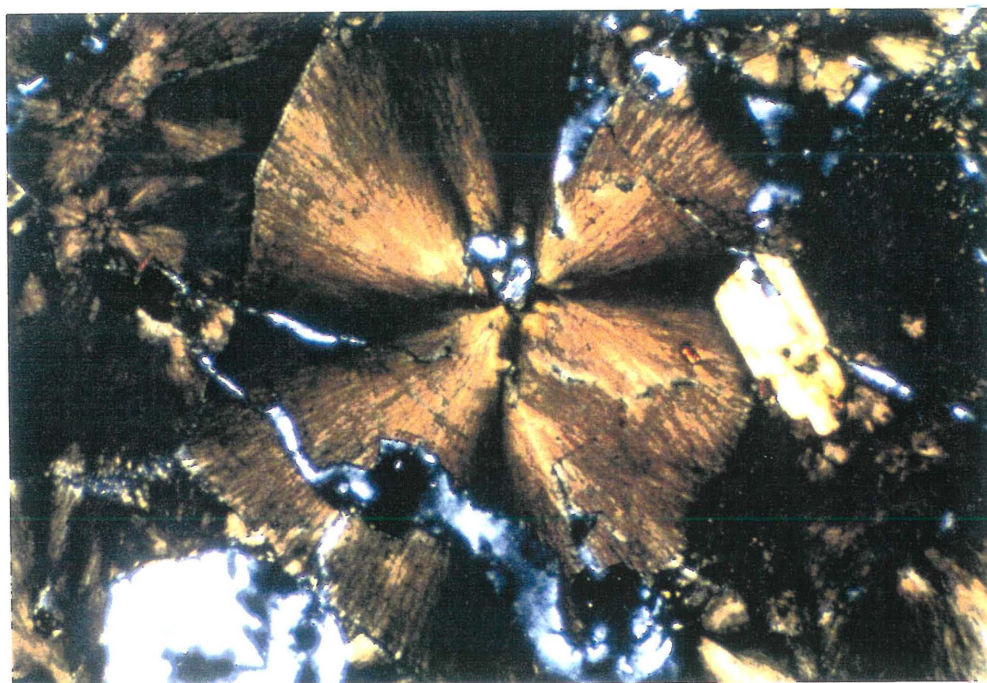


Fig. 3.1 Photomicrograph of Minden Peak rhyolite showing spherulites radiating out from a quartz grain and interstitial to hornblende, X40 magnification, crossed polarised light.

Table 3.1 Modal analyses of whole rock samples from the Western Tauranga Basin

Unit	Rock type	Sample No	matrix %	Plag. %	Quartz %	Hrnblde %	Biotite %	Hyper. %	Opagues %	Zircon %	Pumice %	Sec.Min %	Lithics %
Minden	rhyolite	6	81.2	11.2	4.8	1	1.4	0	0.2	0	0	0	0
Minden	rhyolite	7	89	8	0.2	1.2	1.6	0	0	0	0	0	0
Kaikaikaroro	rhyolite	13	60	26.2	7.2	4	0	1.4	0.8	0.4	0	0	0
Kaikaikaroro	rhyolite	14	59.2	31.8	1	3.6	0.2	2.8	1.2	0.2	0	0	0
Manawata	rhyolite	15	86	9	0.4	2.4	1.4	0	0.8	0	0	0	0
Manawata	rhyolite	16	91.2	4.4	1	0.8	2.2	0	0.4	0	0	0	0
Te Puna	ignim.	24	57	15.2	0.8	0.6	0	0	0	0	23	0.6	0.4
Te Puna	ignim.	26	55.2	23	0.6	1.8	0	0.2	0.4	0	13	1.4	4.8
Te Puna	ignim.	28	54.8	19.6	2.8	0.4	0	0	0.2	0	18.2	0.4	3.6
Waiteariki	ignim.	32	69.8	20.6	2.8	0.2	0	1.8	1	0.2	3.4	0	0.2
Waiteariki	ignim.	32	57.8	18.4	0.4	0.4	0	2.8	0.2	0	17.8	0	0.2
Minden	rhyolite	33	77.6	19	0.2	0.6	0.8	1.6	0.4	0	0	0	0
Minden	rhyolite	35	86.4	10.4	0.4	1.6	0	0.6	0.6	0	0	0	0
Minden	rhyolite	36	82.8	12.6	2	1	0.2	0.4	0.4	0	0	0	0
Minden	rhyolite	41	84.6	11.2	0.4	2.4	0.2	0.8	0.4	0	0	0	0
Kaimai	rhyolite	53	89.2	7	1	1.8	0.2	2	0.6	0	0	0	0
Waiteariki	ignim.	62	58	34	1.2	1.2	0.6	4	0.6	0	0	0	0
Waiteariki	lithic	22	67.8	24.2	0.8	2	0.4	3.8	0.6	0	0	0	0.2
Waiteariki	lithic	23	65.6	27	1	3.6	0.2	2	0.6	0	0	0	0

Table 3.2 Representative microprobe analyses for plagioclase phenocrysts of the Western Tauranga Basin. Kia (Kaikaikaroro Rhyolite), Min (Minden Peak Rhyolite), Wai (Waiteariki Ignimbrite), TeP (Te Puna Ignimbrite).

Sample	Kia 13	Kia 13	Min 7	Min 41	Min 41	Wai 12	Wai 51	Wai 51	Wai 62	Wai 62	TeP 28	TeP 28
	Plag	Plag	Plag	Plag Core	Plag Rim	Plag	Plag Rim	Plag Core	Plag Rim	Plag Core	Plag Core	Plag Core
SiO <sub>2</sub>	57.89	58.23	59.55	58.05	59.35	60.24	57.89	57.81	56.95	57	59.93	57.98
TiO <sub>2</sub>	0.1	0.05	0.09	0	0.05	0.01	0.05	0.02	0.11	0.11	0.06	0.06
Al <sub>2</sub> O <sub>3</sub>	26.21	25.78	25.13	26.12	24.91	23.95	25.92	26.63	26.62	25.7	24.17	26.54
FeO	0.34	0.3	0.12	0.26	0.11	0.12	0.27	0.28	0.16	0.12	0.1	0.2
MnO	0.21	0.09	0.08	0.18	0.04	0.13	0.03	0.02	0.04	0.07	0.05	0.02
MgO	0.1	0.02	0.08	0.03	0.12	0.06	0.1	0.06	0.1	0.18	0.08	0.09
CaO	8.02	7.63	6.46	7.91	6.65	5.63	7.83	8.23	8.79	8.03	6.09	8.12
K <sub>2</sub> O	0.35	0.43	0.61	0.41	0.54	0.67	0.37	0.38	0.37	0.38	0.53	0.36
Na <sub>2</sub> O	6.54	6.78	7.39	6.63	7.05	7.5	6.65	6.29	5.98	6.28	7.45	6.62
P <sub>2</sub> O <sub>5</sub>	0.06	0.05	0.26	0.15	0.14	0.25	0.12	0.23	0.01	0.09	0.18	0.02
Total	99.55	99.15	99.14	99.37	98.49	97.98	98.92	99.61	98.7	97.38	98.97	99.61
Albite	58.4	60.1	65	58.8	63.6	67.9	59.3	56.7	54	57.3	66.7	58.4
Anorthite	39.6	37.4	31.4	38.8	33.2	28.2	38.6	41	43.8	40.5	30.1	39.6
Orthoclase	2.1	2.5	3.5	2.4	3.2	4	2.2	2.3	2.2	2.3	3.1	2.1

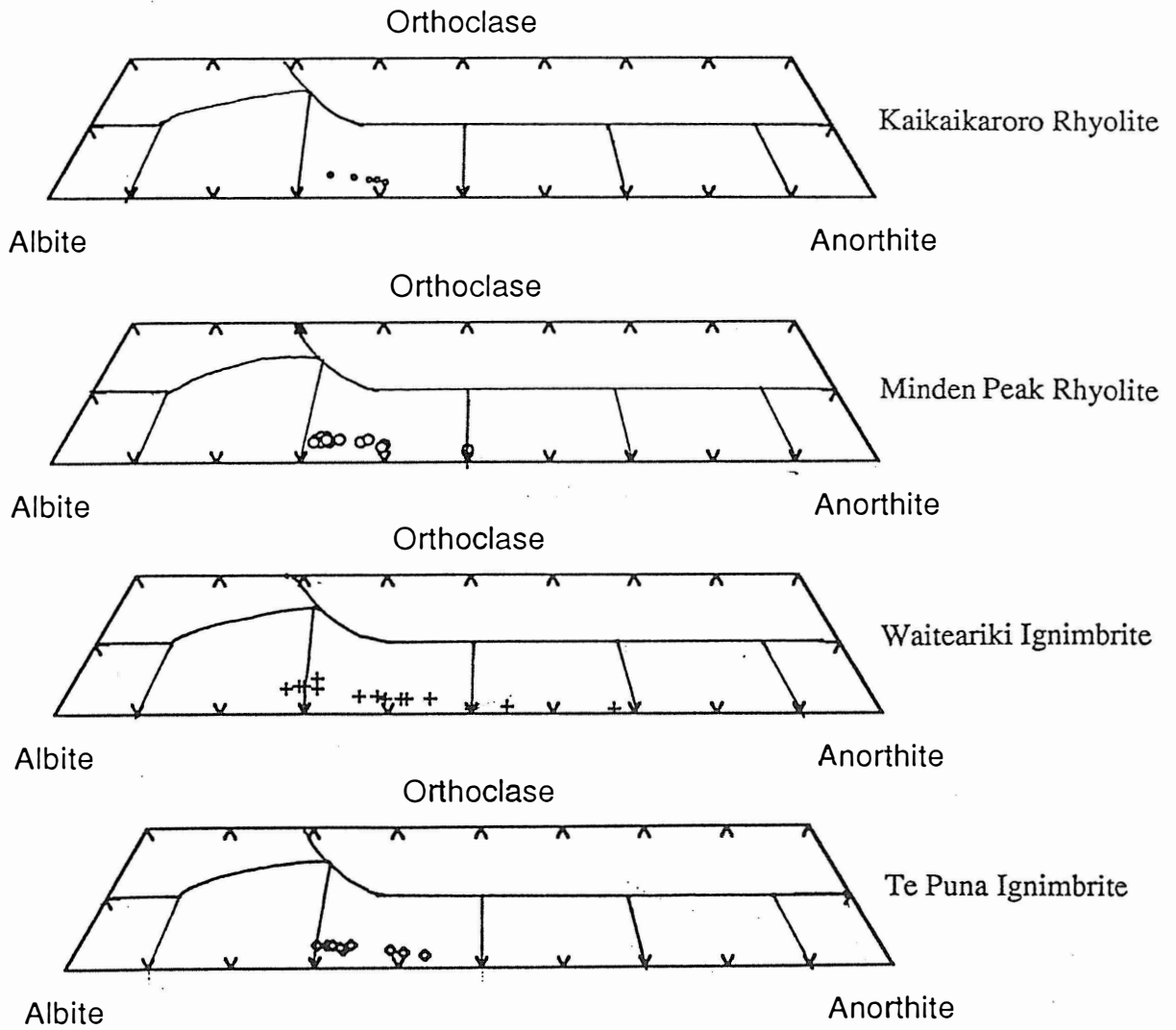
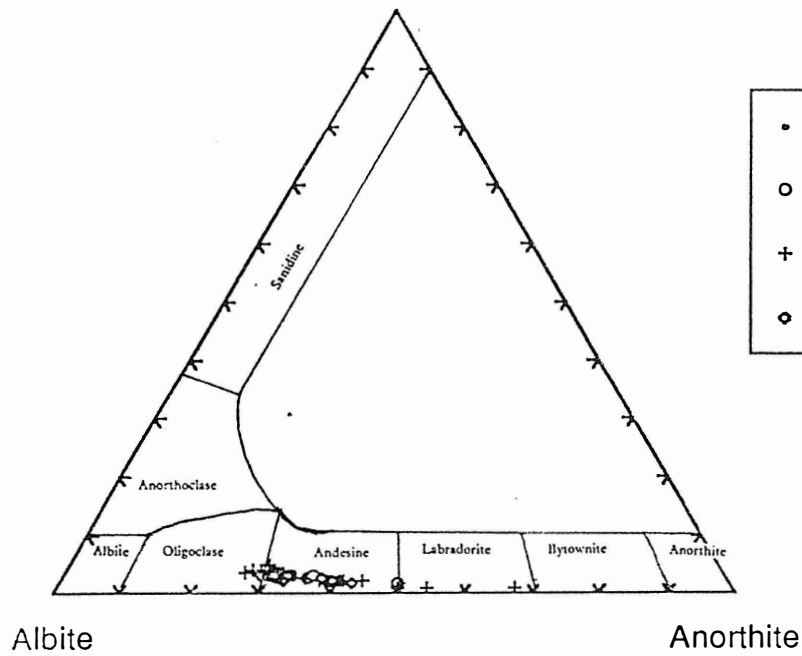


Fig 3.2 An-Ab-Or classification diagram for plagioclase feldspars of the Western Tauranga Basin.

Table 3.3 Representative microprobe analyses for amphibole phenocrysts of the Western Tauranga Basin. Kia (Kaikaikaroro Rhyolite), Min (Minden Peak Rhyolite), Wai (Waiteariki Ignimbrite), TeP (Te Puna Ignimbrite).

Sample	Kaikai 13	Kaikai 13	Min 7	Wai 12	Te P 28	Te P 28	Min 41	Wai 51	Min 33	Wai 62
SiO <sub>2</sub>	46.24	41.83	46.18	43.54	46.36	44.81	45.19	41.7	45.22	44.06
TiO <sub>2</sub>	1.38	2.59	1.19	19.4	1.3	1.54	0.98	2.02	1.34	1.8
Al <sub>2</sub> O <sub>3</sub>	8.21	10.8	6.73	8.41	6.75	7.08	7.3	8.88	7.52	8.14
FeO	14.57	19.66	19.89	19.49	19.97	18.37	21.91	20.59	20.07	18.82
MnO	0.34	0.35	0.74	0.5	0.5	0.45	0.78	0.28	0.55	0.29
MgO	14.02	9.86	11.03	10.38	11.89	11.6	9.81	8.82	10.51	10.57
CaO	11.04	10.55	10.42	10.69	10.12	10.6	10.33	10.26	9.96	10.97
K <sub>2</sub> O	0.27	0.44	0.41	0.51	0.47	0.35	0.57	0.46	0.53	0.52
Na <sub>2</sub> O	1.45	2.09	1.03	1.83	1.37	1.66	1.1	1.58	0.93	1.67
P <sub>2</sub> O <sub>5</sub>	0.19	0.2	0.02	0.02	0.05	0.09	0.04	0.08	0.04	0.06
Total	97.54	98.18	97.61	97.28	98.73	96.15	97.88	94.6	96.62	98.24

Table 3.4 Representative microprobe analyses for biotite phenocrysts of the Western Tauranga Basin. Man (Manawata Rhyolite), Min (Minden Peak Rhyolite), Wai (Waiteariki Ignimbrite).

Sample	Min 7	Man 15	Man 15	Min 41	Min 41	Wai 51
SiO <sub>2</sub>	45.86	35.13	34.64	35.55	36.27	34.99
TiO <sub>2</sub>	1.21	4.1	5.2	4.74	4.9	4.98
Al <sub>2</sub> O <sub>3</sub>	7.22	15.73	13.33	13.76	14.1	16.63
FeO	18.15	21.98	25.07	20.85	21.16	24.23
MnO	0.46	0.29	0.22	0.09	0.06	0.03
MgO	12.03	8.28	8.36	11.46	11.65	9.06
CaO	10.23	0.15	0.03	0.13	0	0.09
K <sub>2</sub> O	0.36	7.96	8.56	8.66	8.72	8.47
Na <sub>2</sub> O	1.278	0.41	0.54	0.08	0.69	0.6
P <sub>2</sub> O <sub>5</sub>	0.08	0	0.11	0.23	0.01	0.11
Total	96.79	94.02	95.69	95.83	97.49	95.96

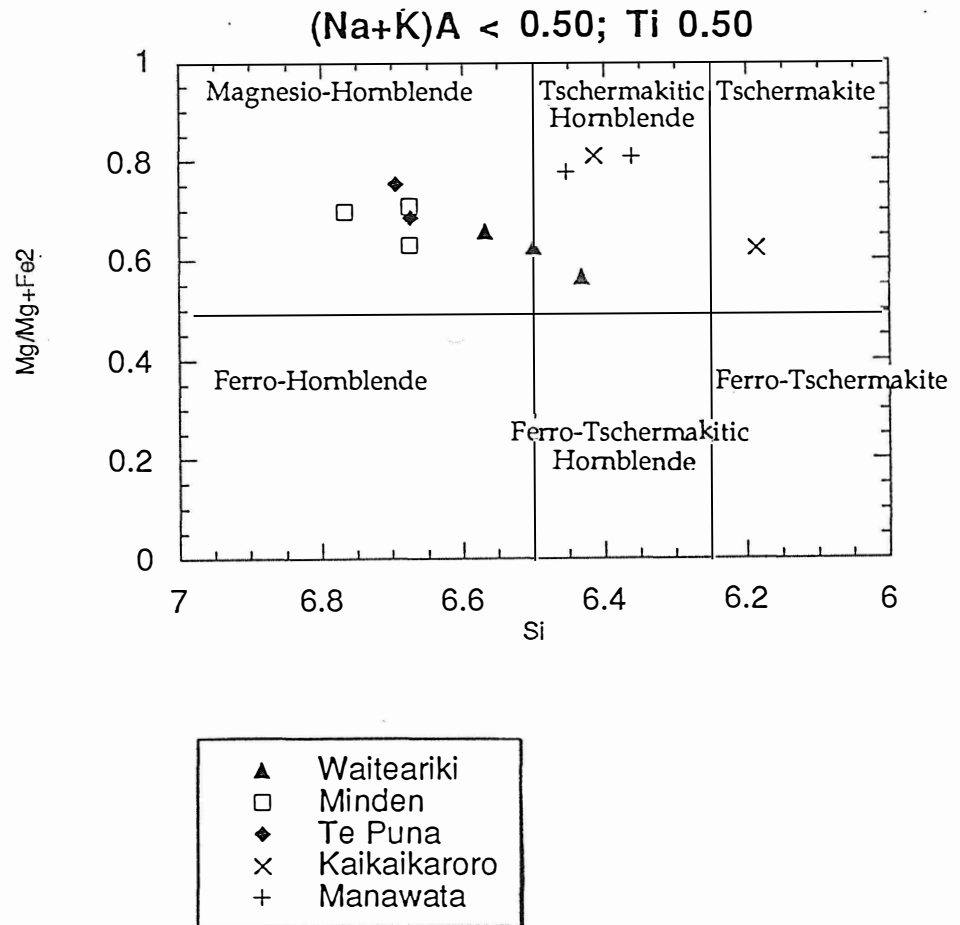


Fig 3.3 Amphibole compositions within the Western Tauranga Basin, classified according to Leake (1978).

Table 3.5 Representative microprobe analyses for orthopyroxene phenocrysts of the Western Tauranga Basin. Kai (Kaikaikaroro Rhyolite), Min (Minden Peak Rhyolite), Wai (Waiteariki Ignimbrite).

Sample	Kia 13	Kia 13	Kia 13	Min 7	Wai 12	Wai 12	Min 41	Min 41	Wai 51	Wai 51	Min 33	Min 33	Wai 62	Wai 62
SiO <sub>2</sub>	46.24	44.29	41.83	49.77	49.54	49.5	48.39	50.31	50.14	49.41	50.7	50.06	50.84	51.74
TiO <sub>2</sub>	1.38	1.76	2.59	0.07	0.14	0.05	0.05	0.11	0.18	0.23	0.3	0.06	0.23	0.52
Al <sub>2</sub> O <sub>3</sub>	8.21	9.34	10.8	0.67	0.49	0.53	14.73	0.6	1.08	0.99	0.65	0.27	0.8	1.56
FeO	14.57	15.86	19.66	31.3	33.55	33.92	26.08	30.88	30.63	32.9	30.35	32.26	28.02	22.65
MnO	0.34	0.37	0.35	1.53	1.15	1.67	0.98	1.57	0.87	0.93	1.46	1.49	0.45	0.49
MgO	14.02	13.13	9.86	15.6	14.66	13.47	15.64	16.15	15.44	14.76	16.68	15.63	18.12	21.78
CaO	11.04	11.07	10.55	0.71	1.18	1.36	0.73	0.84	1.57	0.94	0.76	0.7	1.1	1.87
K <sub>2</sub> O	0.27	0.19	0.44	0.05	0.12	0.03	0.03	0.02	0.01	0.1	0.05	0.05	0.01	0.02
Na <sub>2</sub> O	1.45	1.64	2.09	0.01	0.07	0.03	0.14	0	0.02	0.08	0.07	0.15	0.01	0.06
P <sub>2</sub> O <sub>5</sub>	0.19	0.05	0.2	0.18	0.18	0.04	0.02	0.22	0.03	0.21	0.1	0.17	0.09	0.18
Total	97.54	97.66	98.18	99.59	101.04	100.45	106.56	100.35	99.73	100.15	100.6	100.41	99.57	100.6
En	46.5	43.8	34.7	48.1	45.2	41.8	50.8	49.1	46.5	45.3	50.1	47.8	53.4	62.8
Fs	27.1	29.7	38.6	50.4	52.2	55.2	47.5	49	50.1	52.6	48.2	50.6	44.3	33.3
Wo	26.3	26.5	26.7	1.6	2.6	3	1.7	1.8	3.4	2.1	1.6	1.5	2.3	3.9



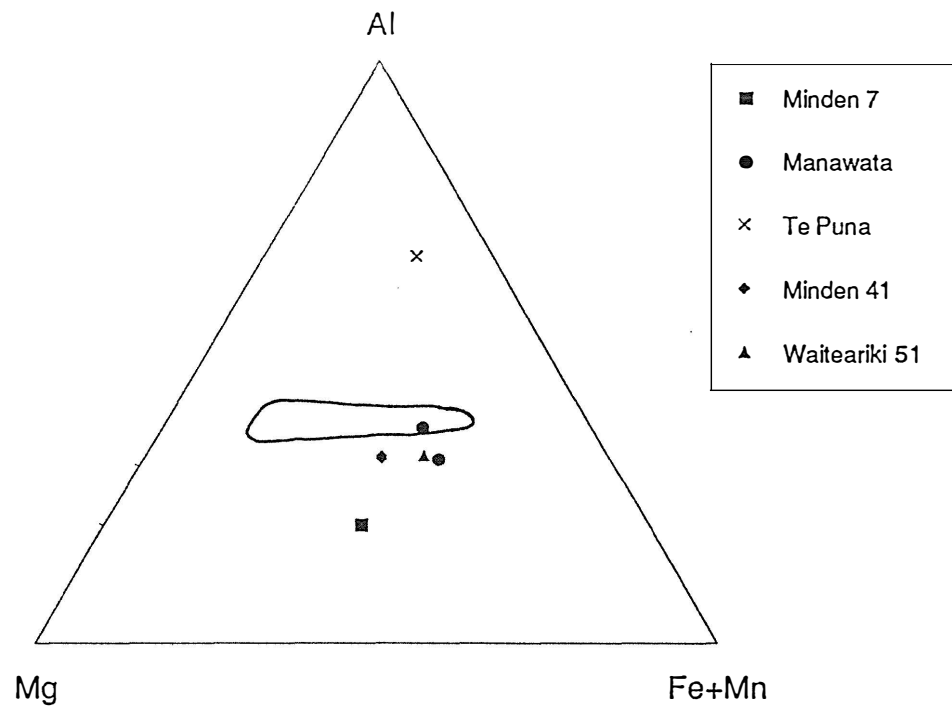


Fig 3.5 Al-Mg-Fe+Mn ternary diagram for biotite of the Western Tauranga Basin. Field is also plotted for TVZ biotite rhyolite (solid) after Ewart (1979).

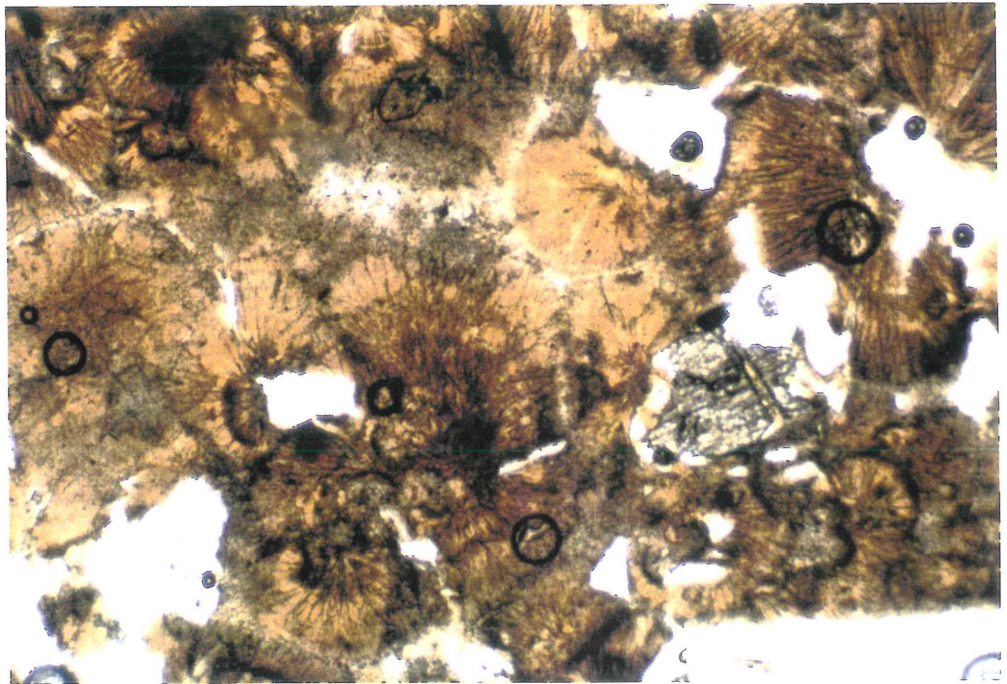


Fig. 3.6. Photomicrograph of spherulitic rhyolite from Kaikaikaroro showing hypersthene and hornblende within a spherulitic groundmass. X 40 magnification, plane polarised light.

### *Plagioclase*

Plagioclase phenocryst compositions for the rhyolites are presented on the An-Ab-Or feldspar ternary classification diagram (Fig 3.2) and representative analyses are presented in Table 3.2. Plagioclase phenocryst composition is classed within the andesine (An 35-50) range.

Plagioclase within the rhyolite occurs as medium grained (1-4mm) euhedral to subhedral phenocrysts, up to 12.6%. The plagioclase phenocrysts show polysynthetic twinning and occasional zoning (An 33-38). Some grains are glomeroporphyritic or have inclusions of biotite or zircon.

### *Quartz*

Quartz occurs as euhedral to anhedral phenocrysts up to 2 mm in length. Quartz occurs in all rocks but it is low in abundance at 0.2%. Phenocrysts are frequently embayed indicating that they are not in equilibrium with the surrounding material.

### *Amphibole*

Calcic amphibole occurs at 0.6 modal percent and is magnesio hornblende using parameters by Mogessie *et.al.* (1988) and classified according to Leake (1978) (Fig 3.3).

Phenocrysts occur up to 2 mm in length and are generally anhedral to euhedral (Fig 3.1). Crystals occasionally show simple twinning and vary in shades of green to green-brown pleochroism. Embayment of the amphiboles can be seen in a number of crystals.

### *Orthopyroxene*

The orthopyroxene phenocryst compositions for the rhyolites are presented on the Wo-En-Fs pyroxene ternary classification diagram (Fig 3.4) and representative analyses are presented in Table 3.5.

The orthopyroxenes present are hypersthene (En 80-50) and ferrohypersthene (En 50-12). Minden Peak contains both hypersthene and ferrohypersthene as En (51-41). Phenocrysts are generally anhedral to subhedral and have a maximum size of 2 mm. Pleochroism within the crystal is from pink to green to varying intensities.

### *Biotite*

Biotite is not a dominant mineral within Minden Peak rhyolite and constitutes only 0.2 modal percent. Phenocrysts are generally subhedral to euhedral and reach 1mm in length. Opaque inclusions within the phenocrysts are common. Phenocryst compositions are presented on the Al-Mg-Fe+Mn ternary diagram (Fig 3.5) and are compared to Taupo Volcanic Zone (TVZ) biotite rhyolites of Ewart (1979). Minden rhyolite biotite shows a lower Al content than the TVZ rhyolites. Representative analyses are presented in Table 3.4.

### *Fe--Ti Oxides*

Titanomagnetite occurs as anhedral grains, which commonly have zircon inclusions. Titanomagnetite also occurs with maghemite, haematite or with ilmenite lamellae. Ilmenite generally occurs as euhedral grains but some grains show embayment.

### **3.2.2 Kaikaikaroro**

Kaikaikaroro rhyolite is a grey hypocrystalline rhyolite with medium to coarse grained (1->5mm) crystals. It is crystal-rich (40%) with visible euhedral hornblende to lengths of 5mm, plagioclase to lengths of 7mm, and quartz. The texture in thin section is spherulitic, which is embedded within a felsitic groundmass.

### *Plagioclase*

Plagioclase phenocryst compositions are presented on the An-Ab-Or feldspar ternary classification diagram (Fig 3.2) and representative analyses are presented in Table 3.2. Phenocryst compositions are classified as andesine. Plagioclase (An 57-58) occurs as subhedral coarse grained (up to 7mm) phenocrysts and constitute up to 31.8% of the whole rock. Phenocrysts show zonation and polysynthetic twinning.

### *Quartz*

Quartz occurs as medium grained (up to 2mm) subhedral phenocrysts and are frequently embayed. Their abundance is 7.2 % of the whole rock.

### *Amphibole*

Calcic amphibole occurs in Kaikaikaroro as tschermakitic hornblende, using parameters by Mogessie et al. (1988) and classified according to Leake (1978) (Fig 3.3).

Phenocrysts are medium grained, up to 5mm in length, are generally euhedral, and show pleochroism from brown to green. Phenocryst abundance is up to 3.6% at Kaikaikaroro.

### *Biotite*

Biotite is low in abundance at 0.2% of the whole rock. It occurs as fine grained, less than 1mm, euhedral phenocrysts.

### *Orthopyroxene*

Hypersthene and ferrohypersthene (En 42-51) are present (Fig 3.4). They occur as fine grained, less than 1mm, subhedral to anhedral phenocrysts with tabular and prismatic forms and make up 2.4% of the whole rock (Fig3.6). Phenocrysts contain occasional inclusions of opaques.

### *Fe-Ti Oxides*

Fe-Ti oxides are euhedral ilmenite and anhedral titanomagnetite and make up 1.2% of the whole rock. Titanomagnetite grains can show exsolution and replacement by ilmenite lamellae. Magnetite and ilmenite commonly contain zircon inclusions.

### **3.2.3 Manawata**

Manawata rhyolite is a light grey to pink hypocrySTALLINE rock. It is phaneritic with medium grained (1-3mm) phenocrysts of quartz, plagioclase and hornblende within a spherulitic groundmass. Manawata rhyolite shows flow banding which is distinguishable due to colour changes in the bands from light grey to pink and by the alignment of hornblende crystals.

It weathers to a light grey to white soft rock with a pocky nature due to the weathering out of plagioclase.

### *Plagioclase*

Plagioclase phenocryst compositions for the rhyolites are presented on the An-Ab-Or feldspar ternary classification diagram (Fig 3.2) and representative analyses are presented in Table 3.2. Phenocryst compositions fall within the andesine (An 35-50) range.

Plagioclase within the rhyolite occurs as medium grained (1-4mm) euhedral to subhedral phenocrysts, constituting 4.4% of the rock. The plagioclase phenocrysts show polysynthetic twinning and occasional normal zoning (An 33-38).

### *Quartz*

Quartz occurs as euhedral to anhedral phenocrysts up to 2 mm in length and up to 1 modal percent. Phenocrysts are frequently embayed indicating that they are not in equilibrium with the surrounding material.

### *Amphibole*

Calcic amphibole abundance is 2.4% at Manawata. Manawata contains tschermakitic hornblende, using parameters by Mogessie *et al.* (1988) and classified according to Leake (1978) (Fig 3.3).

Phenocrysts occur up to 2 mm in length, are generally anhedral to euhedral (Fig 3.3), and have green-brown pleochroism. Some crystals show simple twinning.

### *Orthopyroxene*

In Manawata Rhyolite the hypersthene has been weathered, leaving only a remnant of the original crystal.

### *Biotite*

Biotite occurs in abundance from 1.4-2.2%, is generally subhedral to euhedral, and reaches 1mm in length. Opaque inclusions within the phenocrysts are common.

Phenocryst compositions are presented on the Al-Mg-Fe+Mn ternary diagram (Fig 3.5) and compared to Taupo Volcanic Zone (TVZ) biotite Rhyolites of Ewart (1979). Manawata rhyolite biotite is more similar chemically to the TVZ

rhyolites. Representative analyses of the western Tauranga biotites are presented in Table 3.4.

#### *Fe--Ti Oxides*

Titanomagnetite occurs as anhedral grains, which commonly have zircon inclusions. Titanomagnetite also occurs with maghemite, haematite or with ilmenite lamellae. Ilmenite occurs as euhedral grains to subhedral grains .

### 3.3 Waiteariki Ignimbrite

The Waiteariki Ignimbrite is a crystal-rich (22.2 - 41.6%) ignimbrite with 20% pumice up to 400 mm in length. It varies in appearance from cream pumice within a creamy brown matrix to collapsed pumice forming dense, black, glassy fiamme within a light brown matrix. Visible crystals of plagioclase (5mm), hornblende and hypersthene can be seen in hand specimen. Lithics within the ignimbrite have been found up to 300 mm.

#### *Plagioclase*

Plagioclase phenocryst compositions are presented on the An-Ab-Or feldspar ternary classification diagram (Fig 3.2) and representative analyses are presented in Table 3.2. Phenocrysts are classed as oligoclase, andesine and labradorite.

Plagioclase (An 28-70) occurs as medium grained (3mm) euhedral to subhedral phenocrysts and crystals which are commonly fragmented, characteristic of a high energy eruption. Phenocrysts show polysynthetic twinning and normal zoning (An 41-49). It is the most abundant phenocryst and comprises 18.4 - 34% of the total rock.

#### *Quartz*

Quartz abundance is low (<2.8%) and is present as fine grained (<1mm) anhedral crystals which are generally embayed.

### *Orthopyroxene*

Both hypersthene and ferrohypersthene (see Fig 3.4 and Table 3.3) are present with compositions ranging from En 45-62. They occur as subhedral to anhedral phenocrysts with tabular and prismatic form, and make up 2.8-4% of the rock. Phenocrysts show pink-brown pleochroism and are less than 1mm. Opaque inclusions are common.

### *Amphibole*

The calcic amphiboles, magnesio hornblende and tschermakitic hornblende are found within the Waiteariki Ignimbrite as classified by Leake (1978) (Fig3.3). Amphibole analyses are given in Table 3.3.

They are pleochroic from brown to green and occur as subhedral tabular crystals with 120/60° cleavage cross-sections. Phenocrysts have occasional opaque inclusions. It comprises 1.2% of the rock with crystals less than 1mm in length.

### *Biotite*

Biotite is only found in the upper layer of the ignimbrite and is absent elsewhere. It is found at McLaren Falls where the biotite comprises 0.6% of the rock and occurs as euhedral laths with reaction rims.

Only one biotite phenocryst was microprobed and its chemical composition (Table 3.4) is plotted on the Al-Mg-Fe+Mn ternary diagram (Fig 3.5) .

### *Zircon*

Zircon within the rock generally occurs associated with opaques. They occur as prismatic grains and have straight extinction. Their size is generally less than 0.1mm but have been found up to 0.5mm in length.

### *Fe-Ti Oxides*

Fe-Ti oxides are subhedral tabular ilmenite and anhedral titanomagnetite and make up to 1% of the total rock. Titanomagnetite is also found with ilmenite lamellae and occasionally contain marcasite inclusions.

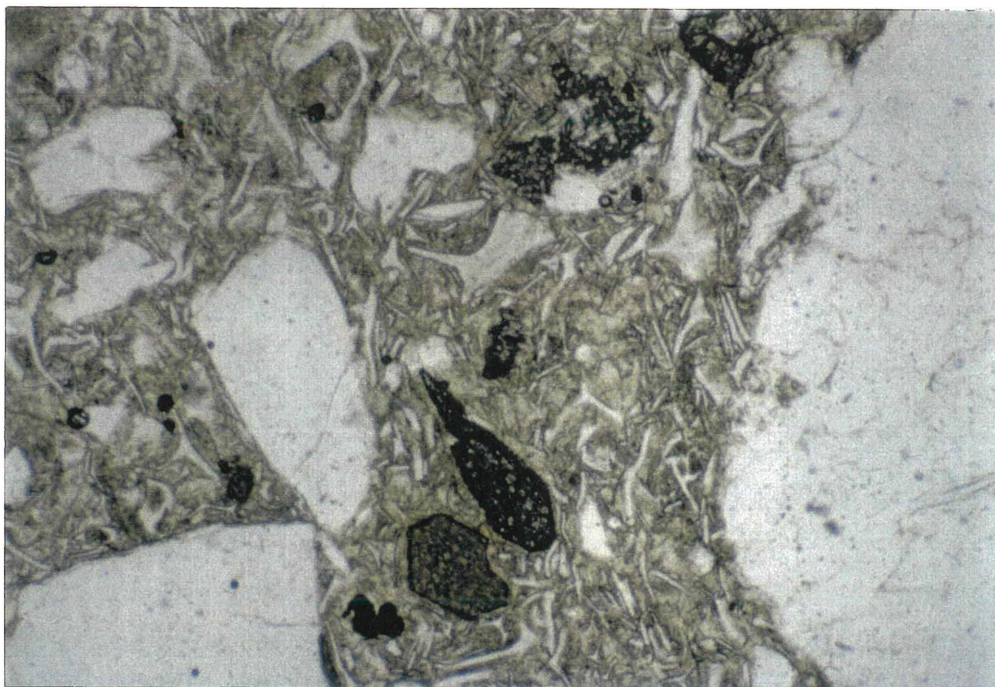


Fig 3.7 Photomicrograph of Waiteariki Ignimbrite with cusped and Y-shaped glass shards and hornblende and zircon crystals in the lower centre. X 40 magnification, plane polarised light.

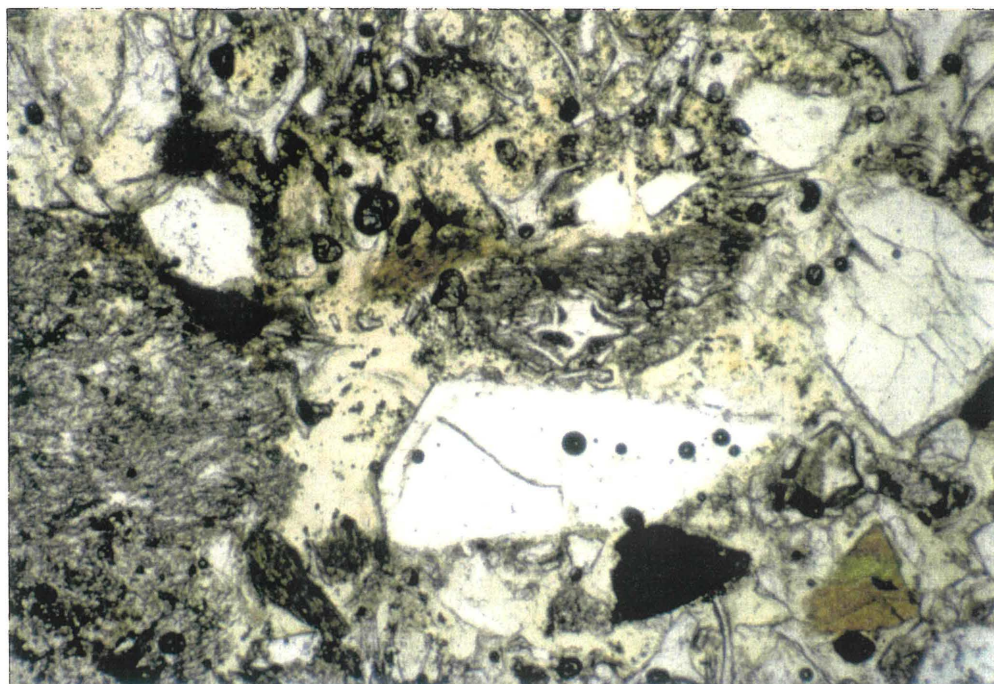


Fig. 3.8 Photomicrograph of Te Puna Ignimbrite with mica, hornblende, plagioclase, and vesicular pumice within a glass shard matrix. X4 objective, plane polarised light.

### *Pumice*

Pumice within the Waiteariki Ignimbrite is fibrous and reaches 30cm in length. It varies in colour from cream to black, and in texture from fibrous to dense, due to the degree of welding and devitrification. Pumice is generally lenticular and shows fiamme characteristics at McLaren Falls. Where the pumice is highly devitrified, spherulites are present.

### *Groundmass*

The groundmass is made up of cusped and Y-shaped glass shards (Fig 3.7). Preferential devitrification occurs from the inside of the shards. Devitrification is greatest at McLaren Falls where it is also densely welded.

Lithics within the ignimbrite are andesitic, rhyolitic and dacitic, and comprise up to 3.6% of the total rock. Andesite lithics, up to 1 mm, contain aligned plagioclase laths in an interstitial groundmass. Rhyolitic lithics, up to 1 mm, are of brown spherulites with phenocrysts of plagioclase and titanomagnetite.

Dacitic lithics up to 30 cm are mineralogically similar to the Waiteariki Ignimbrite. They contain biotite, subhedral to anhedral hornblende, subhedral to anhedral hypersthene, subhedral plagioclase, embayed quartz, Fe-Ti oxides, and zircons in a glassy flow-banded groundmass. These lithics may represent earlier lava flows from the same source.

## **3.4 Te Puna Ignimbrite**

The Te Puna Ignimbrite is holocrystalline nonwelded to partially welded ignimbrite. It contains 23% of white pumice within a buff brown matrix. It is crystal rich with 27% crystals, with visible plagioclase, quartz and hornblende. Lithic abundance is low (1-2%) and lithic types consist of banded and nonbanded rhyolite, and dacite.

### *Quartz*

Quartz abundance within the ignimbrite is 2.8%, and occurs as subhedral to anhedral crystals, which are commonly embayed.

### *Plagioclase*

Plagioclase phenocryst compositions are presented on the An-Ab-Or feldspar ternary classification diagram (Fig 3.2), with samples lying within the andesine range; representative analyses are presented in Table 3.2.

Plagioclase (An 30-39) is the dominant phenocryst and it occurs as medium grained (2mm) euhedral to subhedral crystals that are often fragmented. The crystals show polysynthetic twinning and normal zoning (An 32-37) with occasional inclusions of hornblende, hypersthene and Fe-Ti oxides. Plagioclase abundance is up to 19% of the whole rock.

### *Orthopyroxene*

Hypersthene occurs as subhedral prismatic phenocrysts up to 1mm in length with ragged terminations and occasional opaque inclusions. It constitutes up to 0.4% of the whole rock.

### *Amphibole*

Calcic amphibole occurs as magnesio hornblende within the Te Puna Ignimbrite as classified by Leake (1978) (Fig 3.3). It occurs as medium grained (2mm) prismatic subhedral phenocrysts with poorly developed terminations, or as six sided cross-sections showing 120/60° cleavage. Phenocrysts are pleochroic from dark green to brown and commonly show simple twinning.

### *Secondary minerals*

A Secondary mineral within the Te Puna Ignimbrite may be the result of weathering of biotite within the ignimbrite. The mineral is golden in hand specimen, and light brown in thin section (Fig 3.8). Abundances range from 0.4-1.4% with the length of the crystals reaching 1mm. The compositions are in Table 3.4 and plotted with western Tauranga biotites on the Al-Mg-Fe+Mn ternary diagram (Fig 3.5). The mineral shows a high proportion of Al which has occurred due to weathering.

### *Groundmass*

The groundmass consists of cusped, lunate and Y-shaped glass shards in a yellow matrix and contains accessory lithics.

Brown rhyolite lithics, are up to 2 mm and contain plagioclase phenocrysts and zircon within a spherulitic groundmass. Waiteariki Ignimbrite also occurs up to 2 mm and contains hypersthene, plagioclase, and hornblende in a glass shard groundmass.

### *Pumice*

The pumice is fibrous and makes up to 25% of the ignimbrite. It has a glomeroporphyritic texture and contains euhedral plagioclase, euhedral hornblende, subhedral hypersthene, quartz, biotite and Fe-Ti oxides (Fig 3.9).

### *Fe-Ti Oxides*

Titanomagnetite and ilmenite are the most common opaques. Ilmenite grains occasionally have inclusions of apatite and marcasite.

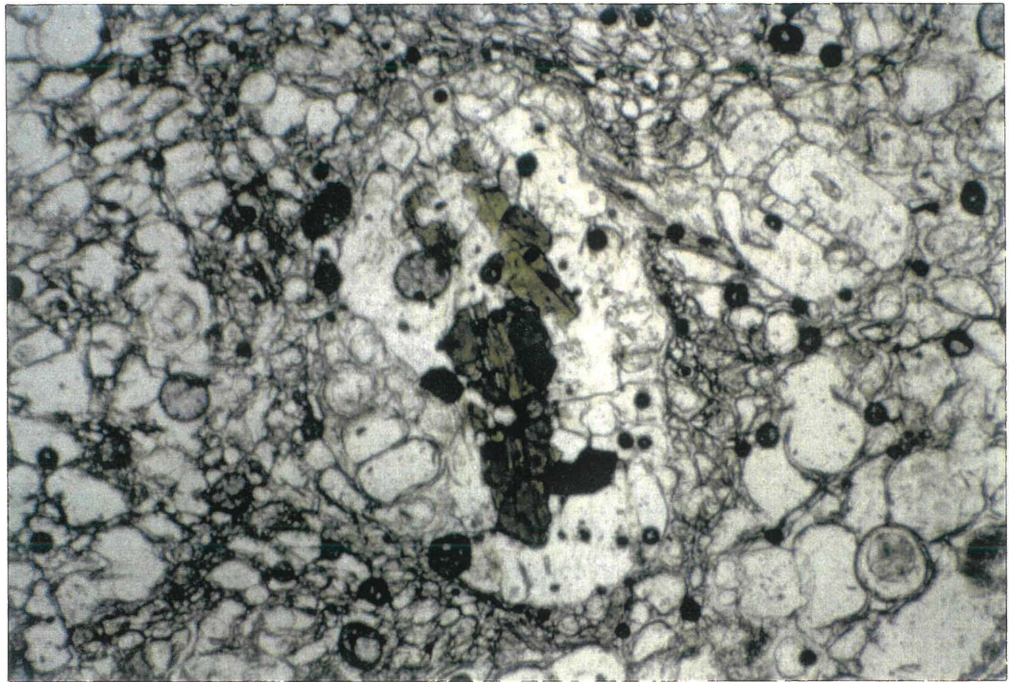


Fig 3.9A Photomicrograph of glomeroporphyritic plagioclase and hornblende within the Te Puna Ignimbrite, X 40 magnification, plane polarised light.

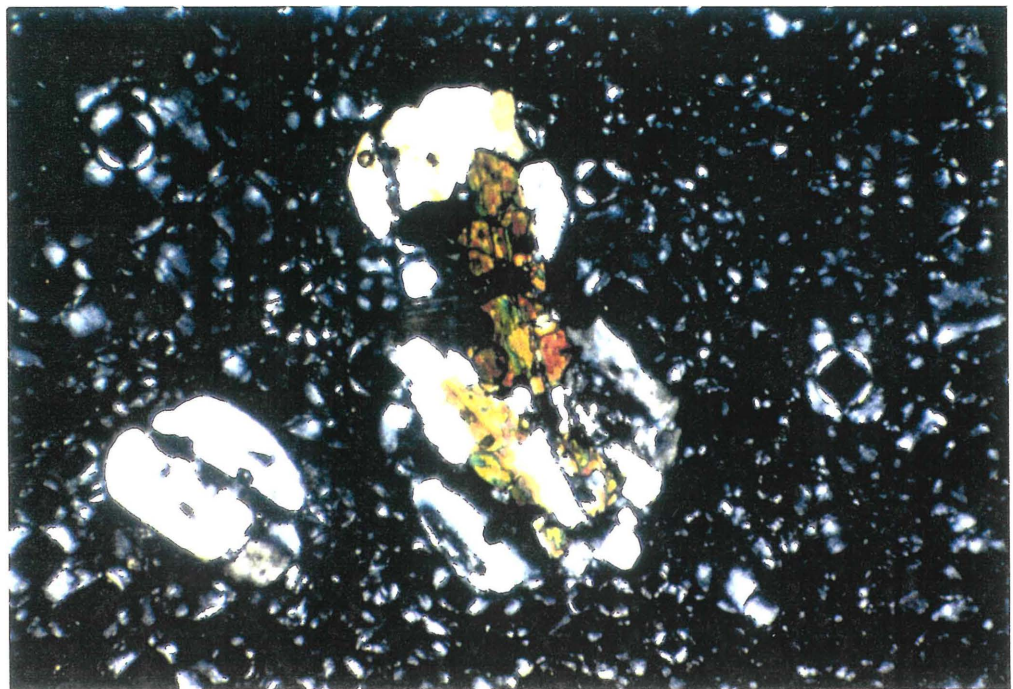


Fig. 3.9B Photomicrograph of glomeroporphyritic plagioclase and hornblende within the Te Puna Ignimbrite, X 40 magnification, crossed polarised light.

*Chapter Four*

**Petrochemistry**

# Chapter Four

## Petrochemistry

### 4.1 Introduction

Twenty four major and trace element analyses were determined on rocks in the western Tauranga Basin by X-ray fluorescence (XRF), and data are presented in Tables 4.1 and 4.2. Analyses were carried out at the Analytical Facility, Victoria University, Wellington.

The following discussion on petrochemistry involves determining if there is any significant chemical relationships between the rocks in the studied area. Also a comparison of the rocks in Coromandel (Adams 1992), Eastern Tauranga basin (Hughes 1992), Motiti Island (Henry 1991) and White Island (Graham and Cole 1989) is undertaken, using primitive mantle-normalised trace element plots.

### 4.2 Classification

Several geochemical variation diagrams can be used to classify the rock types. Peccerillo and Taylor (1976) classified rock types based on the relationship between SiO<sub>2</sub> and K<sub>2</sub>O content. Their classification defines basalts as <52% SiO<sub>2</sub>, basaltic andesites 53-56% SiO<sub>2</sub>, andesites 56-63% SiO<sub>2</sub>, dacites 63-70% SiO<sub>2</sub>, and rhyolites >70% SiO<sub>2</sub>. K<sub>2</sub>O divisions mark the boundaries between arc tholeiite calc-alkaline, high-K calc-alkaline and shoshonite series.

Gill (1981) further divided andesites into high-K, medium-K and low-K andesites, whereas Le Maitre (1984) used SiO<sub>2</sub> vs Na<sub>2</sub>O+K<sub>2</sub>O%.

Using the Peccerillo and Taylor (1976) SiO<sub>2</sub> vs K<sub>2</sub>O (Fig 4.1) and the Le Maitre (1984) SiO<sub>2</sub> vs Na<sub>2</sub>O+K<sub>2</sub>O (Fig 4.2) classification diagrams it is seen that Waiteariki Ignimbrite is dacitic to rhyolitic, Kaikaikaroro, Manawata and Minden Peak are rhyolitic, and Te Puna Ignimbrite is rhyolitic with pumice ranging from rhyolite to high silica rhyolite.

The Western Tauranga basin rocks are subalkaline in nature as classified according to Irvine and Baragar (1971) (Fig 4.3).

Table 4.1 Major (normalised to 100% volatile free) and trace element XRF analyses of the Western Tauranga basin volcanics.  
 Min=Minden Peak Rhy, Kai=Kaikaikaroro Rhy, Man= Manawata Rhy, TeP=Te Puna Ign, Wai=Waitcariki Ig.

Sample	Min 6 rhyolite	Min 7 rhyolite	Kai 13 rhyolite	Man 15 rhyolite	Man15 rhyolite	Te P 28 ignim.	Wai 32 ignim.	Min 33 rhyolite	Min 35 rhyolite	Min 36 rhyolite	Min 41 rhyolite	Min 43 rhyolite
SiO <sub>2</sub>	75.98	75.73	70.92	74.44	76.25	70.52	70.07	74.68	75.36	75.51	75.5	74.56
TiO <sub>2</sub>	0.2	0.2	0.4	0.26	0.22	0.36	0.4	0.22	0.22	0.2	0.2	0.23
Al <sub>2</sub> O <sub>3</sub>	13.82	13.77	15.54	15.92	15.3	17.28	15.91	14.86	14.17	13.56	13.92	15.12
Fe <sub>2</sub> O <sub>3</sub>	0.37	0.36	0.69	0.41	0.4	0.59	0.75	0.41	0.39	0.35	0.35	0.41
FeO	1.33	1.3	2.5	1.48	1.44	2.11	2.68	1.46	1.4	1.28	1.28	1.48
MnO	0.03	0.04	0.06	0.03	0.02	0.09	0.09	0.04	0.03	0.03	0.02	0.05
MgO	0.24	0.23	0.73	0.25	0.13	0.36	0.46	0.26	0.27	0.16	0.2	0.22
CaO	1.06	1.21	2.57	1	0.56	2.31	2.6	1.31	1.2	1.51	1.36	1.32
Na <sub>2</sub> O	3.15	3.4	3.71	2.93	2.08	3.79	4.42	3.47	3.29	3.81	3.5	3.3
K <sub>2</sub> O	3.8	3.73	2.83	3.24	3.57	2.58	2.59	3.26	3.65	3.55	3.64	3.28
P <sub>2</sub> O <sub>5</sub>	0.02	0.02	0.05	0.02	0.01	0.02	0.02	0.02	0.03	0.03	0.02	0.05
LOI	1.98	1.68	2.27	3.4	4.22	4.78	2.78	1.66	1.49	0.69	1.3	2.06
Total	100	100	100	100	100	100	100	100	100	100	100	100
Sc	4	3	9	4	2	7	9	4	4	4	5	5
V	16	15	44	15	11	25	28	14	16	15	15	18
Cr	2	1	5	2	1	2	3	2	1	2	2	3
Ni	1	2	2	3	2	2	4	1	1	1	3	2
Cu	4	4	7	5	5	4	6	3	3	4	3	4
Zn	28	29	54	41	33	58	64	32	28	30	33	29
Ga	14	14	16	15	16	17	17	15	14	14	14	15
As	3	4	4	4	3	4	4	5	4	4	4	4
Rb	133	131	99	120	126	91	82	77	126	127	123	87
Sr	90	92	154	96	57	171	194	99	95	114	99	100
Y	12	14	28	32	16	28	45	17	30	16	80	19
Zr	133	132	158	193	156	209	209	150	142	134	138	148
Nb	8	8	6	7	8	9	8	9	7	7	6	8
Ba	789	794	786	786	681	727	717	820	800	796	771	798
La	18	21	32	89	25	24	52	26	26	23	50	22
Ce	36	39	45	64	46	68	93	38	35	42	40	48
Pb	17	15	15	16	14	18	12	14	15	15	15	18
Th	15	14	10	12	13	12	8	14	13	13	13	15
U	4	4	2	4	3	3	3	3	4	3	4	3

Table 4.2 Continued Major (normalised to 100% volatile free) and trace element XRF analyses of the Western Tauranga basin volcanics.  
Wai=Waiteariki Ignimbrite, TePp=Te Puna Pumice

Sample rhyolite	Wai 62 ignim.	TePp 82 pumice	TePp 83 pumice	TePp 84 pumice	TePp 85 pumice	TePp 86 pumice	TePp 87 pumice	TePp 88 pumice	TePp 89 pumice	TePp90 pumice	TePp91 pumice
SiO <sub>2</sub>	67.54	73.88	75.67	75.09	73.51	75.17	74.41	73.96	73.52	72.58	73.13
TiO <sub>2</sub>	0.54	0.26	0.19	0.2	0.31	0.24	0.27	0.3	0.27	0.24	0.25
Al <sub>2</sub> O <sub>3</sub>	16.84	14.31	13.58	13.83	14.23	13.6	14.07	14.05	14.53	16.1	15.92
Fe <sub>2</sub> O <sub>3</sub>	0.95	0.44	0.35	0.38	0.53	0.39	0.46	0.51	0.47	0.44	0.47
FeO	3.41	1.59	1.25	1.35	1.92	1.4	1.65	1.85	1.68	1.6	1.69
MnO	0.01	0.07	0.06	0.06	0.08	0.05	0.06	0.16	0.08	0.09	0.12
MgO	0.67	0.33	0.25	0.3	0.43	0.35	0.39	0.41	0.38	0.29	0.32
CaO	3.76	2	1.55	1.68	1.96	1.6	1.66	1.77	2.02	1.88	1.55
Na <sub>2</sub> O	3.91	3.55	2.92	3.04	3.46	3.57	3.24	3.3	3.55	3.46	3.28
K <sub>2</sub> O	2.15	3.54	4.18	4.06	3.57	3.62	3.78	3.67	3.5	3.31	3.26
P <sub>2</sub> O <sub>5</sub>	0.02	0.01	0.01	0.01	0.01	0.01	0.01	0.02	0.01	0.01	0.01
LOI	2.28	3.18	3.57	3.66	3.47	2.93	3.35	3.7	3.08	4.41	4.24
Total	100	100	100	100	100	100	100	100	100	100	100
Sc	14	5	4	5	6	4	5	8	7	6	6
V	55	18	12	13	21	14	17	23	17	17	15
Cr	8	2	2	3	4	2	2	4	3	3	3
Ni	5	1	2	2	1	2	2	2	2	2	3
Cu	8	2	3	3	3	3	3	4	4	4	4
Zn	62	46	40	40	52	42	48	54	46	45	46
Ga	17	14	13	15	15	14	16	15	15	17	16
As	3	5	5	4	5	5	5	5	5	4	5
Rb	73	113	132	130	113	122	126	116	110	106	113
Sr	232	150	111	120	140	116	118	122	145	132	106
Y	53	25	23	24	25	23	27	39	27	31	34
Zr	170	174	133	140	209	167	177	209	190	174	173
Nb	7	8	8	7	8	8	8	10	9	8	9
Ba	680	744	793	771	756	739	652	890	777	787	790
La	30	23	25	24	25	27	22	55	30	33	36
Ce	48	49	49	47	50	43	48	94	54	64	75
Pb	12	14	14	14	14	13	13	21	15	19	20
Th	8	11	13	14	12	13	12	12	10	13	16
U	2	2	3	4	3	3	3	3	3	3	3

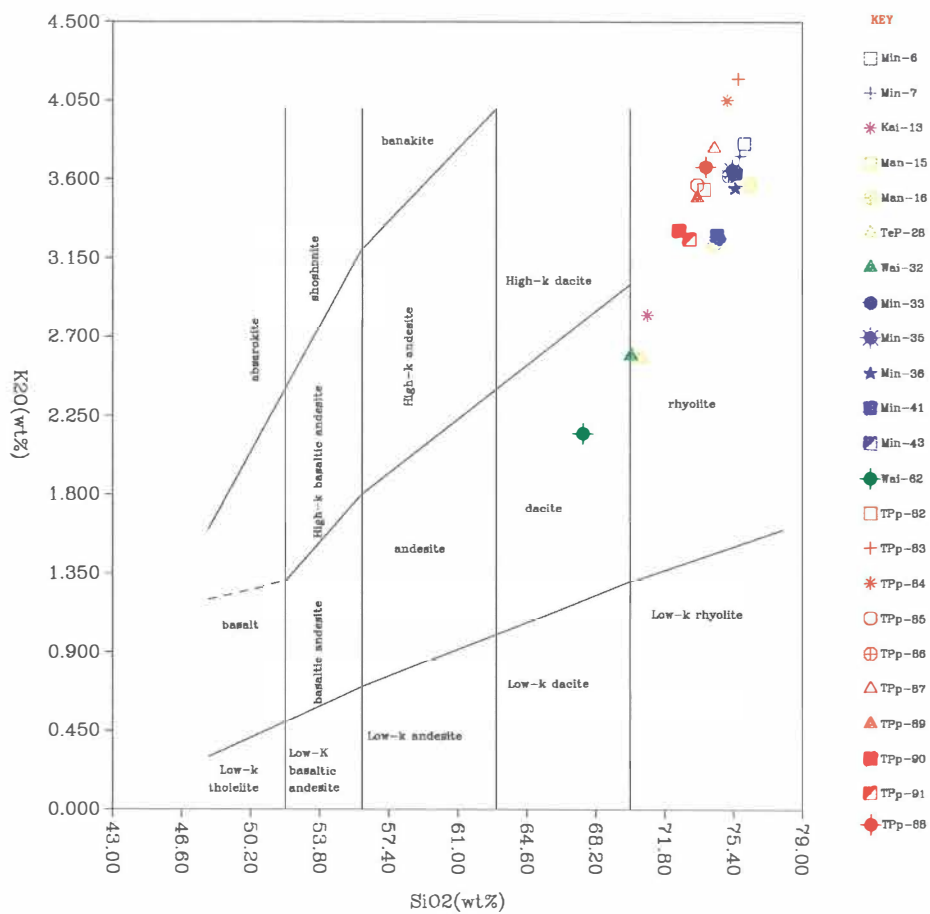


Fig 4.1 Classification of Western Tauranga basin Volcanic rocks using the K<sub>2</sub>O vs SiO<sub>2</sub> diagram of Peccerillo and Taylor (1976).

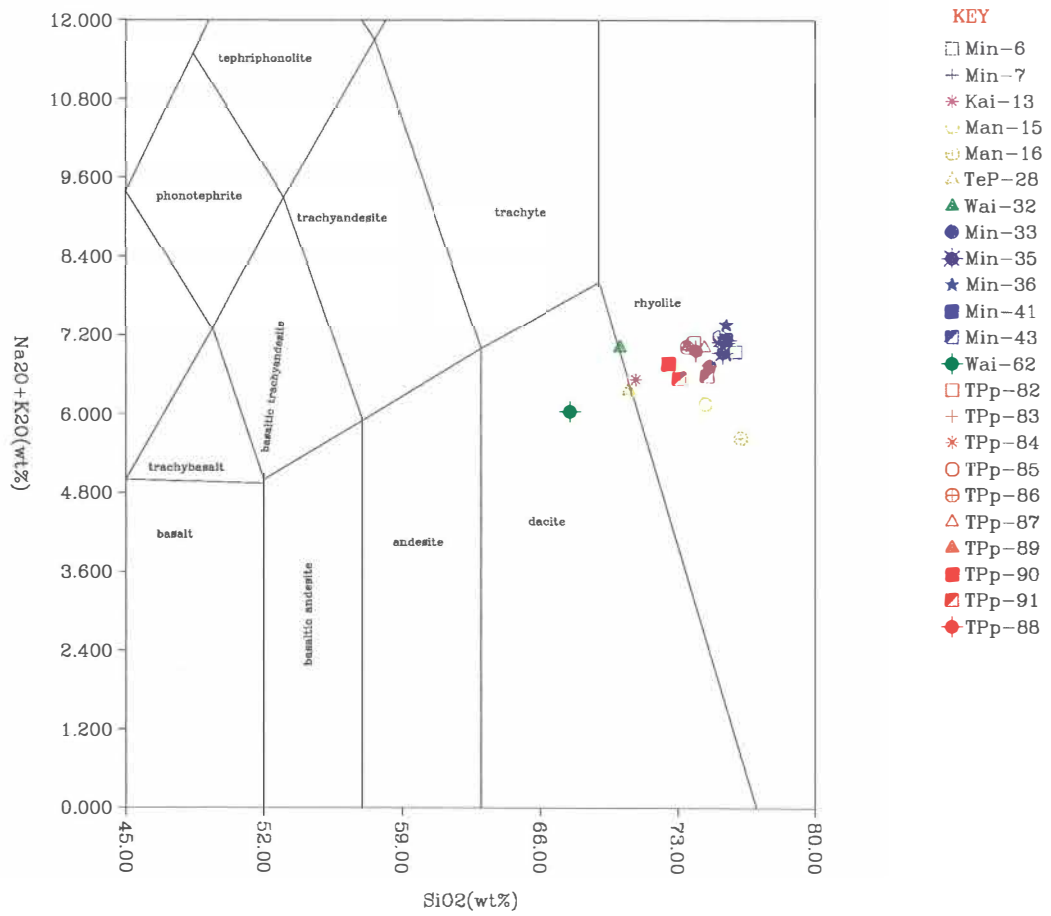


Fig 4.2 Na<sub>2</sub>O + N<sub>2</sub>O vs SiO<sub>2</sub> diagram of Western Tauranga basin rocks (after Le Maitre 1984).

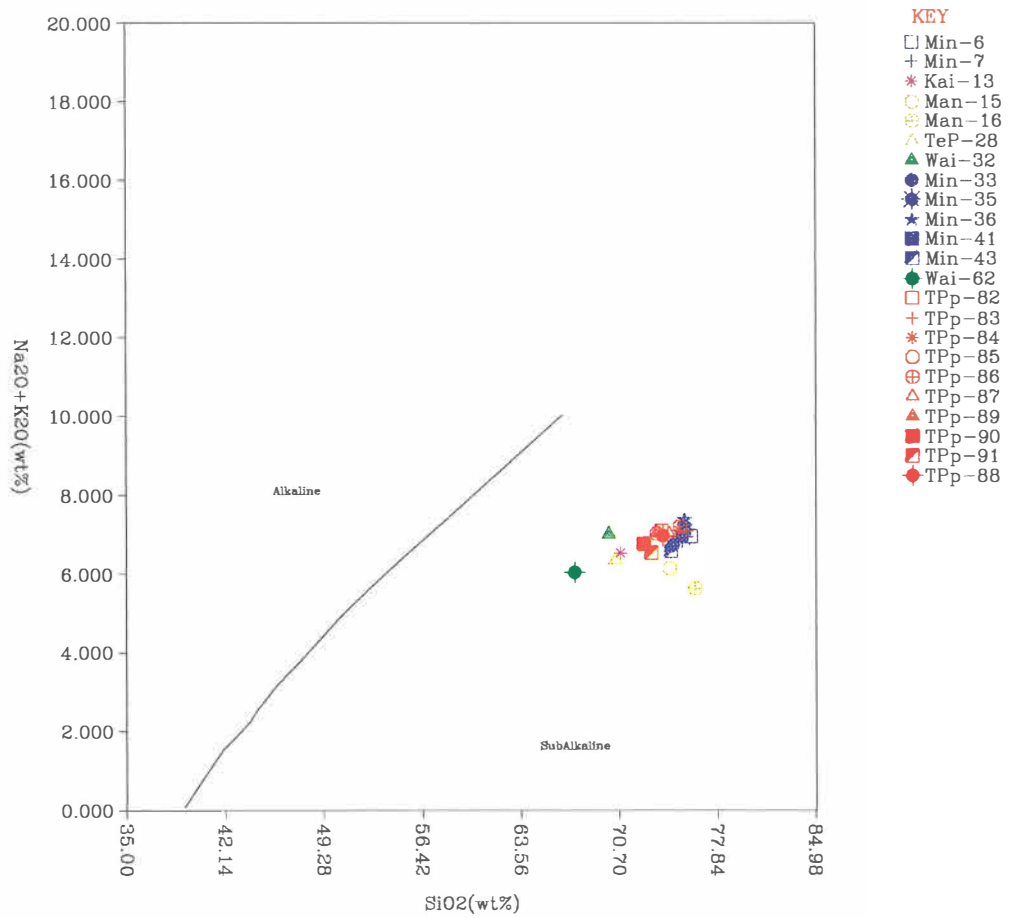


Fig 4.3 Total alkali vs silica plots of Western Tauranga basin rocks. The distinction between alkaline and subalkaline is after Irvine and Barager (1971).

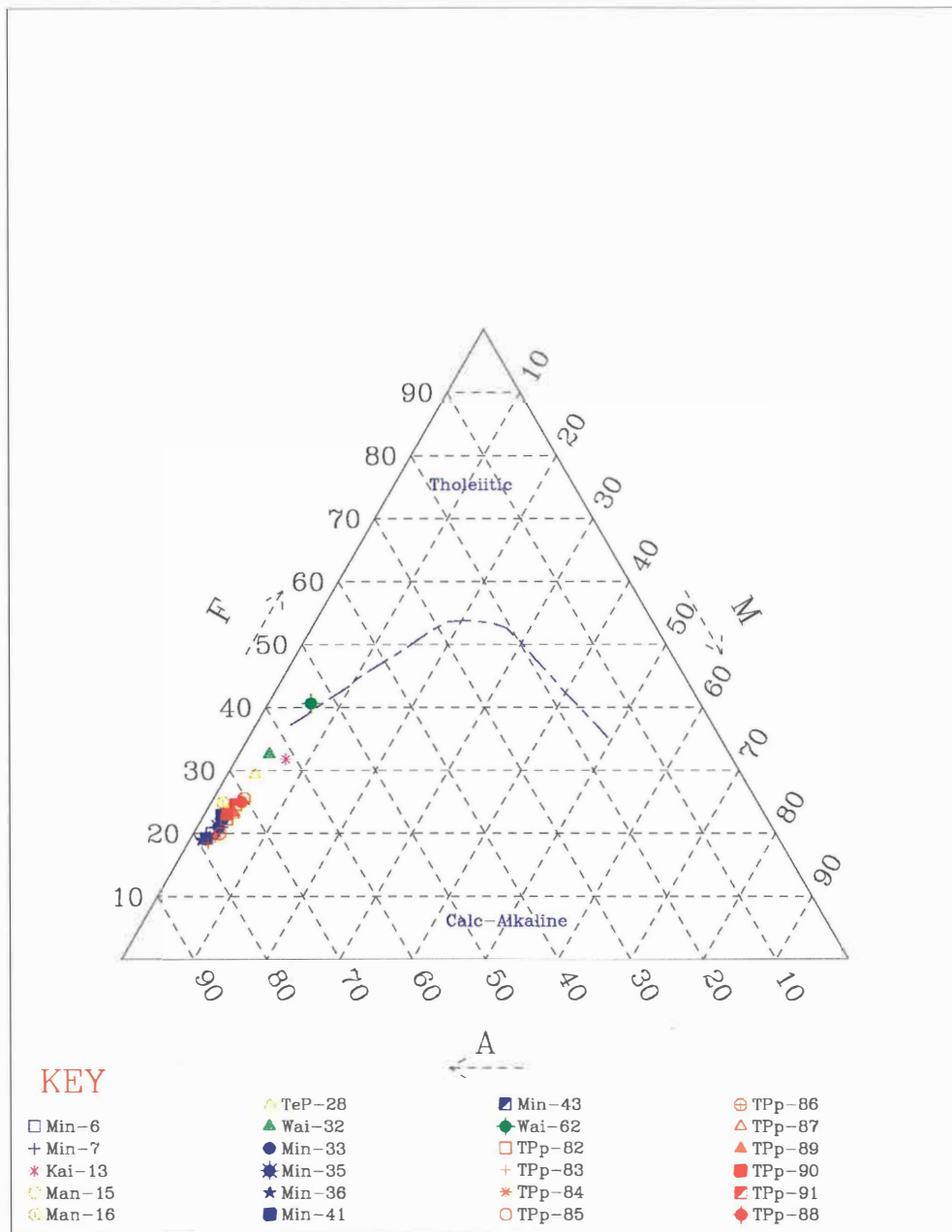


Fig 4.4 AFM diagram of Western Tauranga basin volcanic rocks compared to other North Island rocks (after Irvine and Baragar 1971).  
 1=White Island(Cole & Graham 1989), 2=Motiti Island(Henry 1991)  
 3=Coromandel(Adams 1992), 4=Eastern Tauranga basin(Hughes 1993)

To define the magmatic series involved, the AFM (A= Na<sub>2</sub>O + K<sub>2</sub>O, F= FeO + 0.8998 Fe<sub>2</sub>O<sub>3</sub>, M=MgO) diagram of Irvine and Baragar (1971) has been used which chemically classifies the volcanic rocks into tholeiitic and calc-alkaline suites. These suites are distinguished on the basis of iron enrichment, with tholeiitic rocks containing more iron, and calc-alkaline showing iron depletion. Fig 4.4 shows samples from the western Tauranga basin are calc-alkaline, except for the Waiteariki Ignimbrite (sample 62) which is tholeiitic. Samples show an increase in iron enrichment with a reduction in silica content. The more rhyolitic rocks have less iron enrichment than the dacitic rocks.

Also plotted are data from other areas, White Island, Motiti Island, Coromandel and eastern Tauranga. The western Tauranga rocks show a similar plot to eastern Tauranga basin and Coromandel rocks except for the lower MgO contents in the andesites.

### 4.3 Major Element Chemistry

Harker diagrams are used to present data in a form where trends may represent the course of chemical evolution of a magma. Major element trends are easily seen using Harker variation diagrams, plotting SiO<sub>2</sub> wt % against other major element oxides (Fig 4.5). Silica content provides a convenient relative abscissa to show graphically the variation in concentration of other oxides, and silica correlates positively and significantly with measures of differentiation (Gill 1981).

In general, for suites of cogenetic igneous rocks, pairs of oxides are strongly correlated, either positively or negatively. Such correlations or trends may be generated as a consequence of partial melting, fractional crystallisation, magma mixing or crustal contamination, either individually or in combination (Wilson 1989).

#### 4.3.1 Rhyolites

Minden Peak rhyolite and Manawata rhyolite show similar major element plots. Their data cluster together for MgO, CaO, Fe<sub>2</sub>O<sub>3</sub>, FeO, K<sub>2</sub>O and TiO<sub>2</sub>. This may indicate a similar magmatic source.

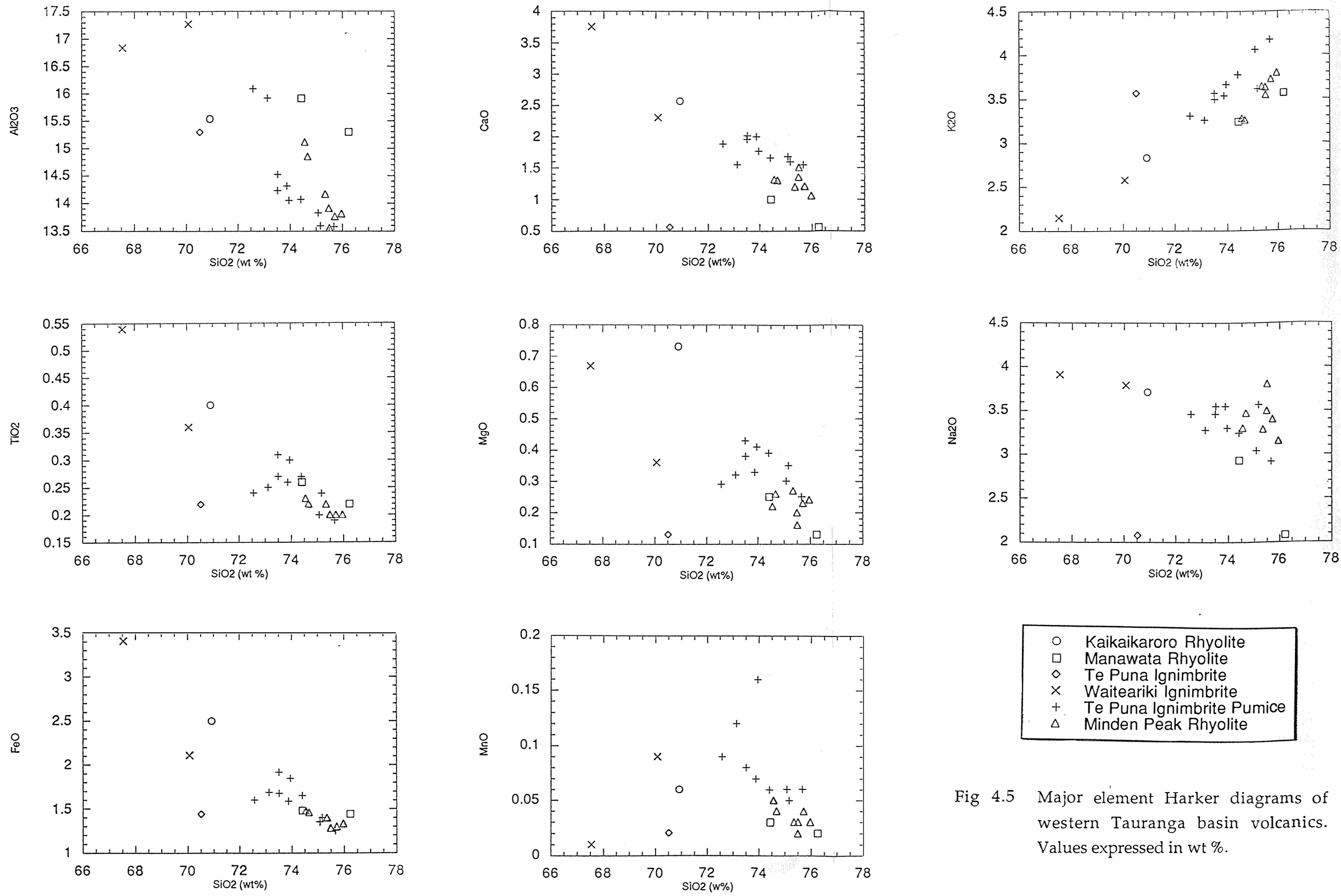


Fig 4.5 Major element Harker diagrams of western Tauranga basin volcanics. Values expressed in wt %.

Kaikaikaroro rhyolite has a lower SiO<sub>2</sub> content than Manawata and Minden Peak. Kaikaikaroro has higher Fe<sub>2</sub>O<sub>3</sub>, CaO, MgO, FeO and TiO<sub>2</sub> values and lower K<sub>2</sub>O values than the other rhyolites.

#### 4.3.2 Waiteariki Ignimbrite

Samples were taken from two different flow units within the Waiteariki Ignimbrite which vary in SiO<sub>2</sub> content. The lower unit contains cream pumice which has a fibrous texture and has a SiO<sub>2</sub> content of 70.07%. The second flow unit is moderately to densely welded with lenticular black pumice and has a SiO<sub>2</sub> content of 67.54%. The dacitic sample has higher FeO, MgO, CaO, Na<sub>2</sub>O, FeO<sub>3</sub> and TiO<sub>2</sub> values. The more rhyolitic unit has higher K<sub>2</sub>O and Al<sub>2</sub>O<sub>3</sub> values. The differences in the oxide contents may be due to differentiation, or zonation in the magma chamber resulting in the two flows having different compositions. If there was zonation in the magma chamber the deeper more dacitic layer may have been tapped first, or an injection of dacitic magma may have erupted through a more rhyolitic magma chamber.

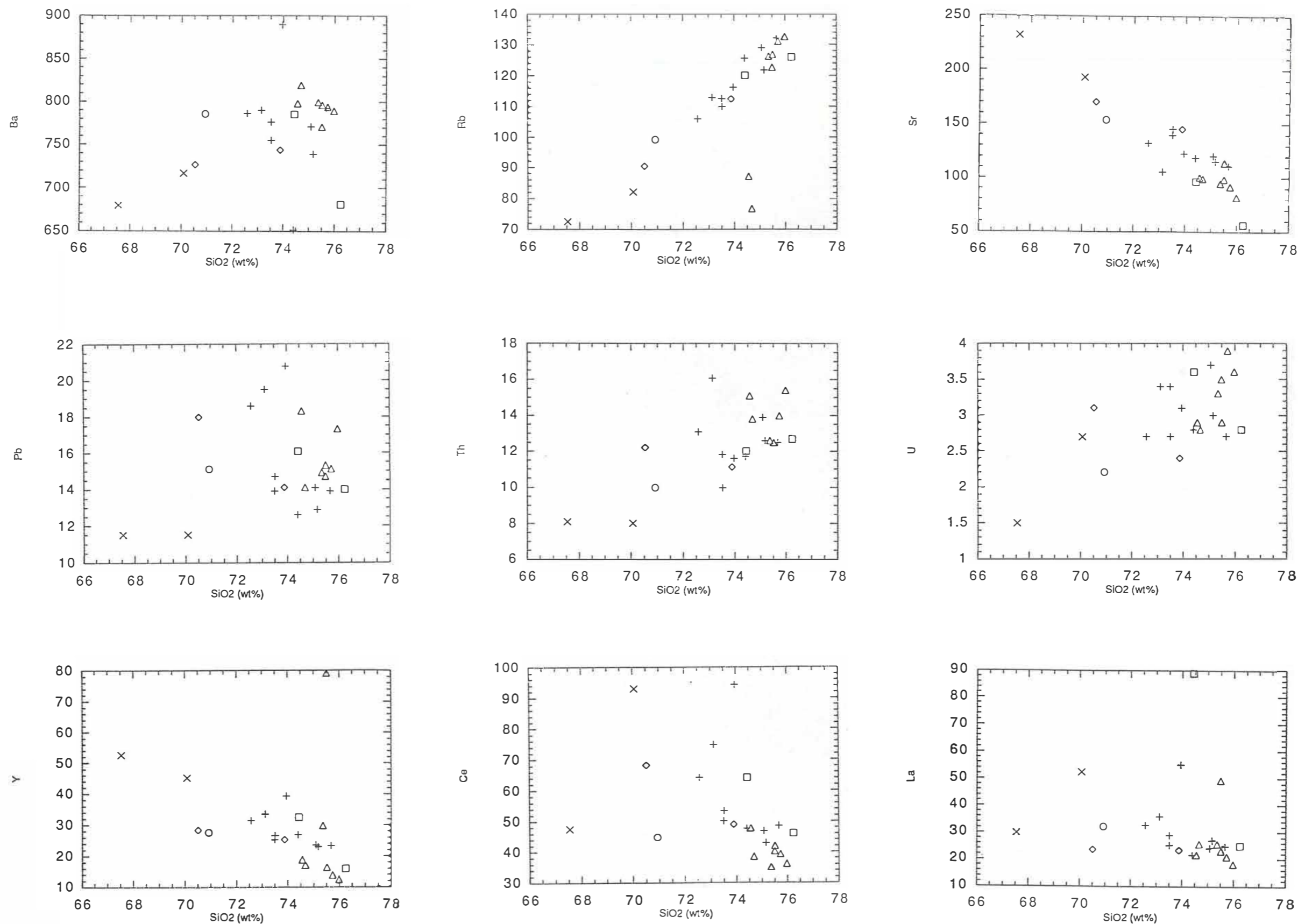
#### 4.3.3 Te Puna Ignimbrite

Pumices from the Te Puna Ignimbrite samples have different SiO<sub>2</sub> values, and range from 72.58 - 75.17% SiO<sub>2</sub>. The most SiO<sub>2</sub>-rich sample has lower K<sub>2</sub>O and higher TiO<sub>2</sub>, FeO, Na<sub>2</sub>O, CaO, K<sub>2</sub>O, Al<sub>2</sub>O<sub>3</sub> and Fe<sub>2</sub>O<sub>3</sub> values. The lower SiO<sub>2</sub> content sample has lower K<sub>2</sub>O and higher TiO<sub>2</sub>, Al<sub>2</sub>O<sub>3</sub>, CaO and Na<sub>2</sub>O values

There is a strong negative correlation in FeO, CaO, Al<sub>2</sub>O<sub>3</sub> and TiO<sub>2</sub> values and positive correlation in K<sub>2</sub>O. The negative correlation indicates that as the magma chamber becomes more SiO<sub>2</sub>-rich, a depletion in these oxides due to crystallisation of the phenocrysts. The phenocrysts are plagioclase (andesine), quartz, calcic amphibole (magnesian hornblende), hypersthene, zircon, magnetite and ilmenite.

### **4.4 Trace Element Chemistry**

A trace element is an element which is present in rocks in concentrations of up to a few thousand parts per million. Different minerals may incorporate or exclude trace elements. Their analyses can lead to constraints on the nature and



△	Minden Peak Rhyolite
○	Kaikaikaroro Rhyolite
□	Manawata Rhyolite
+	Te Puna Ignimbrite Pumice
◇	Te Puna Ignimbrite
×	Waiteariki Ignimbrite

Fig 4.6 Trace element Harker diagrams of western Tauranga basin volcanics. Values expressed in SiO<sub>2</sub> wt% and ppm.

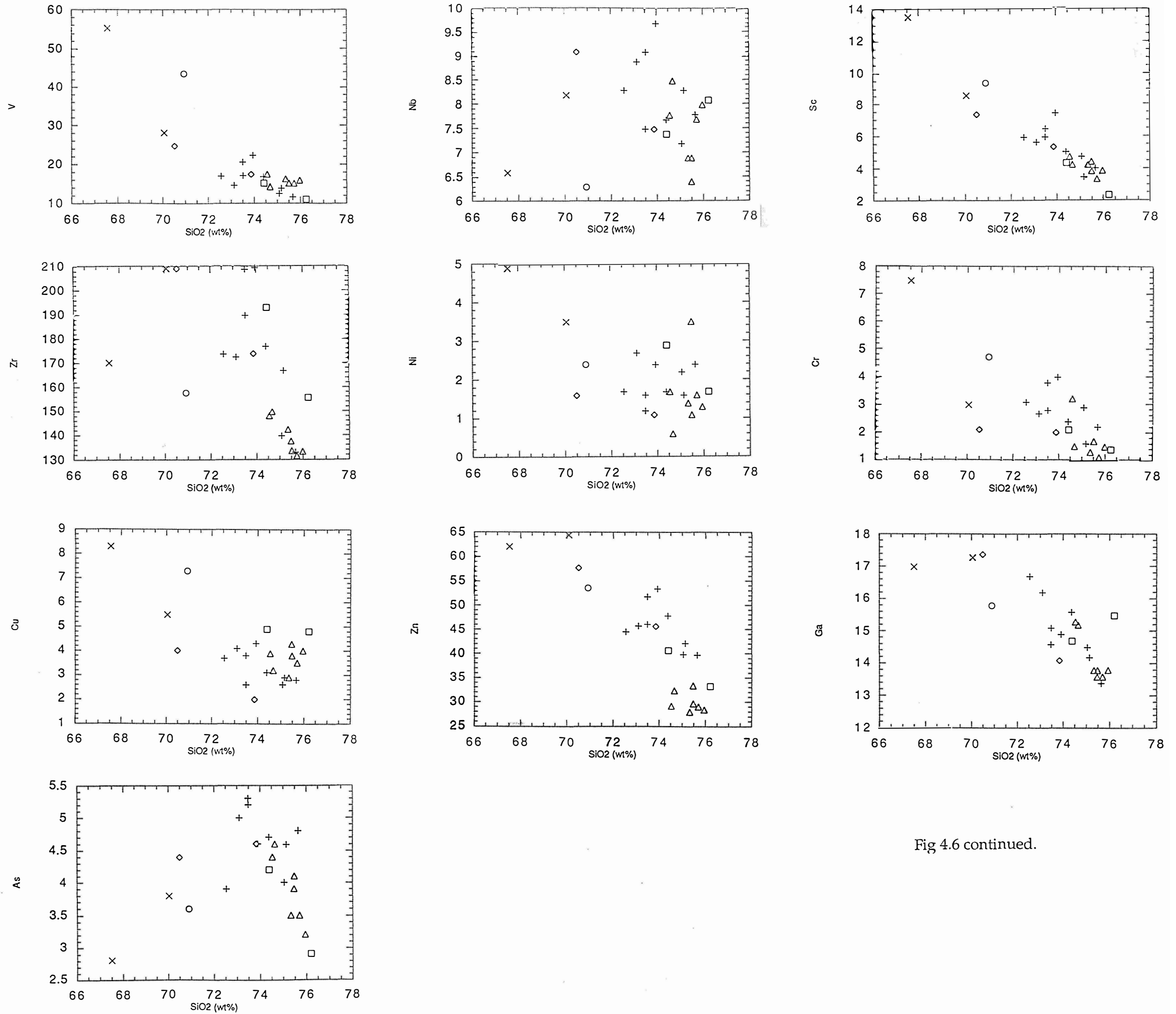


Fig 4.6 continued.

composition of the mineral assemblages with which a magma may have previously equilibrated (Cole 1979). Trace elements plotted against SiO<sub>2</sub> are shown in Fig 4.6.

Sc, Cr and V show negative correlation as these elements are compatible. Compatible elements are preferentially incorporated into crystallising solid phases and therefore their abundance reduces with increasing SiO<sub>2</sub> content. These elements tend to be concentrated in ferromagnesian minerals, than in the co-existing melt. The ferromagnesian minerals within the rocks are hypersthene, ferrohypersthene, biotite and hornblende.

Sr has a negative correlation, which is a similar trend to CaO, which is due to the fractionation of plagioclase.

Cu and Zn have negative correlation as they are compatible with ferromagnesian minerals and therefore incorporated into hypersthene, hornblende and biotite.

Rb, Th and U have positive correlations as they are incompatible elements and are not incorporated into minerals. This results in an increase in element content with increasing SiO<sub>2</sub>.

Ni is compatible and usually shows negative correlation as it is concentrated in ferromagnesian minerals.

The rare earth group (REE), La and Ce, have no correlation to SiO<sub>2</sub> and show a large degree of scatter. A few samples from La, Ce and Y having anomalously high concentrations. Ewart (1979; 1982), Reid and Cole (1983) and Graham and Hackett (1987) indicate that the maximum values for La and Y is about 30ppm, and about 50ppm for Ce. Anomalously high concentrations are found in Manawata Rhyolite with La at 89 ppm, Te Puna Ignimbrite pumice (88) and Waiteariki Ignimbrite (32) have Ce values of 93 ppm, and Minden Peak Rhyolite (41) having a Y concentration of 79 ppm.

REE enrichment, to higher degrees (eg La= 458 ppm, Y=300 ppm) have also been noted in the Kiwitiahi volcanics (Kuschel and Smith 1990; Dunbar 1991; Black et al. 1992) and in Coromandel rocks (Briggs and Fulton 1990, Hunt 1991). These rocks show no mobility in other trace elements and are not petrographically discernible from other rocks in the area. Kuschel and Smith (1990), Dunbar (1991) and Black et al. (1992) have identified submicroscopic

secondary minerals. Black et al. (1992) identified, through SEM backscattered electron imagery, localised REE and Y-enriched silicate minerals on grains of plagioclase. These secondary minerals are thought to be products of weathering or late-stage localised hydrothermal alteration (Fodor et al. 1992).

The major and trace element chemistry of the western Tauranga basin rocks show no distinct variations between the rock units. Concentrations in elements tend to suggest that the units are genetically related as no distinct compositional groups can be seen on the Harker variation diagrams. The main process which can be seen in the geochemistry of the rocks is fractional crystallisation. Several major elements and compatible trace elements show negative correlations with SiO<sub>2</sub>, which is indicative of fractional crystallisation. The major fractionating minerals are plagioclase, biotite, orthopyroxenes and hornblende. Plagioclase fractionation is shown by a negative correlation in Al<sub>2</sub>O<sub>3</sub>, CaO and Sr with SiO<sub>2</sub>. Biotite, orthopyroxenes and hornblende fractionation is shown by strong negative correlations in CaO, MgO, FeO, Sc, Cr, V, Cu, and Zn with SiO<sub>2</sub>. A correlation between SiO<sub>2</sub> and TiO<sub>2</sub> indicates the fractionation of titanomagnetite and ilmenite from the melt.

## 4.5 Spider Diagrams

Spider diagrams are plotted to show the pattern of trace elements within a rock. These diagrams can be used to compare elemental abundances between rock samples.

The abundances of a range of incompatible trace elements are normalised to estimates of their abundances in the primordial Earth. The elements plotted all behave incompatibly ( $D < 1$ ) during most partial melting and fractional crystallisation processes. The main exceptions to this are Sr, which may be compatible with plagioclase, and Ti with magnetite.

Trace elements are normalised using chondrite and primitive mantle data (Taylor and McLennan 1985) which allows comparison between rock samples. A selection of primitive mantle and chondrite normalised spider diagrams from representative Western Tauranga basin rocks are shown in Fig 4.7.

The primitive mantle plot (Fig 4.7a) shows that Ba, Rb, Th, U and K values for the different rock types increase with increasing SiO<sub>2</sub> content. This is due to the incompatible nature of these elements during differentiation which excludes them during crystal growth. Trace elements on the right hand side of the

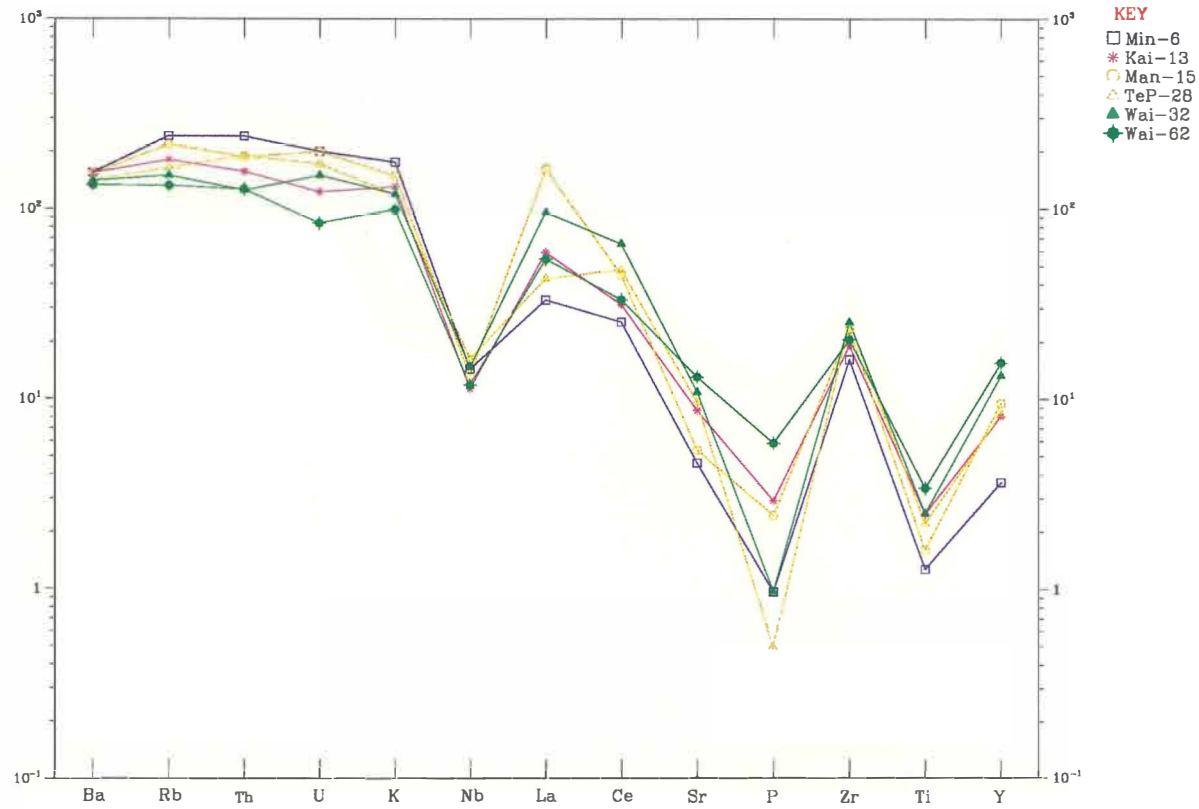


Fig 4.7a Spider diagram of trace element concentration normalised to Primitive mantle for selected Western Tauranga rocks. Values for primitive mantle are after Taylor and McLennan (1985).

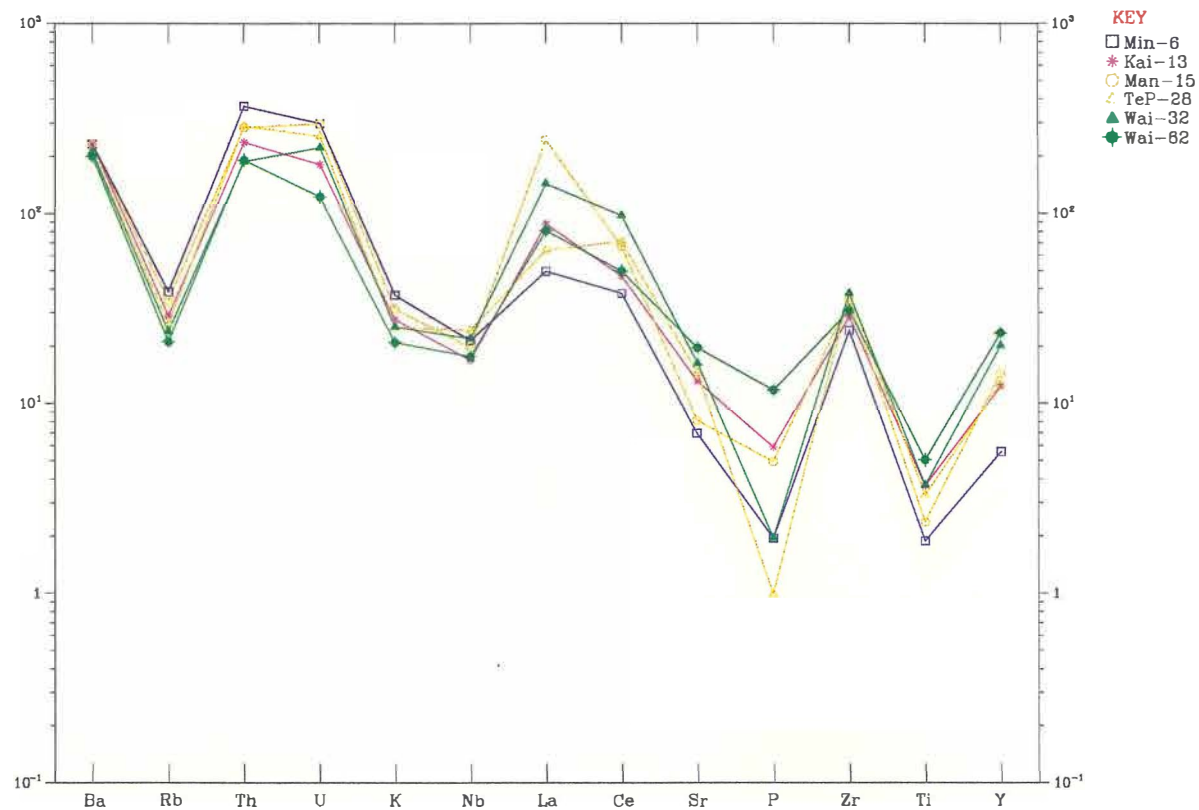


Fig 4.7b Spider diagram of trace element concentrations normalised to chondrite for selected Western Tauranga rocks. Values for chondrite are after Taylor and McLennan (1985).

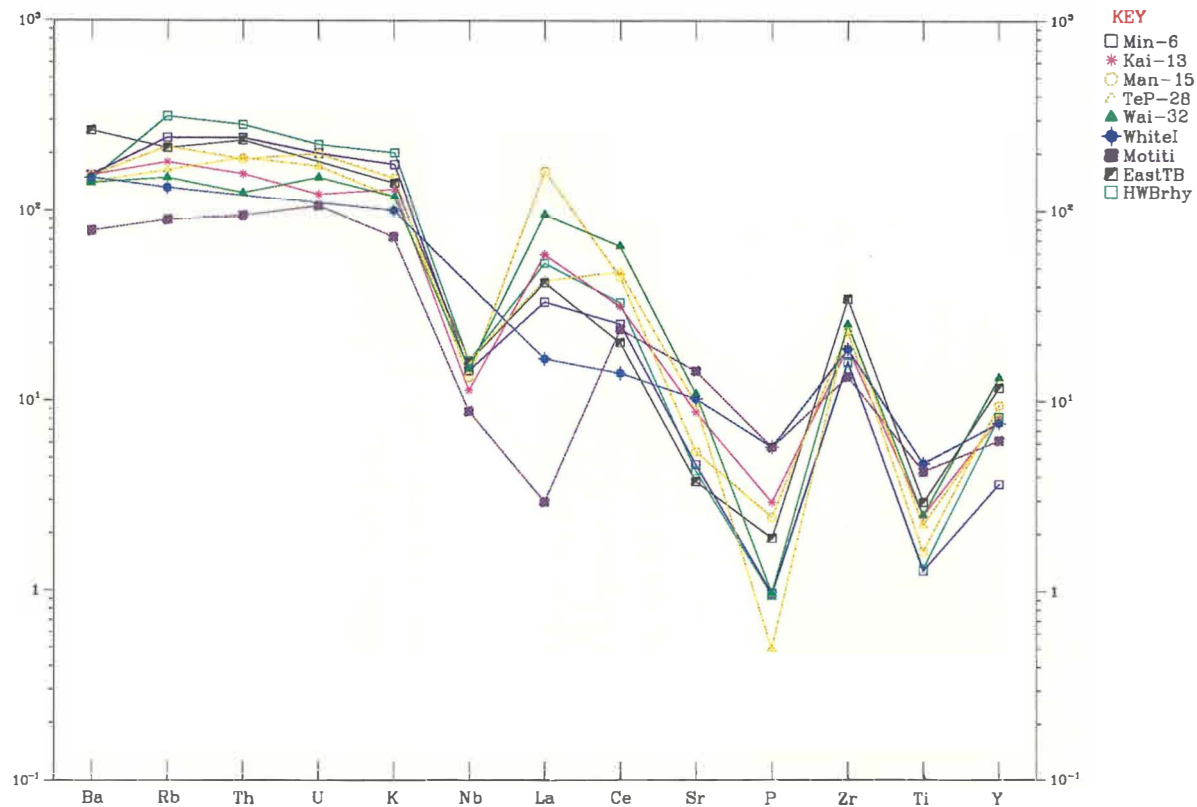


Fig 4.7c Western Tauranga rocks compared to White Island (Graham & Cole 1989), Motiti Island (Henry 1991), Coromandel (HWB) (Adams 1992), and Eastern Tauranga basin (EastTB) (Hughes 1993), normalised to primitive mantle using values of Taylor & McLennan (1985).

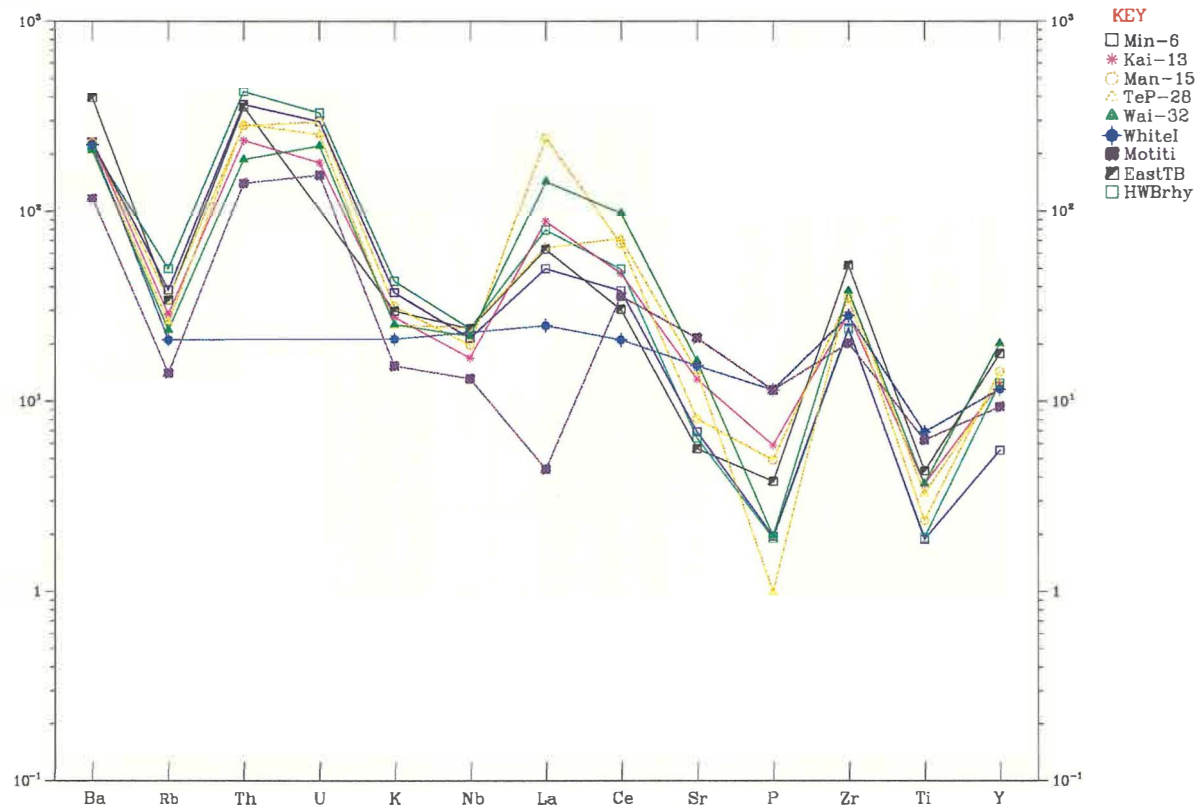


Fig 4.7d Western Tauranga basin rocks compared with White Island (Graham & Cole 1989), Motiti Island (Henry 1991), Coromandel (HWBrhy) (Adams 1992), and Eastern Tauranga basin (EastTB) (Hughes 1993) normalised to chondrite values of Taylor and McLennan (1985).

diagram are less incompatible and therefore are depleted during partial melting.

The large abundance of Zr is a characteristic, and expressed in the petrography of the rocks by the ubiquitous presence of zircon as an accessory mineral. This is also a feature of rocks in other areas, for example the Tauranga basin (Hughes 1993) and CVZ (Adams 1992) and TVZ rocks.

The depletion of Nb and Ti in both the primitive and chondrite normalised spider diagrams (Fig 4.7 a,b) is characteristic of subducted rocks. Rocks at convergent plate boundaries have lower TiO<sub>2</sub> contents than in volcanic rocks from intra-plate localities. This depletion of arc magmas in all the Ti-group elements is used to distinguish arc-derived rocks (Gill 1981). Samples from Western Tauranga basin are compared to Coromandel (Adams 1992), Eastern Tauranga basin (Hughes 1993), Motiti Island (Henry 1991) and White Island (Graham and Cole 1989) using primitive mantle and chondrite normalised trace element plots (Fig 4.7 c,d).

Motiti and White Island show different patterns to the other samples. This may be due to them being andesitic in composition compared to the more rhyolitic nature of the other rocks. Motiti Island has a depletion in La whereas the other rocks have a higher value.

Coromandel (HWB rhy) has higher incompatible elements and lower amounts of lesser incompatible elements. This may suggest that more partial melting or fractionation has occurred in these rocks.

Rhyolites from eastern Tauranga basin (East TB) plot with similar patterns to the rhyolites from within the field area. These same patterns may indicate that the rocks originated from the same magmatic source.

#### 4.6 Fe-Ti Geothermometry

The temperature and oxygen fugacity of equilibrium between coexisting magnetite-ulvospinel (spinel phase) and ilmenite-haematite solid solution (rhombohedral phase) can be obtained from the compositions of the two phases. The Computer program of Stormer (1983) was used to calculate possible temperatures of the rocks within the western Tauranga area. The program uses the model of Spencer and Lindsley (1981) and calculates the mole

fractions of ilmenite and ulvospinel using the Anderson (1968), Carmichael (1967), Lindsley and Spencer (1982), and Stormer (1983) schemes.

Temperatures of the western Tauranga basin rocks can be seen in Table 4.3. The rhyolites vary in temperature from 795-839°C. Other rhyolites within New Zealand which also contain plagioclase, quartz, hornblende, biotite and hypersthene have temperatures of 720-765°C. Their lower temperatures of crystallisation may be due to a slightly higher water content (Ewart 1979).

Waiteariki Ignimbrite (805°C) and Te Puna Ignimbrite (765-780°C) have similar crystallisation temperatures to other plagioclase, quartz, hornblende and hypersthene rocks in New Zealand and Japan (Ewart 1979).

Table 4.3 Temperatures of Western Tauranga basin rocks (after Stormer 1983).

Sample	Model			
	Stormer T °C	Anderson T °C	Carmichael T °C	Lindsley T °C
Minden Rhyolite	795	791	815	785
Kaikaikaroro Rhyolite	838	835	838	829
	839	836	839	830
Manawata Rhyolite	809	803	809	796
Waiteariki Ignimbrite	805	810	799	797
Te Puna Ignimbrite	765	770	770	761
	780	784	801	774

*Chapter Five*

**Te Puna  
Ignimbrite**

# Chapter Five

## Te Puna Ignimbrite

### 5.1 Introduction

The Te Puna Ignimbrite was first described by Harmsworth (1983) as a nonwelded to partially welded buff brown ignimbrite containing white to grey pumice. His work concentrated on the stratigraphy of this unit, and no work was undertaken on the geochemistry. This chapter examines in more detail the geochemistry of the Te Puna Ignimbrite.

### 5.2 Distribution

The Te Puna Ignimbrite is exposed at Clarke Road, Omokoroa Point, Pahoia Point, Motuhoa Island and Matakana Island. It varies in thickness from >17m at Clarke Road to 2 m at Omokoroa Point. The variation in thickness is due to the nature of the undulating pre-existing topography and suggests a low energy flow. The Te Puna Ignimbrite stratigraphically overlies lignite and underlies the Pahoia Tephra.

### 5.3 Mineralogy

The Te Puna Ignimbrite is a buff brown nonwelded to partially welded ignimbrite containing white to grey pumice within a crystal-rich (27%) matrix. Plagioclase phenocrysts are euhedral to subhedral and are andesine in composition with normal zoning (An 32-37). Hypersthene is subhedral and constitutes up to 0.4% of the rock. Amphiboles are calcic and occur as magnesio hornblende. The subhedral grains show 120/60° cleavage in cross section and are pleochroic from dark green to brown. Quartz is subhedral to anhedral and constitutes 2.8% of the rock. Fe-Ti oxides occur as titanomagnetite and ilmenite. Ilmenite contains occasional inclusions of apatite and marcasite.

Lithic abundance within the ignimbrite is low (1-2%) and consist of spherulitic grey, red, and green rhyolites, the basal flow unit of the Waiteariki Ignimbrite,

obsidian and charcoal. The red and grey rhyolite lithics have the same mineralogy as the rhyolite domes within the field area. Any of these domes may have been the source of the lithics.

## 5.4 Stratigraphic Section

A measured stratigraphic section (Fig 5.1) was selected at Clarke Road (U14 828859) on the basis of suitable vertical exposure and where the pumice was as fresh as possible for geochemical analysis.

The base of the Te Puna Ignimbrite at this location is not seen indicating that the ignimbrite is > 17 m. The ignimbrite is buff brown to light grey brown and contains white and grey vesicular pumice which has visible phenocrysts of quartz, plagioclase and hornblende. Pumice abundance varies from 20 % at the base, to 12 % at the top of the unit. Flattening ratios of the pumice are also greatest at the base of the unit.

Lithics within the section vary from 1-2 % and consist of obsidian, grey rhyolite, red brown rhyolite, black rhyolite, green-grey rhyolite, and orange hornblende dacite.

The top of Te Puna Ignimbrite is deeply eroded and overlain by 3.8 m of colluvium, tephra and Maori middens.

## 5.5 Geochemistry

Samples of pumice at 1 m intervals were taken from the stratigraphic section on Clarke Road, except where samples were inaccessible between 10-15m. These samples were analysed using XRF at Victoria University. Major and trace element geochemical data of the representative pumice samples in the Te Puna Ignimbrite are presented in Table 5.1.

Plots of geochemical data versus SiO<sub>2</sub> in Figs 5.2 and 5.3 and geochemical data versus height are shown in Figs 5.4 and 5.5.

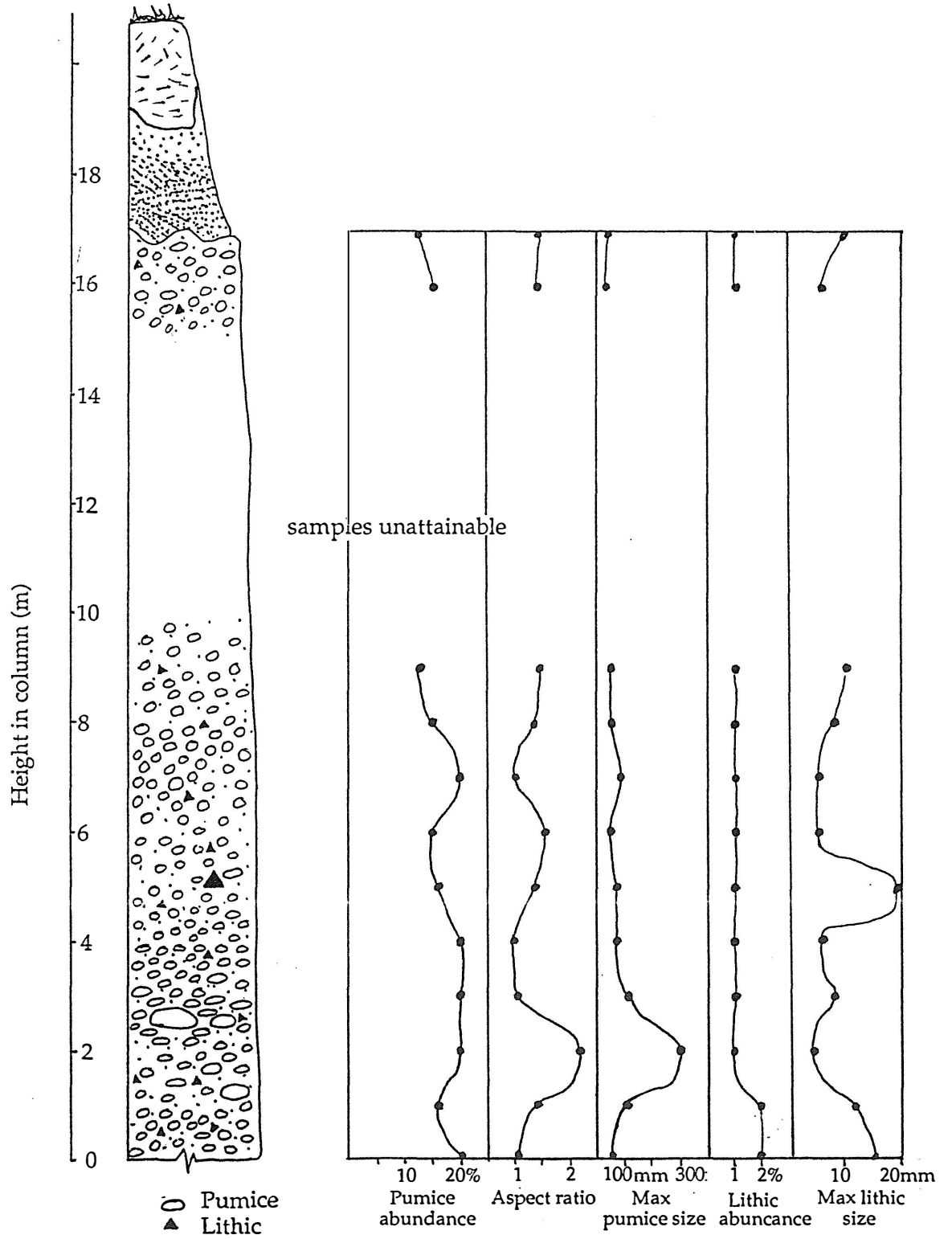


Fig 5.1 Stratigraphic Section of Te Puna Ignimbrite showing pumice and lithic abundances, Clarke Road (U14 828859)

Table 5.1 Major (wt%) and trace element (ppm) XRF compositions of pumices in the Te Puna Ignimbrite.

Sample	82	83	84	85	86	87	88	89	90	91
Height(m)	0.0	1.0	2.0	3.0	4.0	5.0	6.0	7.0	9.0	16.0
SiO <sub>2</sub>	73.87	75.67	75.09	73.51	75.17	74.41	73.96	73.52	72.58	73.13
TiO <sub>2</sub>	0.26	0.19	0.20	0.31	0.24	0.27	0.30	0.27	0.24	0.25
Al <sub>2</sub> O <sub>3</sub>	14.31	13.58	13.83	14.23	13.60	14.07	14.05	14.53	16.10	15.92
Fe <sub>2</sub> O <sub>3</sub>	0.44	0.35	0.38	0.53	0.39	0.46	0.51	0.47	0.44	0.47
FeO	1.59	1.25	1.35	1.92	1.4	1.65	1.85	1.68	1.60	1.69
MnO	0.07	0.06	0.06	0.08	0.05	0.06	0.16	0.08	0.09	0.12
MgO	0.33	0.25	0.30	0.43	0.35	0.39	0.41	0.38	0.29	0.32
CaO	2.00	1.55	1.68	1.96	1.60	1.66	1.77	2.02	1.88	1.55
Na <sub>2</sub> O	3.55	2.92	3.04	3.46	3.57	3.24	3.30	3.55	3.46	3.28
K <sub>2</sub> O	3.54	4.18	4.06	3.57	3.62	3.78	3.67	3.50	3.31	3.26
P <sub>2</sub> O <sub>5</sub>	0.02	0.01	0.01	0.01	0.01	0.01	0.02	0.01	0.01	0.01
LOI#	3.18	3.57	3.66	3.47	2.93	3.35	3.70	3.08	4.41	4.24
Total	100	100	100	100	100	100	100	100	100	100
Sc	5	4	5	6	4	5	8	7	6	6
V	18	12	13	21	14	17	23	17	17	15
Cr	2	2	3	4	2	2	4	3	3	3
Ni	1	2	2	1	2	2	2	2	2	3
Cu	2	3	3	3	3	3	4	4	4	4
Zn	46	40	40	52	42	48	54	46	45	46
Ga	14	13	15	15	14	16	15	15	17	16
As	5	5	4	5	5	5	5	5	4	5
Rb	113	132	129	113	122	126	116	110	106	113
Sr	145	111	120	139	115	118	122	145	132	106
Y	25	23	24	25	23	27	40	27	31	34
Zr	174	133	140	209	167	177	209	190	174	173
Nb	8	8	7	8	8	8	10	9	8	9
Ba	744	793	771	756	739	652	890	777	787	790
La	23	25	24	25	27	22	55	30	33	36
Ce	49	49	47	50	43	48	94	54	64	75
Pb	14	14	14	14	18	18	21	15	19	20
Th	11	13	14	12	13	12	12	10	13	16
U	2	3	4	3	3	3	3	3	3	3

#Original values

### 5.5.1 Pumice geochemistry

The chemistry of the pumice ranges from low to high silica rhyolite (72.6-75.7% SiO<sub>2</sub>) which may indicate a zonation in the magma chamber due to the large range in the SiO<sub>2</sub> content.

Positive correlation of incompatible elements and negative correlation of compatible elements indicates that differentiation has occurred (Gill 1991). Positive correlation for Al<sub>2</sub>O<sub>3</sub> and CaO may signify plagioclase fractionation.

A positive correlation for K<sub>2</sub>O implies that it behaves as an incompatible element, resulting in higher concentrations in more siliceous rocks. This is consistent with the petrography as there is no biotite or major K-bearing phase.

A negative Fe<sub>2</sub>O<sub>3</sub> correlation and a slightly negative correlation for TiO<sub>2</sub> could reflect the fractionation of titanomagnetite and ilmenite.

Sc and V show negative correlation indicating these elements are compatible. Compatible elements are preferentially incorporated into crystallising solid phases and therefore their abundance reduces with increasing SiO<sub>2</sub> content. These elements tend to be concentrated in ferromagnesian minerals, rather than in the co-existing melt. The ferromagnesian minerals within the Te Puna Ignimbrite are hornblende and hypersthene.

Sr has a slightly negative correlation, which is a similar trend to CaO, which is probably due to the fractionation of plagioclase.

Rb has a positive correlation indicating that it is an incompatible element and it is not significantly incorporated into any of the phenocrysts in the Te Puna pumice. This results in an increase in element content with increasing SiO<sub>2</sub>.

Zr has a slightly negative correlation which is due to the crystallisation of zircon which is an accessory mineral. As differentiation occurs the concentration of Zr left in the melt reduces.

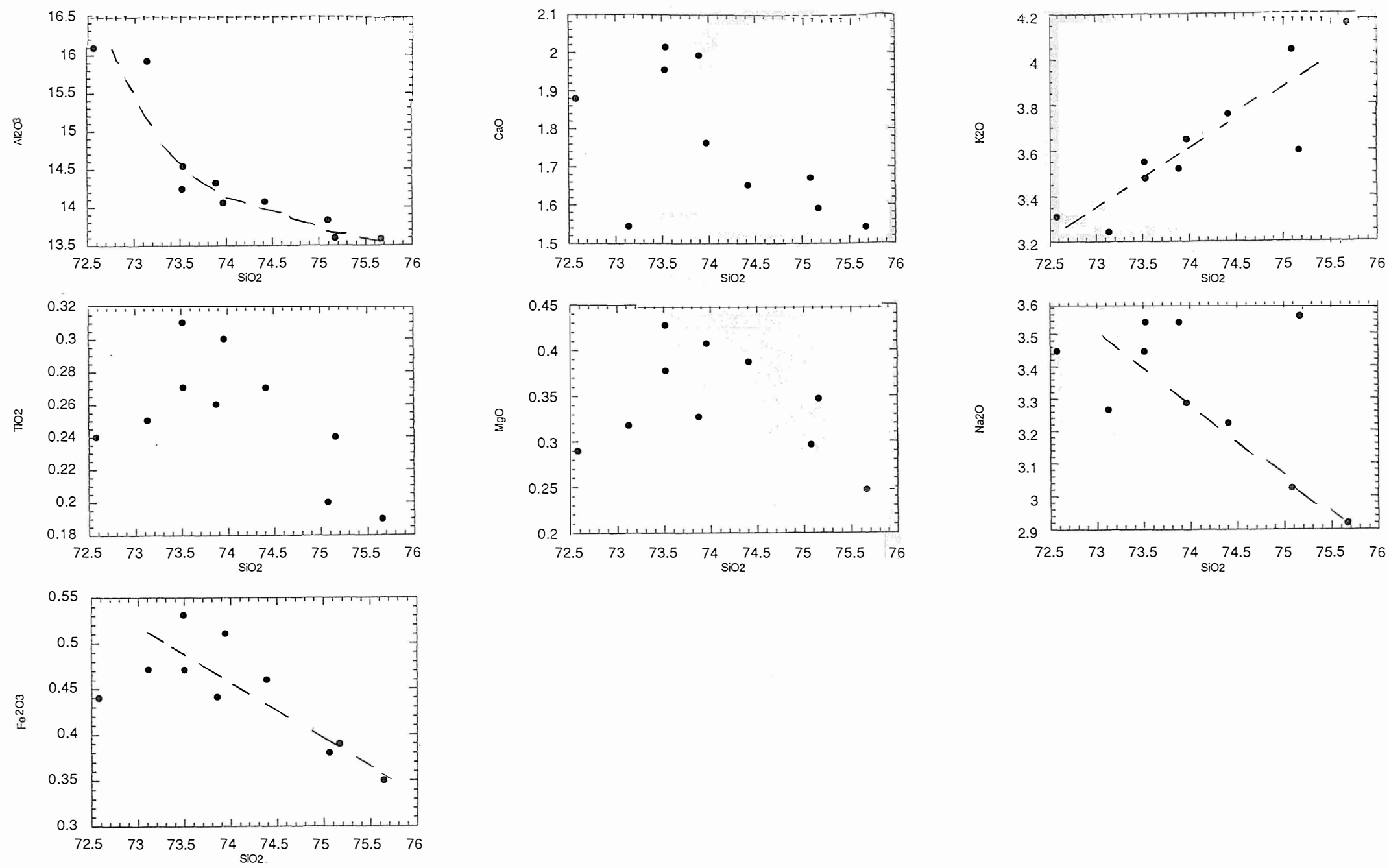


Fig 5.2 Major element concentrations (wt%) of Te Puna pumice plotted against SiO<sub>2</sub> content.

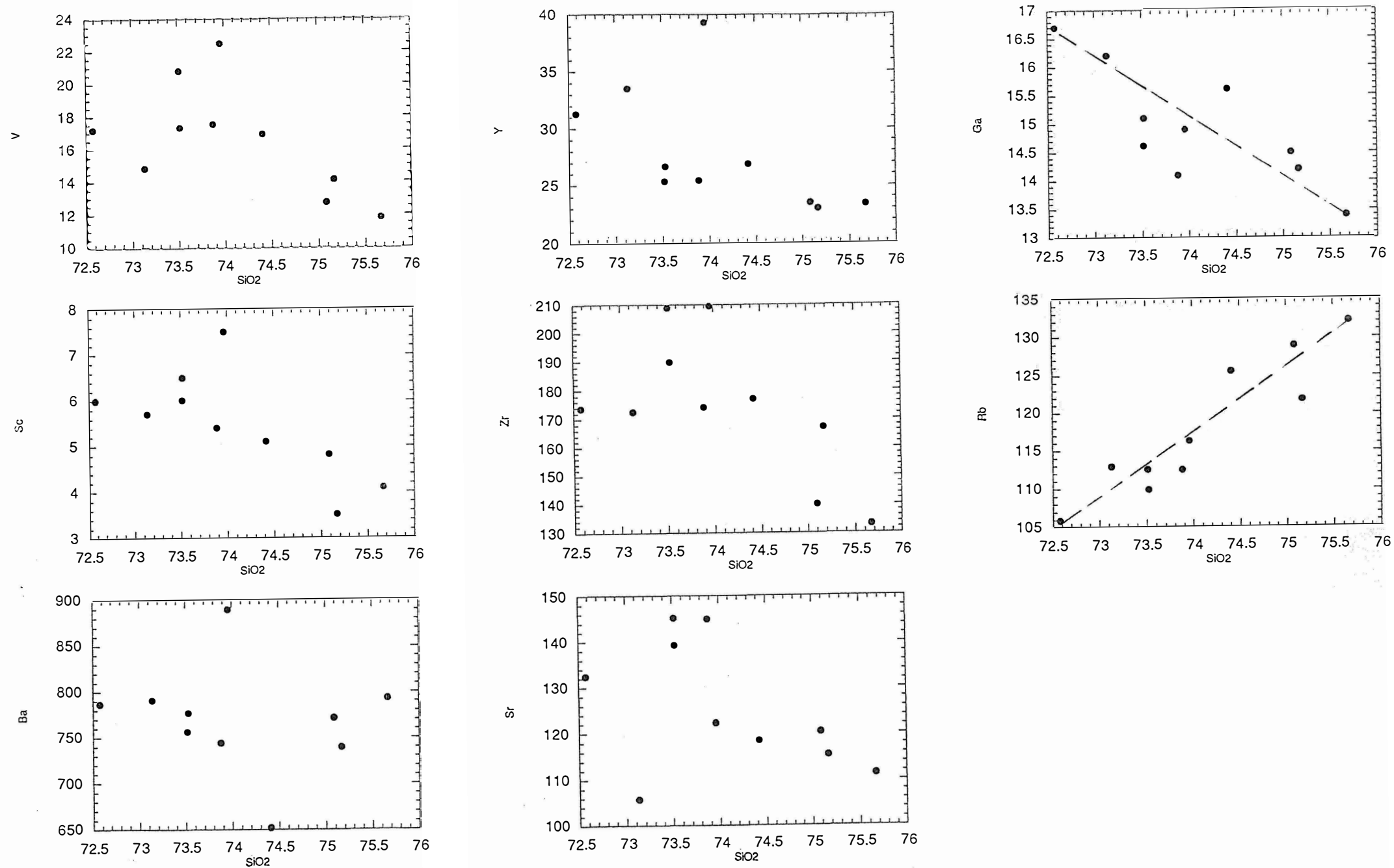


Fig 5.3 Trace element concentrations (ppm) of Te Puna pumice plotted against SiO<sub>2</sub> content.

### 5.5.2 Pumice geochemistry related to stratigraphic height

When examining the chemistry of the pumices in relation with their stratigraphic height there are a number of correlations both for major and minor elements. These correlations may be due to a zoned magma chamber.

In the major elements SiO<sub>2</sub> and K<sub>2</sub>O decrease with an increase in height, while Fe<sub>2</sub>O<sub>3</sub> increases with an increase in height. Trace elements which increase with height are Cu, La, Nb, Ga, Ce and Y, while Rb decreases with stratigraphic height.

Samples at 0.0m and 16.0m are commonly inconsistent with the trends. This may be due to mixing of the magma as they tend to plot away from the trend in the major element vs SiO<sub>2</sub> plots.

The sample at 6.0m has anomalously high abundances of Y (40 ppm), Ce (94 ppm), and La (55 ppm), however its Al<sub>2</sub>O<sub>3</sub> content is normal. Weathering or vapour-phase alteration may have caused the high abundances of the elements even though the samples look petrographically fresh. Black et al. (1992) found that samples which had anomalously high abundances of REE and Y, which petrographically looked fresh, contained secondary minerals when observed using the SEM backscattered electron imagery.

#### Theory number 1 - crystal settling in a non-convecting magma chamber

A liquid magma chamber cools with heat loss being greater towards the top of the chamber. This results in more crystallisation occurring at the top than elsewhere, so that the residual liquid composition must take on a vertical zonation. The more evolved liquid lying at the top of the chamber and the less evolved below. This results in the existence of a vertical temperature gradient in the chamber which produces higher temperature (more basic) crystals at lower levels than exist at the same time at higher levels (Cox et al. 1979).

#### Theory number 2- Convection and mixing in magma chamber

Magma chambers are multi component systems which are controlled by the size and shape of the chamber, the density and viscosity of the magma and by processes which operate at the boundaries of the chamber (Wilson 1989).

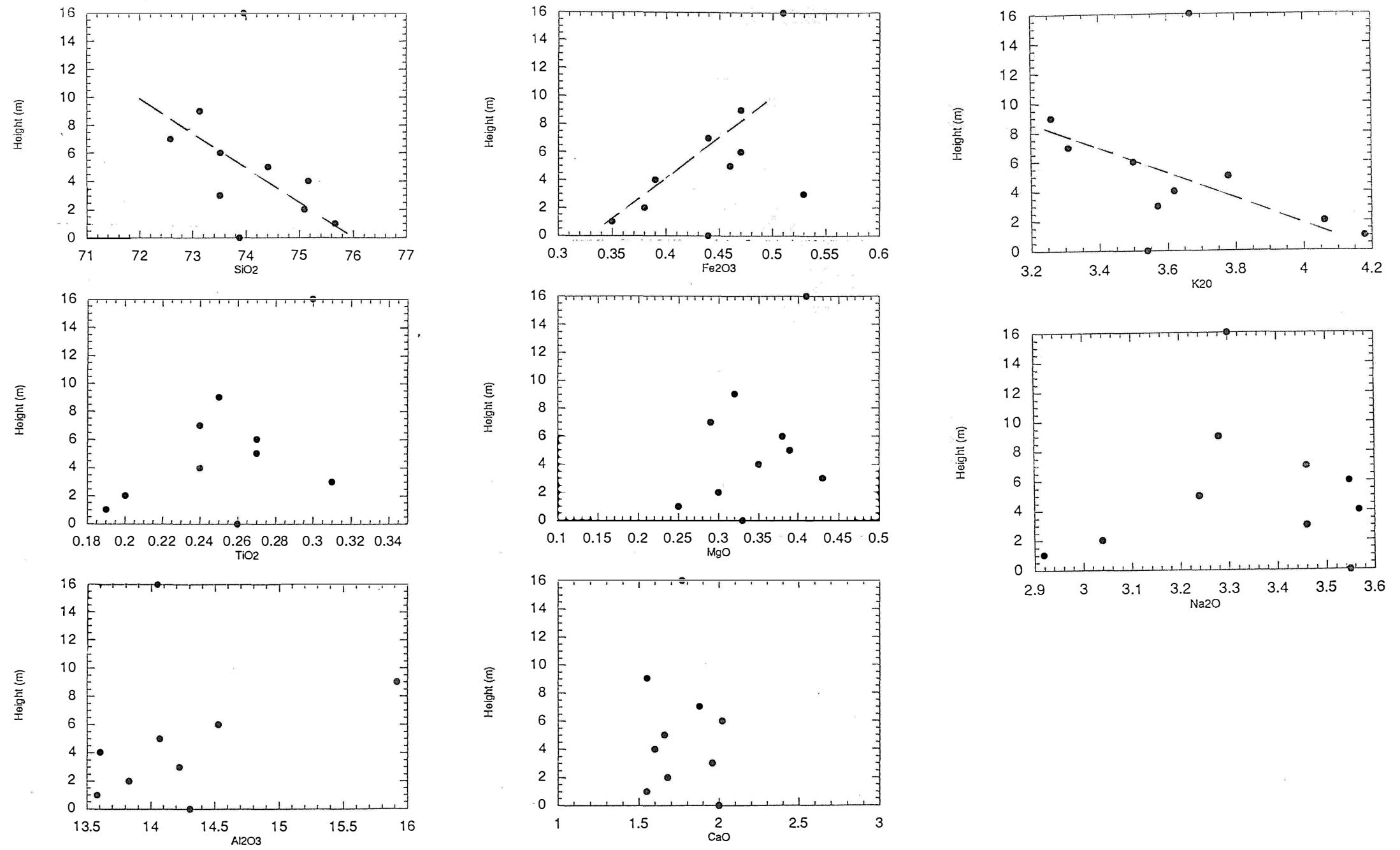


Fig 5.4 Major element concentrations of Te Puna pumice plotted against stratigraphic height. Major elements in wt %.

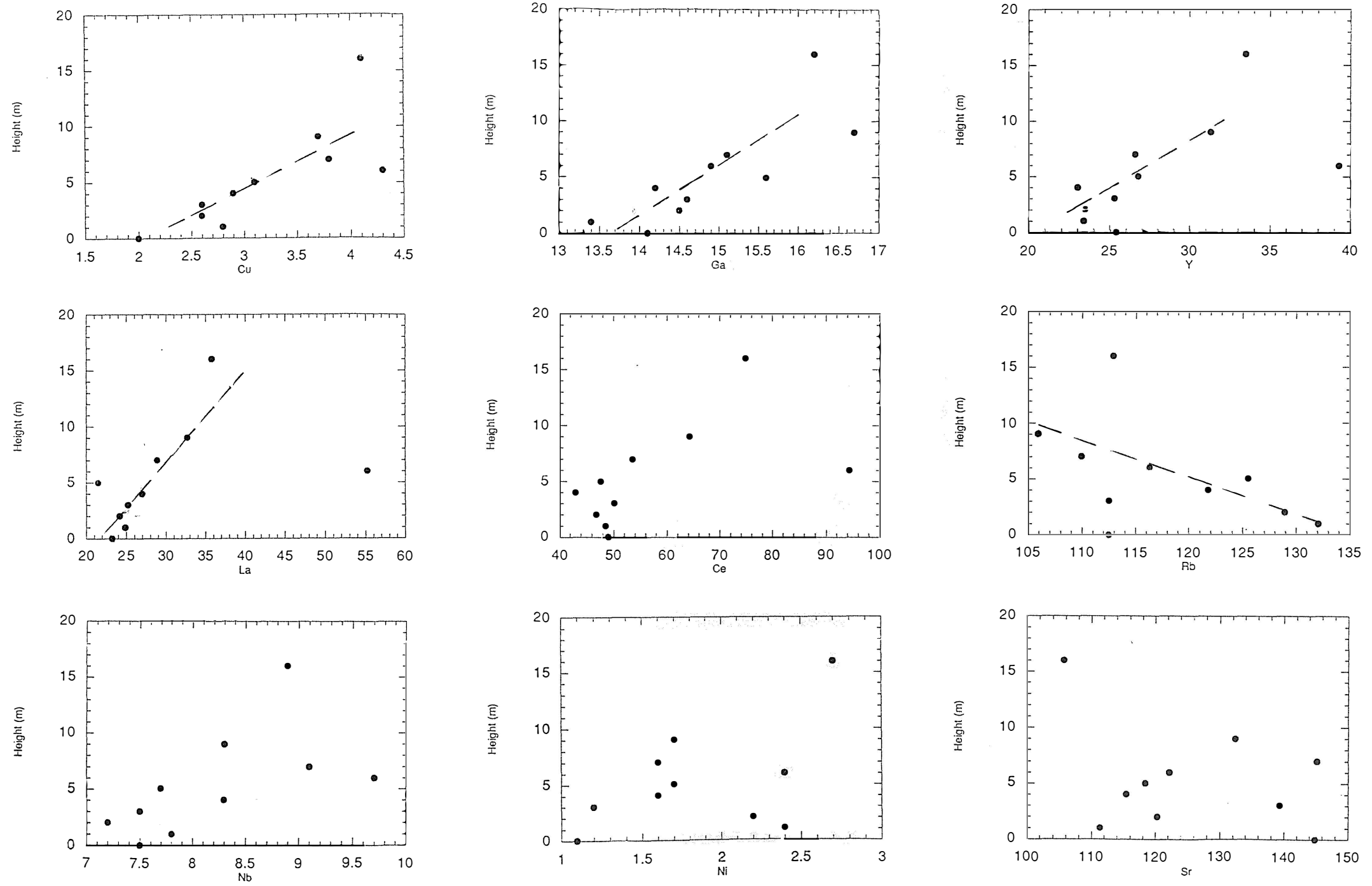


Fig 5.5. Selected trace element concentrations (ppm) of Te Puna pumice plotted against stratigraphic height.

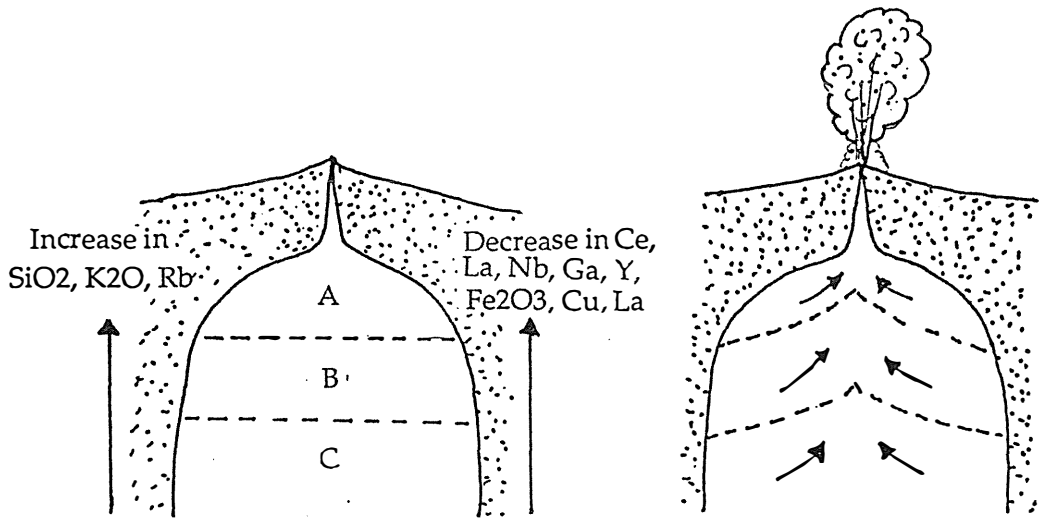
When crystallisation occurs in a magma the fluid next to the growing crystals may become either enriched or depleted in heavy components, depending upon the minerals crystallising. The density of this layer will therefore be different from that of the main chamber magma. As a result, the liquid will convect away from the crystal faces. Fluids may become vertically stratified with respect to density, composition and temperature (Wilson 1989).

## 5.6 Inversion of the Magma Chamber

Upon eruption the magma chamber may be inverted within the ignimbrite (Fig 5.6). In the magma chamber where SiO<sub>2</sub> increases near the top it increases towards the base of the ignimbrite. This occurs as magma is withdrawn from the top of the magma chamber first. However during the eruption the zoned magma chamber may be disrupted and mixing of the layers may occur.

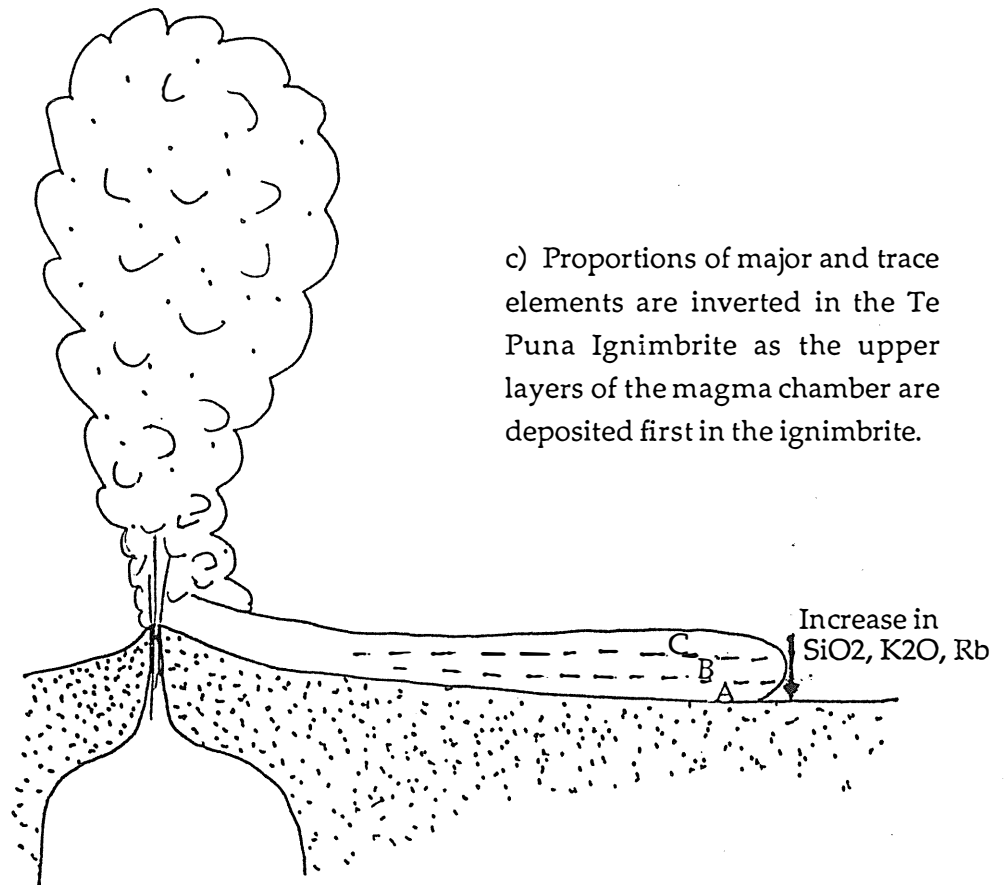
Blake and Ivey (1986) through modelling found that the liquid being sampled from a draining reservoir of density-stratified fluid, such as an erupting zoned magma chamber, is derived from a relatively thin withdrawal layer adjacent to the level of the chamber outlet. This is a consequence of the buoyancy force associated with the density gradient inhibiting vertical motion so that the opportunity for widely separate density levels to be tapped and mingled syneruptively is suppressed. If the caldera collapse distance is much greater than the withdrawal layer then the selective withdrawal process leads to successive levels of the chamber being skimmed. This allows the compositional stratigraphy of the chamber to be inverted by the eruptive processes, with little opportunity for syneruptive mixing between diverse magma compositions.

The sample at 0.0m has a lower SiO<sub>2</sub> content than the expected trend. This may be due to an injection of material into the magma chamber which has caused less SiO<sub>2</sub> rich magma to be erupted first. The sample at 16.0m also does not follow the trend. This layer may have been at the end of the eruption where the magma within the magma chamber has become highly disrupted and more SiO<sub>2</sub> magma than expected is erupted.



a) Zonation of the major and trace elements within the magma chamber

b) Upon eruption, magma is tapped from the top layers and progressively taken from greater depths.



c) Proportions of major and trace elements are inverted in the Te Puna Ignimbrite as the upper layers of the magma chamber are deposited first in the ignimbrite.

Fig 5.2 Inversion of a zoned magma chamber within the erupted Te Puna Ignimbrite.

## 5.7 Previous studies into zoned magma chambers

Zonation in magma chambers, particularly from acidic ignimbrites have been described by Smith and Bailey (1965) in the Bandelier Tuff, Lipman (1967) from the Aso caldera, Schuraytz et al. (1989) in the Topopah Spring Tuff in southwest Nevada, and Vogel et al. (1989) in the Black Mountain Volcanic Centre.

Within New Zealand very few ignimbrites derived from zoned magma chambers have been identified. Ewart (1965) found that in the Whakamaru ignimbrite there was a reversal of the magma chamber in the two ignimbrite sheets, with mineral abundances and elemental abundances altering with height.

Blake et al. (1992) suggests a three-layered stratified chamber from andesite at the base to rhyodacite to rhyolite at the top as the source of the Waimihi eruption from Taupo. The zonation occurred due to the injection of andesite into a rhyolite chamber and mixing to form a rhyodacite layer. The eruption tapped the magma chamber which preferentially withdrew the layers of lowest density. The extent to which the dense layers are tapped being governed by the thickness of overlying layers and the withdrawal rate. A chamber with a thin cap and high discharge rate favoured the lower layers being tapped.

Briggs et al. (1993) investigated the mineralogy, geochemistry and isotopic composition of the pumice clasts in ignimbrites from the Mangakino volcanic centre. They found that the magma chamber was originally zoned, shown by trends in major and trace elements, but the zonation was disrupted during eruption of the ignimbrites when mixing occur.

## 5.8 Discussion

The Te Puna Ignimbrite is one of only a few known ignimbrites which have originated from a zoned magma chamber in New Zealand in which the magma erupted by simple inversion of the magma chamber from the top down. The major and trace element chemistry show zonation as their abundances vary with stratigraphic height. The ignimbrite represents a simple inversion of the magma chamber as mixing does not occur to any large extent.

## *Chapter Six*

# Summary

## Chapter Six

# Conclusions

The Western Tauranga basin is an area which is bounded to the west by the Kaimai Range and to the south by the Whakamarama Plateau which dips into the basin. The major features within the area are three rhyolitic domes. These domes are surrounded and lapped on to by the Waiteariki Ignimbrite which becomes progressively eroded in a northerly direction. To the north, peninsulas extend out into the Tauranga Harbour which contain the Te Puna Ignimbrite, volcanic fluvial material from the Matua subgroup, which are overlain by the Pahoia tephra, Hamilton Ash and tephra from the Taupo Volcanic Zone.

The oldest unit consists of three rhyolite domes which are aligned in a north-northeasterly direction which suggests that their alignment may be fault controlled. The rhyolites, Minden Peak, Manawata and Kaikaikaroro form complexes of domes and lavas.

Minden Peak Rhyolite contains plagioclase (within the andesine range), quartz, calcic amphibole (magnesian hornblende), orthopyroxene (hypersthene and ferrohypersthene), biotite, titanomagnetite, ilmenite and zircon. Kaikaikaroro Rhyolite consists of andesine, quartz, tschermakitic hornblende, biotite, hypersthene and ferrohypersthene, titanomagnetite, ilmenite and zircon. Manawata Rhyolite contains andesine, quartz, tschermakitic hornblende, hypersthene, biotite, titanomagnetite, ilmenite and zircon.

Minden Peak and Manawata rhyolite are similar in chemical composition with Kaikaikaroro contains higher amounts of  $\text{Fe}_2\text{O}_3^*$ , CaO, MgO,  $\text{TiO}_2$  and lower  $\text{SiO}_2$ .

Waiteariki Ignimbrite is younger than the rhyolites and has a fission track age of  $0.84 \pm 0.11$  Ma (Kohn 1973). The Waiteariki Ignimbrite forms the dipping Whakamarama plateau and surrounds and laps onto the rhyolite domes. The ignimbrite is crystal-rich (30%) and is divided into three flow units which have different degrees of welding. Within the field area the lower flow unit of the Waiteariki Ignimbrite is light grey-brown with 20% lenticular cream pumice. Flow unit two is densely welded and contains black lenticular pumice. It contains crystals of plagioclase (varying from oligoclase to labradorite), quartz,

orthopyroxene (hypersthene and ferrohypersthene), calcic amphibole (magnesian hornblende and tschermakitic hornblende), biotite, zircon, titanomagnetite and ilmenite.

Samples from the two different flow units from within the Waiteariki Ignimbrite vary in geochemistry. The lower sample stratigraphically, is higher in SiO<sub>2</sub> content (70.1%) than the younger flow unit with 67.5% SiO<sub>2</sub>. This may indicate that the magma chamber was zoned and that inversion of the magma chamber occurred on eruption resulting in a more rhyolitic flow overlain by a dacitic flow.

The Matua Subgroup overlies the Waiteariki Ignimbrite and contains lignite and fluvial sediments. The fluvial sediments are predominantly volcanic in origin and comprise of pumice and ash.

The Te Puna Ignimbrite is a nonwelded to partially welded buff brown ignimbrite. It contains 15-20% white to grey pumice in a crystal-rich (27%) matrix. The ignimbrite was deposited into a swamp or estuarine environment as it overlies fluvial material and lignite from the Matua subgroup. The crystals within the ignimbrite are plagioclase (An 30-39.5), quartz, hypersthene, calcic amphibole (magnesian hornblende), titanomagnetite, ilmenite and zircon.

Pumices from within the Te Puna Ignimbrite have different SiO<sub>2</sub> contents (72.58-75.67%), which vary stratigraphically, tending to decrease with stratigraphic height. This indicates that the magma chamber was zoned and therefore varied in SiO<sub>2</sub> composition with more silicous magma near the top of the chamber. Upon eruption magma was withdrawn from the top of the magma chamber and inverted into the ignimbrite. This resulted in more SiO<sub>2</sub> rich pumice at the base of the stratigraphic column, compared to the top.

The rocks within the western Tauranga basin are calc-alkaline in composition except for the middle flow unit in the Waiteariki Ignimbrite which is tholeiitic. The rocks distribution on the AFM diagram (Irvine and Baragar, 1971) plot in a similar manner to rocks from Coromandel and eastern Tauranga basin, this shows that the rocks have similar amounts of iron and MgO. On chondrite and primitive mantle normalised spiderdiagrams, the rocks from western Tauranga basin have similar incompatible trace element contents to those of eastern Tauranga rocks, but higher incompatible trace elements contents than the Coromandel rocks. This suggests that the eastern and western Tauranga basin rocks are likely to have formed from the same processes. Their similar

proportion of incompatible elements are likely to be due to similar amounts of differentiation of the magma or partial melting of the crust.

## 6.1 Tectonic Setting

New Zealand is an active continental margin where oceanic crust (Pacific Plate) is subducted beneath continental crust (Australian Plate). As the subducted plate melts, magma rises which may cause partial melting of the continental crust. This causes continental margin magmas to be more silica-rich than those in island arcs (which contain no continental crust). In any destructive plate margin environment the nature and distribution of magmatic activity in the overriding plate is directly linked to the geometry of the subducted slab, which is a function of the convergence rate of the lithospheric plates and the age of the subducted lithosphere (Wilson 1989).

Within the North Island the present volcanic arc is expressed in the Taupo Volcanic Zone which extends from Mt Ruapehu to White Island. This volcanic arc is thought to have migrated with time as the ages of the rocks tend to become younger from Whangarei to Taupo (Kear 1959, Brothers 1984, Ballance 1986). Migration of the volcanic front in the North Island is suggested to be the result of plate rotation and migration southward and south westward in the last 25 Ma. With an increase in plate motion the direction of the volcanic front has become more easterly with time (Kamp 1992).

Kear (1959) noted an apparent south-eastward migration of volcanism with time across the northern and central North Island based on K/Ar ages of rocks with low-K andesite character. Brothers (1984) using additional ages constructed time lines which represent the oldest dated rocks, and thus the initiation of volcanism at each volcanic centre throughout the northern North Island. This gave western Tauranga basin rocks an approximate age of 3 Ma. He proposed that the steepening of the subducting plate from the Miocene resulted in the migration of calc-alkaline volcanism from Tokatoka and Whangarei to Taupo in a NE-SW orientation.

Ballance (1976) and Ballance et al. (1982) define six spatially separated magmatic arcs since 20 Ma when the Australian-Pacific plate boundary spread through the North Island. Stern (1987) suggests that the movement of the active volcanic front is not just migrating at 20 mm/y but also a rotation of 30° has occurred over the last 4 Ma (Fig 6.1).

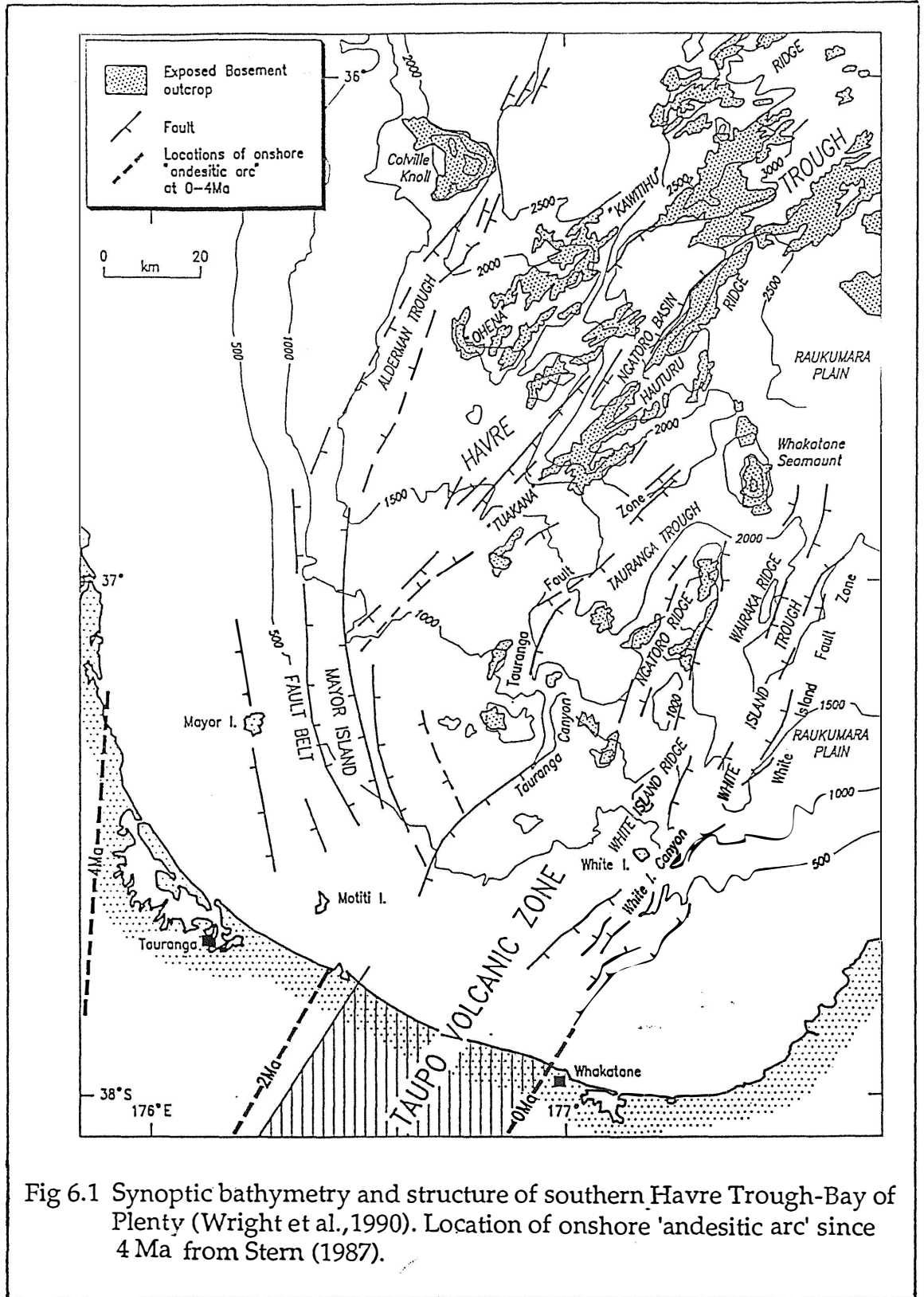


Fig 6.1 Synoptic bathymetry and structure of southern Havre Trough-Bay of Plenty (Wright et al., 1990). Location of onshore 'andesitic arc' since 4 Ma from Stern (1987).

Kamp (1984) used the  $K_2O-h$  parameter of depth of magma generation together with age distribution of andesites to define the geometry of the subducting slab. However, using the  $K_2O-h$  relationship may not be correct (Reynors 1990) as the  $K_2O$  abundance in basalts and andesites is also controlled by other magmatic processes other than depth. These processes may be partial melting, crystal fractionation or crustal contamination.

Ballance et al. (1985) and Ballance (1988) challenged Brothers and Kamp's isochrons as some of the ages used for isochrons did not represent the initial eruptions from the areas. Also within the Coromandel Peninsula the dates may not be correct due to hydrothermal alteration which alters the age of the rock.

Karig (1970) suggested that the Tonga, Kermadec and Taupo arcs formed part of a single arc system and the arc continued directly into the North Island, into the Taupo Volcanic Zone. However, Cole (1978) considered that the arcs were separate and that the Havre Trough, an active intraoceanic back-arc basin, extended south-westward into the Ngatoro Basin intersecting the coast of New Zealand at Tauranga and not the Taupo Volcanic Zone (Fig 6.1).

Feden et al. (1976) suggests that the Havre Trough developed at about 5 Ma and this resulted in tensional graben structures and active marginal basins, initially on the eastern side of Coromandel, later (2-3Ma) forming the volcanism in the Tauranga area, and finally the Taupo Volcanic Zone.

In offshore Bay of Plenty, the basement structure is comprised of a series of parallel basement ridges and basins aligned in a NE-SW direction (Wright 1992) (Fig 6.1). Within the field area in the western Tauranga basin the alignment of the rhyolite domes is in a north-northeasterly direction. The domes alignment may be due to faulting in the basement rock which may represent an onshore continuation of the Ngatoro Basin.

Wright et al. (1990) found through a side-scan sonar survey in the Bay of Plenty, that the Havre Trough tectonism and volcanism relates to a series of laterally discontinuous, multiple spreading rifts which terminate southward at the 3 km deep Ngatoro Basin. A 45 km sinistral offset, attributed to an en echelon synthetic shearing, separates the basin from the actively spreading Taupo Volcanic Zone. Before plate movement and rotation caused the en echelon synthetic shearing the volcanic front would have been centred in the Tauranga area. With plate movement and rotation the volcanic front would have migrated southward into the present day Taupo Volcanic Zone.

## 6.2 Comparison of the Tauranga basin to other Volcanic Zones

The Tauranga basin includes the western and eastern Tauranga basin which was studied by Hughes (1993). The Tauranga basin is cited between the Coromandel Volcanic Zone (CVZ) and the Taupo Volcanic Zone (TVZ) and may represent the migration of the volcanic front from north to south. The CVZ ranges in age from 18 Ma at its northern extent to 3 Ma to the south (Skinner 1986). Within this zone the ages of the rocks become progressive younger towards the south. The Tauranga basin has relatively few ages and some may be unreliable as fission track analyses were undertaken on volcanic glass. Volcanic glass may give incorrect ages if devitrification of the glass has occurred. The estimated age is between 2-4 Ma. Currently the Institute of Geological and Nuclear Science is dating rhyolites and ignimbrites from within the Tauranga basin and Kaimai Range by Ar/Ar dating, which will give a better age restraint on the zone. The TVZ is younger than the Tauranga basin with an age of < 1.6 Ma (Pringle 1992).

The mineralogy of the rhyolites varies within the three zones. Coromandel rhyolites (Adams 1992) contains plagioclase (oligoclase-labradorite), rare sanidine, calcic amphibole, hypersthene, augite, biotite, quartz and zircon. Western Tauranga rhyolites contain andesine, magnesio-hornblende, tschermakitic-hornblende, hypersthene-ferrohypersthene, biotite, quartz and zircon.

Rhyolites of the TVZ (Ewart 1979) contain plagioclase (labradorite to oligoclase), rare sanidine, hypersthene-ferrohypersthene, augite, cummingtonite, hornblende, biotite, quartz and zircon.

The CVZ and TVZ range in composition from basalt to rhyolite with numerous ignimbrites. Tauranga basin has andesite to rhyolite and numerous ignimbrites with basaltic andesite pumice found within the Papamoa Ignimbrite (Hughes 1993).

Within the three areas the trace element chemistry ratios of Ba/La, Ba/Nb, K/Rb and Rb/Sr show that the Tauranga basin dacites are in between the values for the CVZ and the TVZ (Table 6.1). This shows that the Tauranga basin has features of both zones which was also noted by Hughes (1993). The rhyolite ratios are generally within the range of both the CVZ and TVZ.

Table 6.2 Comparison of incompatible trace element ratios for the CVZ, Tauranga basin and TVZ after Hughes (1993). Data for CVZ adapted from Briggs and Fulton (1990), Eastern Tauranga Basin from Hughes (1993), and TVZ from Cole and Graham (1989), Reid and Cole (1983) and Ewart (1979). \*=K/Ar ages from Skinner (1986), # = Ar/Ar ages from Pringle et al. (1992).

	Coromandel Volcanic Zone	Tauranga basin		Taupo Volcanic Zone
		Western Tauranga basin	Eastern Tauranga basin	
Age Range	3-18 My*		2-3 My*	0-1.6 My#
Dacites				
Ba/La	11-19	22	34-51	63-84
Ba/Nb	107-123	97	62-88	62-70
K/Rb	226-230	244	227-341	223-576
Rb/Sr	0.41-0.43	0.31	0.27-0.42	0.05-0.46
Rhyolites				
Ba/La	20-34	24-48	14-52	25-33
Ba/Nb	88-99	85-131	92-155	110-152
K/Rb	228-237	224-312	160-240	186-244
Rb/Sr	1.89-4.44	0.64-2.21	0.56-3.24	0.98-2.89

### 6.3 Caldera Identification

The Coromandel Volcanic Zone and the Taupo Volcanic Zone are dominated by silicic volcanism and contain several calderas. Within the Tauranga basin the presence of rhyolite domes and flows and ignimbrites suggest that caldera formation is likely to have occurred. Rhyolite calderas can be recognised by a number of features, including:

- a Geophysically defined subcircular basement depressions indicated by gravity anomalies,
- b Late-stage rhyolite domes and flows which lie within or at the margins of the caldera, forming intracaldera complexes or arcs of domes along ring fractures,
- c Hydrothermal systems including epithermal mineral deposits,

- d A variety of caldera-fill or moat deposits eg lake sediments, fluvial epiclastic sediments, caldera-collapse or post-collapse breccias,
- e Circular or arcuate structures observed by remote sensing techniques
- f Thick intracaldera ignimbrites and co-ignimbrite breccias, and thin outflow sheets (Cas and Wright 1987).

Hughes (1993) proposed a possible caldera which linked rhyolite domes, faults and hydrothermal systems in the eastern Tauranga basin.

## 6.4 Evidence for the Katikati Caldera

The western Tauranga basin shows no surface expressions of a caldera. Nevertheless, the Te Puna Ignimbrite which outcrops in the area is likely to be the result of caldera collapse, and there is some evidence for a caldera based on the above features.

Geophysical data from gravity maps of the Tauranga area (Woodward and Ferry 1973) show a large negative isostatic vertical gradient anomaly east of Katikati in the Tauranga Harbour (Fig 6.2), and isostatic and Bouguer anomaly maps show low values also east of Katikati. A negative anomaly can indicate a caldera as it gives a lower value than expected due to the low density nature of the pyroclastic material which infills the caldera. The anomaly is  $<-40$  Eotvos which is the same value as over the Okataina, Reporoa and Mangakino calderas. This large negative anomaly may therefore be indicative of a caldera.

On Matakana Island there are very finely layered lake sediments, indicating that fine material settled out of still water as apposed to a stream or river. These sediments overlie the Te Puna Ignimbrite. The lake sediments may represent moat deposits within the caldera. These occur due to formation of the caldera, resulting in a depression, from which water can not drain and therefore a lake forms.

A dacitic dome occurs at U14 788952 just southwest off Matakana Island. This dome may represent a late-stage dacite dome which lies within or at the margins of the caldera.

The thin outflow sheet which is associated with the caldera may be the Te Puna Ignimbrite. At its thickest point it is  $>16$ m and 2m at its thinnest.

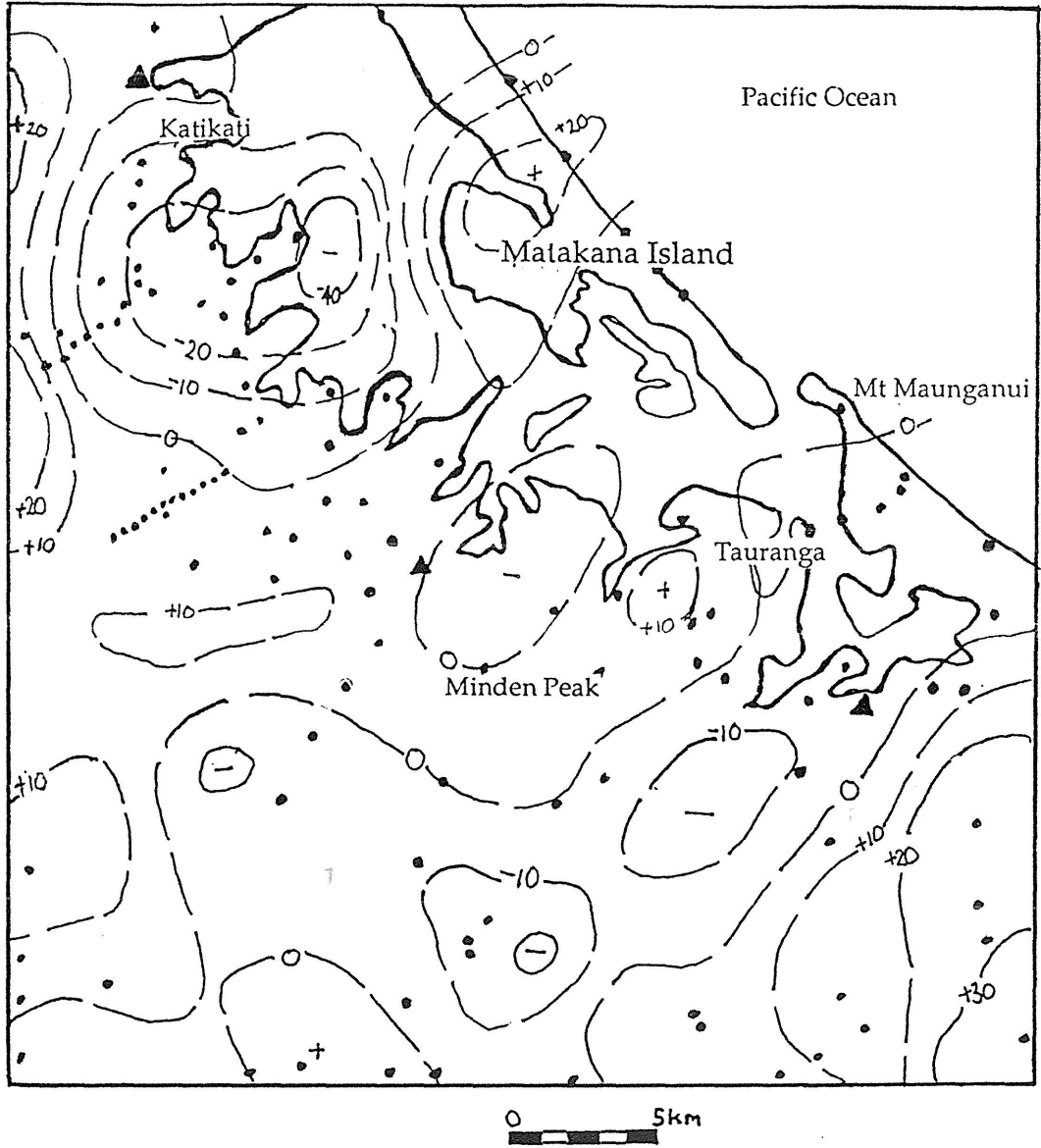


Fig 6.2 Isostatic vertical gradient anomalies in the Tauranga area, (after Woodward and Ferry 1973) units in Eotvos ( $10^{-9}$  N/kgm)

- Gravity station
- ▲ Gravity station of NZ Primary gravity network

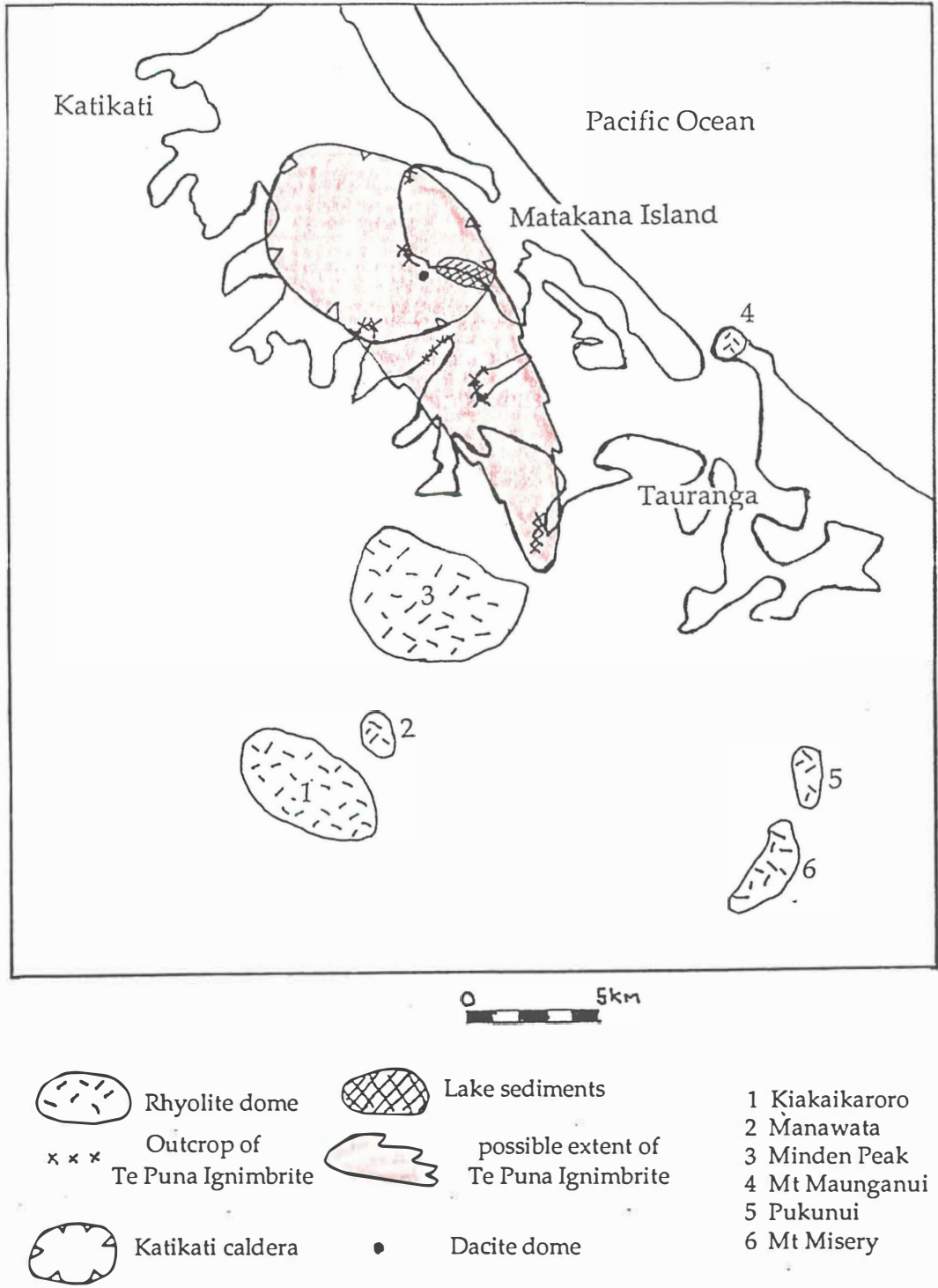


Fig 6.3 Position of the proposed Katikati caldera within the Tauranga basin. Te Puna Ignimbrite assumed to be associated with caldera formation.

The evidence given above suggests that there could be a caldera within the Tauranga basin. The proposed position of the caldera is given in Fig 6.3 based mainly on the location of the negative gravity anomaly. The boundary of the negative anomaly is based on contouring of the values between each gravity station. The eastern boundary of the anomaly at Matakana Island is not precise enough to indicate the caldera boundary as contouring occurs between fewer gravity stations.

It is also based on the position of the lake sediments which would lie within the caldera. Te Puna Ignimbrite outcrops are indicated as well as a suggested original distribution before any erosion of the ignimbrite occurred. This indicates a possible direction of flow in an easterly direction.

## References

- Adams, J.C., 1992: A Facies Approach to the Geology of the Hot Water Beach-Whenuakite Region, Coromandel Volcanic Zone. Unpublished MSc Thesis housed at the University of Waikato.
- Anderson, A.T. 1968: Oxidation of the LaBlache Lake titaniferous magnetite deposits, Quebec. *Journal of Geology*. 76 : 528-547.
- Ballance, P.F., 1976: Evolution of the upper Cenozoic magmatic arc and plate boundary in Northland, New Zealand. *Earth and Planetary Science Letters*. 28: 356-370.
- 1988: Late Cenozoic time lines and calc-alkaline volcanic arcs in northern New Zealand- further discussion. *Journal of the Royal Society of New Zealand*, 18 no 4.
- Ballance, F.F., Hayward, B.W., Brook, F.J., 1985: Subduction regression of volcanism in New Zealand. *Nature*, 313 : 820-821.
- Ballance, P.F., Pettinga, J.F., Webb, C., 1982: A model of the Cenozoic evolution of northern New Zealand and adjacent areas of the southwest Pacific. *Tectonophysics*, 87: 37-48
- Bird, G.A. 1981: The nature and causes of coastal landsliding on the Maungatapu Peninsula, Tauranga, New Zealand. Unpublished MSc Thesis housed in the Library, University of Waikato.
- Black, P.M., Briggs, R.M., Itayam, T., Dewes, E.R., Dunbar, H.M., Kawasaki, K., Kuschel, E., Smith, I.E.M. 1992: K-Ar age data and geochemistry of the Kivitahi Volcanics, western Hauraki Rift, North Island, New Zealand. *New Zealand Journal of Geology and Geophysics*, 35 : 403-413.
- Blake, S., Ivey, G.N. 1986: Density and viscosity gradients in zoned magma chambers, and their influence on withdrawal dynamics. *Journal of Volcanology and Geothermal Research*, 30 :201-230
- Blake, S., Wilson, C.J.N., Smith, I.E.M., Walker, G.P.L 1992: Petrology and dynamics of the Waimhia mixed magma eruption, Taupo Volcano, New Zealand. *Journal of the Geological Society*. 149 : 193-208.

- Brathwaite, R.L., 1989: Geology and exploration of the Karangahake gold-silver deposits. *In: Kear, D., ed. Mineral deposits of New Zealand, The Gordon J. Williams Memorial volume.* Monograph 13: 73-78. Australasian Institute of Mining and Metallurgy, Parkville.
- Briggs, R.M., Gifford, M.G., Moyle, A.R., Taylor, S.R., Norman, M.D., Houghton, B.F., Wilson, C.J.N. 1993: Geochemical zoning and Eruptive Mixing in Ignimbrites from Mangakino Volcano, Taupo Volcanic Zone. New Zealand. *Journal of Volcanology and Geothermal Research.*, 56 : 175-203.
- Briggs, R.M., Fulton, B.W.J. 1990: Volcanism, structure, and petrology of the Whiritoa- Whangamata coastal section, Coromandel Volcanic Zone, New Zealand: facies model evidence for the Tunaiti caldera. *New Zealand Journal of Geology and Geophysics*, 33 : 623-633.
- Brothers, F.N. 1984: Subduction regression and oceanward migration of volcanism, North Island, New Zealand. *Nature* , 309 : 698-700.
- Carmichael, I.S.E. 1967: The iron-titanium oxides of salic volcanic rocks and their associated ferromagnesium silicates. *Contribution to Mineralogy and Petrology.*, 14 : 36-64.
- Cole, J.W., 1978: Tectonic setting of Mayor Island Volcano (note). *Journal of Geology and Geophysics*, 12 : 645-647.
- \_\_\_\_ 1979: Structure, petrology and genesis of Cenozoic Volcanism, Taupo Volcanic Zone, New Zealand - a review. *New Zealand Journal of Geology and Geophysics*, 22:631-657.
- Cole, J.W., Graham, I.J. 1989: Petrology of strombolian and phreatomagmatic ejecta from the 1976-82 White Island eruption sequence. *In Houghton, B.F., Nairn, I.A. (ed) The 1976-82 eruption sequence at White Island volcano (Whakaari), Bay of Plenty, New Zealand. New Zealand Geological survey bulletin 103*
- Cox, A. 1969: A paleomagnetic study of secular variation in New Zealand. *Earth and planetary science letters* , 6:257-267.
- Cox, K.G, Bell, J.D., Pankhurst, R.J. 1979: The interpretation of Igneous rocks. George Allen & Unwin.

- Davidge, S.C. 1982: A geophysical study of the South Hauraki Lowlands. Unpublished MSc Thesis housed in the Library, University of Auckland.
- Dunbar, H.M. 1991: Petrology and geochemistry of the Southern Kiwitahi Volcanics. Unpublished MSc thesis lodged in the library, University of Waikato.
- Ewart, A. 1965: Mineralogy and Petrogenesis of the Whakamaru ignimbrite in the Maraetai area of the Taupo Volcanic Zone, New Zealand. *New Zealand Journal of Geology and Geophysics*, 8 : 611-77
- \_\_\_\_\_ 1967: Mineralogy and Petrogenesis of the Whakamaru ignimbrite in the maraetai are of the Taupo Volcanic Zone, New Zealand. *New Zealand Journal of Geology and Geophysic.*, 8 : 611-677.
- \_\_\_\_\_ 1979: A review of the mineralogy and Chemistry of Tertiary-Recent Dacitic, latitic, Rhyolitic and Related salic Volcanic rocks. *In* Barker. F. (Ed) *Trondhjemites, Cacites and Related Rocks*. Elsevier. New York
- \_\_\_\_\_ 1982: The mineralogy and petrology of Tertiary - Recent orogenic volcanic rocks: with special reference to the andesite-basaltic compositional range. *In* R.S. Thorpe (ed). *Andesites: Orogenic Andesites and Related Rocks*. pp 25-98 .John Wiley and Sons, Chichester.
- Feden, R. H., Fleming, K.S., Malahoff, A. 1976: Crustal extension processes in the Havre Trough and South Fiji Basin. Abstract. International Symposium on Dynamics in the South West Pacific.
- Fodor, R.V., Dobosi, G., Bauer, G.R. 1992: Anomalously high rare-earth element abundances in Hawaiian lavas. *Analytical chemistry*, 64 : 639-643.
- Fransen, P.J.B., 1982; Geology of the Western mamaku Plateau and variations in the Mamaku Ignimbrite. Unpublished M.Sc Thesis, University of Waikato.
- Fraser, C. 1910: The Geology of the Thames Subdivision, Hauraki, Auckland. New Zealand Geological Survey Bulletin 10.

- Fraser, C., Adams, J. H. 1907: The Geology of the Coromandel Subdivision, Hauraki, Auckland. New Zealand Geological Survey Bulletin 4
- Froggatt, P.C., Lowe, D.J. 1990: A review of late Quaternary silicic and some other tephra formations from New Zealand: their stratigraphy, nomenclature, distribution, volume, and age. *New Zealand Journal of Geology and Geophysics*. 33 : 89-109.
- Gill, J.B. 1981: Orogenic Andesites and Plate tectonics. Springer-Verlag. New York.
- Graham, I.J., Hackett, W.R., 1987: Petrology of calc-alkaline lavas from Rhuapehu Volcano and related vents, Taupo Volcanic Zone, New Zealand. *Journal of Petrology*, 28 : 531-567.
- Harmsworth, G. 1983: Quaternary stratigraphy of the Tauranga Basin. Unpublished MSc thesis housed in the Library, University of Waikato.
- Healy, J. 1967: Geology of the Kaimai Tunnel Section (abs.). *Geological Society of New Zealand Conference, 1967*. Unpublished.
- Healy, J., Schofield, J. C., Thompson, B. N. 1964: Sheet 5 Rotorua (1st ed) Geological Map of New Zealand 1:250,000 Dept of Scientific and Industrial Research, Wellington.
- Henderson, J., Bartrum, J. A. 1913: The geology of the Aroha Subdivision Hauraki, Auckland. Geological Survey Branch Bulletin No 16.
- Henry, M.A.C. 1991: The Volcanic geology of Motiti Island. Unpublished MSc thesis, lodged in the library, University of Waikato.
- Houghton, B.F., Cuthbertson, A. B. 1989: Sheet T14 BD-Kaimai. Geological map of New Zealand 1:50 000. Map (1 sheet) and notes. Wellington, New Zealand. Departments of Scientific and Industrial Research
- Hughes, G.R., 1993: Geology of the Eastern Tauranga Basin and Papamoa Range. Unpublished MSc Thesis housed in the Library, University of Waikato.

- Hull, A.G., 1977: Lignite and its relation to the stratigraphy of the eastern Taruanga Basin. Dissertation for B.Sc. (Hons.), Victoria University
- Hunt, P. 1991: The volcanic geology of the Whiritoa Hill area. Unpublished MSc thesis, lodged in the library, University of Waikato.
- Hunt, T.M., Whiteford, C.M. 1979: Sheet 5 Rotorua (1st Ed) Magnetic Map of New Zealand, 1:250000, Total force Anomalies. Department of Scientific and Industrial Research Wellington New Zealand.
- Irvine, I.N., Baragar, W.R.A 1971: A guide to the chemical classification of the common Volcanic Rocks. *Canadian Journal of Earth Sciences*, 8 : 523-548.
- Kamp, P.J.J. 1984: Neogene and Quaternary extent and geometry of the subducted Pacific Plate beneath North Island New Zealand: implications for Kaikoura tectonics. *Tectonophysics*, 108 : 241-266.
- Karig , D.E. 1970: Ridges and Basins of theTonga-Kermadec Island Arc System. *Journal of Geophysical Research*,, 75 : 239-254.
- \_\_\_\_\_ 1974: Evolution of arc systems in the Western Pacific. *Annual review of Earth and Planetary Sciences*, 2 : 51-75.
- Kear, D. 1959: Stratigraphy of New Zealand's Cenozoic volcanism north-west of the volcanic belt. *New Zealand Journal of Geology and Geophysics*, 2 : 578-589.
- Kear, D., Schofield, J.C., 1978: Geology of the Ngaruawahia Subdivision. New Zealand Geological Survey, Bulletin 88: 168p.
- Kohn, B.P. 1973: Some studies of New Zealand pyroclastic rocks. Unpublished PhD thesis housed in the Library, Victoria University of Wellington. 340p
- Kushel, E., Smith, I.E.M., 1990: Rare earth mobility in arc-type volcanic rocks. The Australain Institute of Mining and Metallurgy, Pacific Rim Congress, Australia, 1990.
- Leake, B.E. 1978: Nomenclature of amphiboles. *Candian Mineral*. v 16 p 501-520.

- Le Maitre, R.W. 1976: A new Approach to the Classification of Igneous Rocks Using the Basalt-Andesite-Dacite-Rhyolite Suite as an Example. *Contributions to Mineralogy and Petrology*, 56 : 191-204.
- Lipman, P.W. 1967: Mineral and chemical variation within an ash-flow sheet from Aso caldera, southwestern Japan. *Contributions to Mineralogy and Petrology*, 16 : 300-327.
- Lindsey, D.H., Spencer, K.J. 1982: Fe-Ti oxide geothermometry: Reducing analyse of co-existing Ti-magnetite (Mt) and Ilmenite (Ilm). Transactions, American Geophysical Union 63 p471.
- Lofgren, G. 1971: Experimentally produced devitrification textures in natural rhyolitic glass. *Geological Society of America Bulletin*, 82 : 111-124.
- Ministry of Works and Development. 1976: *The Kaimai Railway Deviation: constructed by the Ministry of Works and Development for New Zealand Railways*. Information services Ministry of Works and Development.
- Morgan, P. C. 1924: The Geology and mines of the Waihi District, Hauraki Goldfield, New Zealand. Geological Survey Branch Bulletin No 26.
- Morgan, M. 1980: Geology of the Northern Mamaku Plateau. Unpublished MSc Thesis housed in the Library, University of Waikato .
- Morimoto, M. 1988: Nomenclature of Pyroxenes. *Mineralogical Magazine.*, 52 : 535-50.
- Murphy, R. A., Seward, D., 1981: Stratigraphy, lithology, paleomagnetism and fission track age of some ignimbrite formations in the Matahina Basin. *New Zealand Journal of Geology and Geophysics*. 24: 325-331
- New Zealand Geological Survey. 1972: North Island (1st Ed). Geological map of New Zealand 1:1,000,000. Department of Scientific and Industrial Research, Wellington New Zealand.

- New Zealand Geological Survey. 1973: Quaternary Geology, North Island, 1,000,000 (1st ed) New Zealand Geological Survey Miscellaneous Series Map 5. Department of Scientific and Industrial Research, Wellington, New Zealand.
- Peccerillo, A., Taylor, S.R. 1976: Geochemistry of Eocene Calc-Alkaline Volcanic Rocks from the Kastamonu Area, North Turkey. *Contributions to Mineralogy and Petrology*, 58 : 63-82
- Pringle, M.S., McWilliams, M., Joughton, B.F., Lanphere, M.A., Wilson, C.J.N. 1992:  $^{40}\text{Ar}/^{39}\text{Ar}$  dating of Quaternary feldspar: Examples from the Taupo Volcanic Zone, New Zealand. *Geology*, 20 : 531-534.
- Pullar, W.A., Birrell, K.S., Heine, J.C., 1973: New Zealand Soil Survey Report 1 and 2. New Zealand Soil Bureau.
- Reid, F.W., Cole, J.W., 1983: Origin of dacites of Taupo volcanic Zone, New Zealand. *Journal of Volcanology and Geothermal Research*, 18 : 191-214.
- Reynors, M.E., 1990: Hikurangi margin seismicity, structure and tectonics before PANDA. *Geological Society of New Zealand Miscellaneous Publications* 50a, 116.
- Rutherford, N.F., 1978: Fission-track age and trace element geochemistry of some Minden Rhyolite obsidians. *New Zealand Journal of Geology and Geophysics*, 21:443-448.
- Schuraytz, B.C., Vogel, T.A., Younker, L.W. 1989: Evidence for Dynamic withdrawal from layered magma body. The Topopah Spring Tuff, Southwestern Nevada. *Journal of geophysical Research.*, 94 : 5925-5942.
- Skinner, D. N. B. 1986: Neogene Volcanism of the Hauraki Volcanic Region. Late Cenozoic Volcanism in New Zealand. Royal Society of New Zealand, Bulletin Number 23.
- \_\_\_\_ 1993: Geology of the Coromandel Harbour area. Scale 1:50000. Institute of Geological and Nuclear Sciences geological map 4. 1 sheet and 44 p. Institute of Geological and Nuclear Sciences Ltd, lower Hutt, New Zealand.

- Smith, R.L, Bailey, R.A. 1966: The Bandelier Tuff: A study of Ash-flow Eruption cycles from zoned magma chambers. *Bulletin of Volcanology*. 29 : 83-104.
- Spencer, K.J., Lindsley, D.H. 1981: A solution for coexisting iron-titanium oxides. *American Mineralogist*, 66 : 1189-1201
- Stern, T. A. 1986: Geophysical Studies of the Upper Crust within the Central Volcanic Region, New Zealand. Late Cenozoic Volcanism in New Zealand. Royal Society of New Zealand, Bulletin Number 23.
- \_\_\_\_\_ 1987: Asymmetric back-arc spreading, heat flux and structure associated with the Central Volcanic Region of New Zealand. *Earth and Planetary Science Letters*, 85 : 265-276.
- Stipp, J.J., 1968: The geochronology and petrogenesis of the Cenozoic volcanics of the North Island, New Zealand. Unpublished Ph.D. Thesis, Australian national University.
- Stormer, J.C. 1983: The effects of recalculation on estimates of temperature and oxygen fugacity from analyses of multicomponent iron-titanium oxides. *American Mineralogist*, 68 : 586-594.
- Tonkin and Taylor 1991: Unpublished report on the stability of the Minden Area.
- Wilson, C.J.N., Houghton, B.F., Lamphere, M.A, Weaver, R.R., 1992: A new radiometric age estimate for the Rotoehu Ash from Mayor Island Volcano, New Zealand. *New Zealand Journal of Geology and Geophysics*. 35: 371-374.
- Wilson, M. 1989: Igneous Petrogenesis. Unwin Hyman, London 456p.
- Woodward, D.J., Ferry, L.M., 1973: Sheet 5, Rotorua (1st Ed) Gravity Map of New Zealand, 1:25000, Isostatic Vertical Gradient Anomalies. Department of scientific and Industrial Research Wellington, New Zealand.

\_\_\_\_\_ Sheet 5, Rotorua (1st Ed) Gravity Map of New Zealand, 1:25000, Bouguer Anomalies. Department of scientific and Industrail Research Wellington, New Zealand.

\_\_\_\_\_ Sheet 5, Rotorua (1st Ed) Isostatic Anomalies of New Zealand, 1:25000, Isostatic Anomalies. Department of scientific and Industrail Research Wellington, New Zealand.

Wright, I.C. 1992: Shallow structure and active tectonism of an offshore continental back-arc spreading system: the Taupo Volcanic Zone, New Zealand. *Marine Geology*, 103 : 287-309.

Wright, I.C., Carter, L., Lewis, K. 1990: GLORIA Survey of the Oceanic-Continental Transition of the Havre-Taupo Back-Arc Basin. *Geo-Marine Letters* , 10 : 59-67.

## Appendix - 1

### Catalogue of rock samples

Samples are referred to in the text by their field number, but are catalogued in the University of Waikato Earth Sciences Department rock store under a different number (W number). 'W' numbers are prefixed by the year e.g. 94, and consequently read as follows: W9401.

Grid references refer to NZMS 260 U14 Tauranga Edition 1 (1:50000).

TS - thin section, XRF - X-ray fluorescence, MA - modal analysis, MP - microprobe analyses.

Catalogue No	Sample No	Rock Name	Location	Application
W94320	1	Alluvium	829844	TS
W94321	3	Waiteariki	827824	TS
W94322	6	Minden	807818	TS,XRF,MA
W94323	7	Minden	807815	TS,XRF,MP,MA
W94324	8	Waiteariki	791790	TS
W94325	9	Waiteariki	795805	TS
W94326	12	Waiteariki	804788	TS,MP
W94327	13	Kaikaikaroro	742754	TS,XRF,MP,MA
W94328	14	Kaikaikaroro	742754	TS,MA
W94329	15	Manawata	762780	TS,XRF,MP,MA
W94330	16	Manawata	762780	TS,XRF,MA
W94331	22	Waiteariki lithic	736732	TS,MA
W94331	23	Waiteariki lithic	736732	TS,MA
W94332	24	Te Puna Ig	798928	TS,MA
W94333	25	Te Puna Ig	798928	TS,MA
W94334	26	Te Puna Ig	798928	TS,MA
W94335	28	Te Puna Ig	798928	TS,XRF,MP,MA
W94336	31	unknown	787757	TS
W94337	32	Waiteariki Ig	795795	TS,XRF,MA
W94338	33	Minden	788740	TS,XRF,MP,MA
W94339	34	Minden	788740	TS,
W94340	35	Minden	788740	TS,XRF,MA
W94341	36	Minden	788740	TS,XRF,MA
W94342	37	Minden	788740	TS
W94343	41	Minden	797823	TS,XRF,MP,MA

Catalogue No	Sample No	Rock Name	Location	Application
W94344	43	Minden	804841	TS,XRF,
W94345	50	Minden	787840	TS
W94346	51	Waiteariki Ig	750720	TS,MP
W94347	53	Kaimai	summit	TS,XRF,MP,MA
W94348	60	Te Puna Ig	827855	TS
W94349	61	Te Puna Ig	827855	TS
W94350	62	Waiteariki Ig	783729	TS,XRF,MP,MA
W94351	64	Waiteariki Ig	785758	TS
W94352	65	Waiteariki Ig	788756	TS
W94353	71	Te Puna	798928	TS
W94354	72	Te Puna	798928	TS
W94355	74	Te Puna	760928	TS
W94356	75	Te Puna	786920	TS
W94357	76	Te Puna	786920	TS
W94358	77	Te Puna	789925	TS
W94359	78	Te Puna	789924	TS
W94360	79	Te Puna	827855	TS
W94361	80	Te Puna	828856	TS
W94362	81	Te Puna	828856	TS
W94363	82	Te Puna	828856	TS,XRF
W94364	83	Te Puna	828856	TS,XRF
W94365	84	Te Puna	828856	TS,XRF
W94366	85	Te Puna	828856	TS,XRF
W94367	86	Te Puna	828856	TS,XRF
W94368	87	Te Puna	828856	TS,XRF
W94369	88	Te Puna	828856	TS,XRF
W94370	89	Te Puna	828856	TS,XRF
W94371	90	Te Puna	828856	TS,XRF
W94372	91	Te Puna	828856	TS,XRF

Micro probe analyses data

Tables of microprobe data for representative phenocrysts of the Western Tauranga basin volcanic rocks are presented below. Samples were prepared using standard techniques to produce polished and carbon coated thin sections which were analysed on the electron microprobe at the University of Auckland.

Plagioclase

Unit	Kaikaikaroro				Minden				
Sample	13	13	13	13	7	7	7	7	
SiO <sub>2</sub>	57.89	58.23	57.86	58.86	59.85	58.35	59.52	59.55	54.41
TiO <sub>2</sub>	0.1	0.05	0.14	0.02	0.09	0.05	0.06	0.09	0.12
Al <sub>2</sub> O <sub>3</sub>	26.21	25.78	25.98	25.51	25.12	25	24.77	25.13	27.72
FeO	0.34	0.3	0.24	0.09	0.26	0.06	0.33	0.12	0.3
Fe <sub>2</sub> O <sub>3</sub>	0	0	0	0	0	0	0	0	0
MnO	0.21	0.09	0.03	0.07	0.04	0.05	0.02	0.08	0.01
MgO	0.1	0.02	0.03	0.06	0	0.04	0.06	0.08	0.17
CaO	8.02	7.63	7.78	7.14	6.6	7.13	6.08	6.46	10.03
K <sub>2</sub> O	0.35	0.43	0.45	0.46	0.56	0.47	0.55	0.61	0.31
Na <sub>2</sub> O	6.54	6.78	6.6	6.85	7.26	6.76	7.43	7.39	5.57
P <sub>2</sub> O <sub>5</sub>	0.06	0.05	0.2	0.17	0.2	0.16	0.16	0.26	0.26
Total	99.55	99.15	98.91	98.83	99.62	97.71	98.68	99.14	98.34
Albite	58.38	60.11	58.95	61.72	64.39	61.40	66.63	65.05	49.22
Anorthite	39.56	37.38	38.40	35.55	32.35	35.79	30.13	31.42	48.98
Orthoclase	2.06	2.51	2.65	2.73	3.27	2.81	3.25	3.53	1.80

Unit	Minden		Waiteariki				Te Puna		
Sample	7	7	12	12	12	12	12	28 Plag Rim	28 Plag Core
SiO <sub>2</sub>	59.16	58.47	60.24	59.07	59.79	60.65	59.35	59.98	59.93
TiO <sub>2</sub>	0.05	0.12	0.01	0.1	0.03	0.04	0.06	0.04	0.06
Al <sub>2</sub> O <sub>3</sub>	25.27	25.07	23.95	24.19	23.49	23.79	24.42	24.47	24.17
FeO	0.15	0.24	0.12	0.4	0.23	0.08	0.18	0.08	0.1
Fe <sub>2</sub> O <sub>3</sub>	0	0	0	0	0	0	0	0	0
MnO	0.05	0.05	0.13	0.11	0.12	0.04	0.07	0.13	0.05
MgO	0.05	0	0.06	0.07	0.1	0.07	0.07	0.1	0.08
CaO	6.64	7.14	5.63	5.96	5.46	5.41	5.97	6.67	6.09
K <sub>2</sub> O	0.52	0.52	0.67	0.62	0.69	0.66	0.89	0.41	0.53
Na <sub>2</sub> O	7.48	6.55	7.5	7.41	7.61	8.08	7.47	7.43	7.45
P <sub>2</sub> O <sub>5</sub>	0.22	0.27	0.25	0.02	0.15	0.1	0.26	0.11	0.18
Total	99.06	97.75	97.98	97.65	97.04	98.59	97.8	98.97	98.97
Albite	65.09	60.44	67.86	66.69	68.68	70.24	65.79	65.26	66.73
Anorthite	31.93	36.41	28.15	29.64	27.23	25.99	29.06	32.37	30.15
Orthoclase	2.98	3.16	3.99	3.67	4.10	3.78	5.16	2.37	3.12

Unit	Minden	Waiteariki	Waiteariki	Waiteariki	Waiteariki	Waiteariki	Waiteariki	Waiteariki	Minden
Sample	41 Plag	51 Plag Core	51 Plag Rim	51 Plag core	51 Plag Rim	A51 Plag Cor	51 Plag Rim	51 Plag Core	33 Plag Rim
SiO2	60.2	53.81	58.68	57.15	57.89	57.81	54.4	50.1	59.25
TiO2	0.05	0.13	0.08	0.05	0.05	0.02	0	0.06	0.16
Al2O3	24.55	28.76	25.59	26.17	25.92	26.63	28.1	31.5	25.12
FeO	0.14	0.23	0.31	0.28	0.27	0.28	0.21	0.37	0.19
Fe2O3	0	0	0	0	0	0	0	0	0
MnO	0	0.12	0.7	0.3	0.03	0.02	0.03	0.02	0.1
MgO	0.08	0.05	0.1	0.1	0.1	0.06	0.01	0.07	0.06
CaO	6.29	10.91	7.2	8.16	7.83	8.23	9.84	13.73	6.46
K2O	0.65	0.16	0.44	0.38	0.37	0.38	0.15	0.12	0.49
Na2O	7.48	5.05	7	6.41	6.65	6.29	5.43	3.64	7.59
P2O5	0.19	0.16	0.02	0.24	0.12	0.23	0.08	0.21	0.12
Total	99.18	98.68	99.21	98.54	98.92	99.61	97.92	99.46	98.91
Albite	65.71	45.15	62.12	57.39	59.27	56.73	49.52	32.20	66.10
Anorthite	30.53	53.91	35.31	40.37	38.56	41.02	49.59	67.11	31.09
Orthoclase	3.76	0.94	2.57	2.24	2.17	2.26	0.90	0.70	2.81

Unit	Te Puna	Te Puna	Te Puna	Te Puna	Te Puna	Te Puna	Te Puna	Minden	Minden
Sample	28 Plag Core	28 Plag Rim	28 Plag Core	28 Plag Rim	28	28 Plag Core	28 Plag Rim	41 Plag Core	41 Plag Rim
SiO2	57.98	56.52	58.66	59.67	59.04	58.56	57.93	58.05	59.35
TiO2	0.06	0.02	0.05	0.15	0.14	0.15	0.06	0	0.05
Al2O3	26.54	26.48	24.86	24.43	24.38	24.62	25.53	26.12	24.91
FeO	0.2	0.09	0.17	0.17	0.37	0.06	0.3	0.26	0.11
Fe2O3	0	0	0	0	0	0	0	0	0
MnO	0.02	0.09	0.1	0.05	0.15	0	0.02	0.18	0.04
MgO	0.09	0.01	0.07	0.01	0.12	0.15	0.01	0.03	0.12
CaO	8.12	8.4	6.65	5.77	6.39	6.55	7.66	7.91	6.65
K2O	0.36	0.32	0.54	0.52	0.54	0.55	0.44	0.41	0.54
Na2O	6.62	6.14	7.57	7.53	7.66	7.09	6.69	6.63	7.05
P2O5	0.02	0.32	0.23	0.03	0.1	0.03	0.04	0.15	0.14
Total	99.61	97.87	98.27	97.93	98.38	97.37	98.54	99.37	98.49
Albite	58.36	55.86	65.26	68.08	66.34	64.04	59.67	58.82	63.63
Anorthite	39.56	42.23	31.68	28.83	30.58	32.69	37.75	38.78	33.17
Orthoclase	2.09	1.92	3.06	3.09	3.08	3.27	2.58	2.39	3.21

Unit	Minden	Minden	Minden	Kaimai	Kaimai	Kaimai	Kaimai	Kaimai	Kaimai
Sample	33 Plag core	33	33	A53 Plag Rim	53 Plag Core	53 Plag Rim	53 Plag Core	53 Plag Rim	53 Plag Core
SiO <sub>2</sub>	59.83	57.17	59.14	56.62	56.9	57.12	55.86	55.36	55.66
TiO <sub>2</sub>	0.1	0.16	0.06	0.07	0.02	0.04	0.14	0.08	0.02
Al <sub>2</sub> O <sub>3</sub>	24.58	25.84	24.69	26.58	26.23	26.17	26.19	27.35	27.78
FeO	0.17	0.16	0.25	0.13	0.25	0.36	0.1	0.44	0.23
Fe <sub>2</sub> O <sub>3</sub>	0	0	0	0	0	0	0	0	0
MnO	0.02	0.04	0.1	0.04	0.06	0.04	0.14	0.1	0.1
MgO	0.05	0.02	0.03	0.05	0.08	0.07	0.06	0.15	0.11
CaO	6.24	8.02	6.52	8.72	8.19	8.08	8.77	9.53	9.56
K <sub>2</sub> O	0.52	0.4	0.59	0.43	0.37	0.39	0.45	0.35	0.26
Na <sub>2</sub> O	7.64	6.76	7.44	6.12	6.46	6.57	6.23	5.9	5.89
P <sub>2</sub> O <sub>5</sub>	0.03	0.19	0.27	0	0	0.19	0.15	0.09	0.07
Total	98.81	98.19	98.62	98.47	98.39	98.69	97.5	98.92	99.13
Albite	66.84	59.01	65.09	54.54	57.53	58.19	54.78	51.77	51.92
Anorthite	30.17	38.69	31.52	42.94	40.30	39.54	42.62	46.21	46.57
Orthoclase	2.99	2.30	3.40	2.52	2.17	2.27	2.60	2.02	1.51

Unit	Kaimai	Kaimai	Waiteariki	Waiteariki	Waiteariki
Sample	53	53	62 Plag Rim	62 Plag Core	62
SiO <sub>2</sub>	59.18	56.58	56.95	57	57.85
TiO <sub>2</sub>	0.02	0.04	0.11	0.11	0.02
Al <sub>2</sub> O <sub>3</sub>	24.84	26.24	26.62	25.7	25.25
FeO	0.11	0.06	0.16	0.12	0.21
Fe <sub>2</sub> O <sub>3</sub>	0	0	0	0	0
MnO	0.03	0.05	0.04	0.07	0
MgO	0.08	0.01	0.1	0.18	0.03
CaO	7.04	8.06	8.79	8.03	7.53
K <sub>2</sub> O	0.54	0.4	0.37	0.38	0.4
Na <sub>2</sub> O	7.2	5.79	5.98	6.28	6.67
P <sub>2</sub> O <sub>5</sub>	0.14	0.08	0.01	0.09	0
Total	98.8	97.07	98.7	97.38	97.7
Albite	62.91	55.11	53.97	57.26	60.12
Anorthite	33.99	42.39	43.84	40.46	37.51
Orthoclase	3.10	2.51	2.20	2.28	2.37

*Orthopyroxene*

Unit	Kaikaikaroro	Minden	Waiteariki	Waiteariki	Waiteariki	Minden	Minden	Minden	Waiteariki
Sample No	13	7	12	12	12	41	41	41	51
Mineral	PX	PX	PX	PX	PX	PX	PX	PX	PX
SiO2	50.2	49.77	49.54	49.5	49.19	48.39	50.31	50.23	50.14
TiO2	0.18	0.07	0.14	0.05	0.22	0.05	0.11	0.04	0.18
Al2O3	1.31	0.67	0.49	0.53	0.34	14.73	0.6	0.83	1.08
FeO	30.46	31.3	33.55	33.92	33.12	26.08	30.88	30.62	30.63
MnO	0.6	1.53	1.15	1.67	1.54	0.98	1.57	1.42	0.87
MgO	16.16	15.6	14.66	13.47	13.75	15.64	16.15	16.08	15.44
CaO	1.7	0.71	1.18	1.36	1.07	0.73	0.84	0.78	1.57
K2O	0.05	0.05	0.12	0.03	0.3	0.03	0.02	0.05	0.01
Na2O	0.12	0.01	0.07	0.03	0.6	0.14	0	0.22	0.02
P2O5	0.05	0.18	0.18	0.04	0.16	0.02	0.22	0.21	0.03
Total	100.43	99.59	101.04	100.45	99.24	106.56	100.35	99.96	99.73
Enstatite	48.474	48.051	45.188	41.795	43.35	50.788	49.123	48.993	46.489
Ferrosilite	47.861	50.377	52.198	55.172	54.225	47.509	49.04	49.299	50.114
Wollastonite	3.665	1.572	2.614	3.033	2.424	1.704	1.836	1.708	3.397

Unit	Waiteariki	Waiteariki	Minden	Minden	Kaimai	Waiteariki	Waiteariki
Sample No	51	51	33	33	53	62	62
Mineral	PX	PX	PX	PX	PX	PX	PX
SiO2	49.89	49.41	50.7	50.06	50.61	50.84	51.74
TiO2	0.11	0.23	0.3	0.06	0.12	0.23	0.52
Al2O3	0.73	0.99	0.65	0.27	1.04	0.8	1.56
FeO	32.57	32.9	30.35	32.26	27.33	28.02	22.65
MnO	1.04	0.93	1.46	1.49	1.37	0.45	0.49
MgO	15.05	14.76	16.68	15.63	17.57	18.12	21.78
CaO	1.07	0.94	0.76	0.7	0.72	1.1	1.87
K2O	0	0.1	0.05	0.05	0	0.01	0.02
Na2O	0.11	0.08	0.07	0.15	0.25	0.01	0.06
P2O5	0.04	0.21	0.1	0.17	0.15	0.09	0.18
Total	100.35	100.15	100.6	100.41	98.64	99.57	100.6
Enstatite	45.703	45.332	50.173	47.831	52.873	53.379	62.846
Ferrosilite	51.962	52.593	48.184	50.629	45.57	44.292	33.276
Wollastonite	2.335	2.075	1.643	1.54	1.557	2.329	3.878

*Amphibole*

Unit	Minden	Minden	Waiteariki	Waiteariki	Minden	Minden	Minden	Minden	Kaimai	Waiteariki	Waiteariki
Sample No	41	41	51	51	33	33	33	33	53	62	62
mineral	AM	AM	AM	AM	AM	AM	AM	AM	AM	AM	AM
SiO <sub>2</sub>	45.19	45.52	41.7	1.75	45.22	45.65	45.73	46.03	46.2	44.74	44.06
TiO <sub>2</sub>	0.98	1.28	2.02	7.84	1.34	1.22	1.29	1.31	1.21	1.64	1.8
Al <sub>2</sub> O <sub>3</sub>	7.3	8.07	8.88	18.88	7.52	7.31	7.23	7.55	6.89	7.97	8.14
FeO	21.91	21.18	20.59	0	20.07	19.91	18.47	18.27	18.09	20.08	18.82
Fe <sub>2</sub> O <sub>3</sub>	0	0	0	0	0	0	0	0	0	0	0
MnO	0.78	0.52	0.28	0.28	0.55	0.43	0.35	0.53	0.51	0.28	0.29
MgO	9.81	9.89	8.82	10.91	10.51	10.87	12.41	11.93	11.94	10.86	10.57
CaO	10.33	10.58	10.26	10.78	9.96	10.25	10.09	10.18	10.44	10.7	10.97
K <sub>2</sub> O	0.57	0.66	0.46	0.42	0.53	0.52	0.35	0.36	0.46	0.4	0.52
Na <sub>2</sub> O	1.1	1.33	1.58	1.62	0.93	1.17	1.27	1.015	1.02	1.57	1.67
P <sub>2</sub> O <sub>5</sub>	0.04	0.08	0.08	0.12	0.04	0.18	0.03	0.06	0.01	0.06	0.16
Total	97.88	99.02	94.6	97.28	96.62	97.33	97.19	97.31	96.77	98.24	96.85

Unit	Kaikaikaroro	Kaikaikaroro	Kaikaikaroro	Minden	Manawata	Waiteariki	Waiteariki	Waiteariki	Te Puna	Te Puna	Te Puna
Sample No	13	13	13	7	15	12	12	12	28	28	28
mineral	AM	AM	AM	AM	AM	AM	AM	AM	AM	AM	AM
SiO <sub>2</sub>	44.29	41.83	43.74	46.18	44.76	59.03	43.54	44.12	46.36	44.81	46.15
TiO <sub>2</sub>	1.76	2.59	1.91	1.19	1.95	0	1.94	1.74	1.3	1.54	1.29
Al <sub>2</sub> O <sub>3</sub>	9.34	10.8	9.05	6.73	8.96	24.37	8.41	7.46	6.75	7.08	6.85
FeO	15.86	19.66	19.02	19.89	14.83	0.27	19.49	20.46	19.97	18.37	19.32
Fe <sub>2</sub> O <sub>3</sub>	0	0	0	0	0	0	0	0	0	0	0
MnO	0.37	0.35	0.25	0.74	0.41	0.01	0.5	0.39	0.5	0.45	0.52
MgO	13.13	9.86	11.35	11.03	13.05	0.01	10.38	10.29	11.89	11.6	11.57
CaO	11.07	10.55	10.82	10.42	10.9	6.13	10.69	10.59	10.12	10.6	10.24
K <sub>2</sub> O	0.19	0.44	0.45	0.41	0.4	0.59	0.51	0.64	0.47	0.35	0.38
Na <sub>2</sub> O	1.64	2.09	1.79	1.03	1.62	7.22	1.83	1.79	1.37	1.66	1.13
P <sub>2</sub> O <sub>5</sub>	0.05	0.2	0.05	0.02	0	0.13	0.02	0.17	0.05	0.09	0.04
Total	97.66	98.18	98.36	97.61	96.9	97.61	97.28	97.44	98.73	96.15	97.46